BIOMECHANICAL MICRODEVICES TO STUDY CIRCULATING CANCER CELLS IN HEMATOGENEOUS METASTASIS

TAN SWEE JIN

B.Eng (Hons), NUS

A THESIS SUBMITTED

FOR THE DEGREE OF DOCTOR OF PHILSOPHY

Acknowledgements

The author would like to express his most sincere gratitude to everyone who had been instrumental in making this work possible.

First and foremost, the author would like to express his appreciation to his family who had provided unwavering support throughout the duration of his doctoral work. More specifically, he would like to extend his gratefulness to his wife for her patience and support, and to his parents and sisters for their care and concern. In addition, the author would also like to give thanks to his late grandmother who had been pivotal in the choice of the research topic and had pass away from cancer.

Next, the author would like to extend his appreciation to his advisor, Professor Lim Chwee Teck for his guidance and constant support for the work. The project would not have been possible without him and his continual push for excellence. The author would also like to specially thank his co-advisor, Dr. Levent Yobas for his useful discussions and providing equipment support from the Institute of Microelectronics, A*STAR.

Furthermore, the author would like to show gratitude to his colleagues and friends from the Nanobiomechanics Laboratory in the Division of Bioengineering, NUS; from GEM4 Laboratory, NUS; from SMART laboratory, NUS; from NGS, NUS; from the Bioelectronics Group and Silicon Process Technology Group in the Institute of Microelectronics, A*STAR for providing assistance in fabrication, equipment support,

experimentation and creating a lively environment conducive for research. In particular, special thanks are given to Ms Ramkumar Lalitha Lakshmi and Mr Chen Pengfei (final year honours students) for their direct involvement in the experimentations and to Ms Ivy Wee and Ms Vino from the department of NGS who assisted greatly with all the administrative work.

Additionally, the author would like to present his sincere appreciation to his project collaborators for their continual support and active discussions, and for providing cancer cell lines which were used in the study. In particular, the author would like to thank National Cancer Centre, Singapore; National University Hospital, Singapore; Cancer Science Institute, Singapore and KK Women's and Children Hospital, Singapore. More specifically, the author wished to acknowledge Professor Ong Choon Nam for his gift of MCF-7 and MDA-MB-231 breast cancer cell lines which got the project started, and his intriguing discussions. The author would also like to specially thank Dr. Tan Min Han and Dr. Darren Lim for their constructive and positive discussions for working with clinical blood specimens, and their continual faith in the project. Besides the clinical aspects, the author would like to convey his gratitude to ClearBridge Biomedics for advancing the project to automate the system.

Finally, the author wished to acknowledge the ARF and NMRC funding provided by the National University of Singapore and the Ministry of Health respectively for their support in the project. The scholarship provided by A*STAR that funds the doctoral study is also greatly appreciated.

Table of Contents

Summary

The morbidity and mortality of cancer typically arises from metastasis of the primary tumor and it is generally accepted that secondary prevention through early detection yields the opportunity for early intervention. Spreading of cancer to distant sites is usually established through the body circulatory system and thus the number of circulating tumor cells (CTCs) in peripheral blood of cancer patients is strongly associated to the disease development. The technical challenge lies in the rarity of these cells in peripheral blood of cancer patients which makes them hard to be distinguished. Recent advances in microdevice technology have allowed highly sensitive techniques, and the current investigation seeks to demonstrate a system for the effective isolation and study of CTCs. The study presents a label-free microdevice that is capable of isolating cancer cells from whole blood via cancer cells' distinctively different physical properties such as size and deformability. The isolation of CTCs using microfluidics is attractive as the flow conditions can be accurately manipulated to achieve an efficient separation. Using physical structures placed in the path of blood specimens in a microchannel, CTCs which are generally larger and stiffer are retained while most blood constituents are removed. The operations for processing blood are straightforward and permit multiplexing of the microdevices to concurrently work with different samples. The microfluidic device is optically transparent which makes it simple to be integrated to existing laboratory microscopes and immunofluorescence staining can be done in situ to distinguish cancer cells from hematopoietic cells. This also minimizes the use of expensive staining reagents, given the small size of the microdevice.

In the development of this microfluidic device, computational studies of the proposed microfluidic design along with results from feasibility studies are first performed. A full characterization of the microdevice with numerous cancer cell lines from different origins is then conducted. Finally, its direct use with clinical blood specimens is investigated. With the microfluidic system, it was demonstrated that an effective isolation could be attained and the microdevice is versatile to address the heterogeneities associated with different cancer types. The microsystem was verified with studies using cancer cell lines from breast, colorectal, gastric, liver, tongue and throat cancer. Using clinical blood specimens, isolation of CTCs was achieved with high sensitivity and attained close to 100% detection rate. Due to the unique separation technique, it also enabled the capture of a more diverse group of CTCs without the use of antibodies during enrichment. With this system, real-time visualization of CTC isolation can be achieved during blood processing. The microdevice shows promise in the isolation and investigation of CTCs on patients with metastatic cancer.

List of Tables

List of Figures

List of Abbreviations

AR	Androgen receptor
ATCC	American Type Culture Collection
CAD	Computer Aided Design
CEA	Carcinoembryonic antigen
CK	Cytokeratin
CT	Computed Tomography
CTCs	Circulating Tumor Cells
DAPI	4',6-diamidino-2-phenylindole
DMEM	Dulbecco's modified Eagle's medium
DNA	Deoxyribonucleic acid
EDTA	Ethylenediaminetetraacetate
EGFR	Epidermal growth factor receptor
EMA	Epithelial membrane antigen
EpCAM	Epithelial Cell Adhesion Molecule
FACS	Fluorescent Activated Cell Sorter
FAST	Fibre-optic array scanning technology
FBS	Fetal Bovine Serum
FDA	US Food and Drug Administration
FISH	Fluorescent in situ hybridization
FITC	Fluorescein isothiocyanate
mRNA	messenger ribonucleic acid
MUC5B	Mucin-5B
NI	National Instruments
NPC	Nasopharyngeal carcinoma
NSCLC	Non-small cell lung cancer
PBMC	Peripheral blood mono-nucleated cells
PBS	Phosphate Buffered Saline
PDMS	Polydimethylsiloxane
PET	Positron Emission Tomography
PFA	Paraformaldehyde
PSA	Prostate-specific antigen
RCC	Renal Cell Carcinoma
RT-PCR	Reverse transcription polymerase chain reaction
VHL	von Hippel-Lindau
WBC	White blood cell
WHO	World Health Organization

List of Publications

Journals

S.J. Tan, R. Lalitha, L., P. Chen, W-T. Lim, L. Yobas, C.T. Lim, Versatile label free biochip for the detection of circulating tumor cells from peripheral blood in cancer patients *Biosensors & Bioelectronics* (2010) In Press.

A.A. Bhagat, H. Bow, H.W. Hou, S.J. Tan, J. Han, C.T. Lim, Microfluidics for cell separation. *Med Biol Eng Comput*. (2010) In Press.

S.J. Tan, L. Yobas, G.Y. Lee, C.N. Ong, and C.T. Lim, Microdevice for the isolation and enumeration of cancer cells from blood. *Biomed Microdevices* 11 (2009) 883-892.

Book Chapter

S.J. Tan, Q. Li, C.T. Lim, (2010) Manipulation and Isolation of Single Cells and Nuclei. G.V.Shivashankar (Ed.), *Methods in Cell Biology*, In Press. Elsevier.

Provisional Patent

S.J. Tan and C.T. Lim, Microsystem for Isolating Viable Circulating Tumor Cells, US Provisional Application No. 61/172,250

Conferences Attended

S.J. Tan, P. Chen, V. Dissanayake, W.T. Lim, L. Yobas, C.T. Lim, (2010) Cell Size and Deformability Based Microfluidics Chip for Isolation of Circulating Tumor Cells in Cancer Patients. *6th World Congress on Biomechanics,* Singapore.

S.J. Tan, R. Lalitha, L., P. Chen, W-T. Lim, L. Yobas, C.T. Lim, (2010) Trapping of circulating cancer cells from blood using a microfluidic device. *Biosensors 2010*, Glasgow, UK.

S.J. Tan, L. Yobas, M.H. Tan, C.N. Ong, and C.T. Lim, (2009) Isolation, Enumeration & Retrieval of CTCs using a Microfluidic Device, *Circulating Tumor Cells: Emerging Technologies for Detection, Diagnosis, Prognosis and Treatment*, NIH Campus, Bethesda, Maryland, USA. (invited)

S.J. Tan, L. Yobas, G.Y.H. Lee, C.N. Ong, and C.T. Lim, (2009) Microdevice for Trapping Circulating Tumor Cells for Cancer Diagnostics, *13th International Conference on Biomedical Engineering*, Singapore, pp. 774-777.

S.J. Tan, L. Yobas, G.Y.H. Lee, C.N. Ong, and C.T. Lim, (2008) Enumerating Viable Circulating Tumor Cells for Cancer Diagnostics, *The 12th International Conference on Miniaturized Systems for Chemistry and Life Sciences, uTAS 2008*, San Diego, CA, USA.

S.J. Tan, L. Yobas, G.Y.H. Lee, C.N. Ong, and C.T. Lim, (2008) Microdevice for Isolating Viable Circulating Tumor Cells, *International Conference on Biocomputation, Bioinformatics, and Biomedical Technologies, 2008. BIOTECHNO '08.*, Bucharest, Romania, pp. 109-113.

Chapter 1 Introduction

1.1 Background (Disease and Technology)

Cancer has been the interest of medical research for over a century and is usually associated with extreme desperation in patients due to the morbidity and fatalities involved. In 2008 alone, 7.6 million people die from the disease, with an estimation of over 12.6 million newly diagnosed cases (Ferlay J 2008) according to the World Health Organization (WHO). The lack of telltale signs at the onset limits the ability for eradicating or early treatment of cancer (Chambers, Groom et al. 2002). Physical signs associated with the disease include the uncontrolled proliferation of cells which can affect almost any part of the body. More often than not, these signs go unnoticed until serious impairment of bodily functions or pain is experienced. In most cases, the primary cause of cancer related deaths is the result of the intravasation of tumor cells from the primary neoplasm into the circulation and the subsequent growth of a secondary tumor at distant sites (Heyder, Gloria-Maercker et al. 2006; Steeg 2006), a process known as metastasis. The exact mechanism of how tumors spread remains an enigma, although there were early observations showing possibilities of targeted cancer spreading to specific organs in the human body (Paget 1889). In more recent investigations, the pathogenesis of cancer metastasis is now better understood after decades of extensive studies (Gupta and Massague 2006). Figure 1.1 highlights the key processes in metastatic development of cancer.

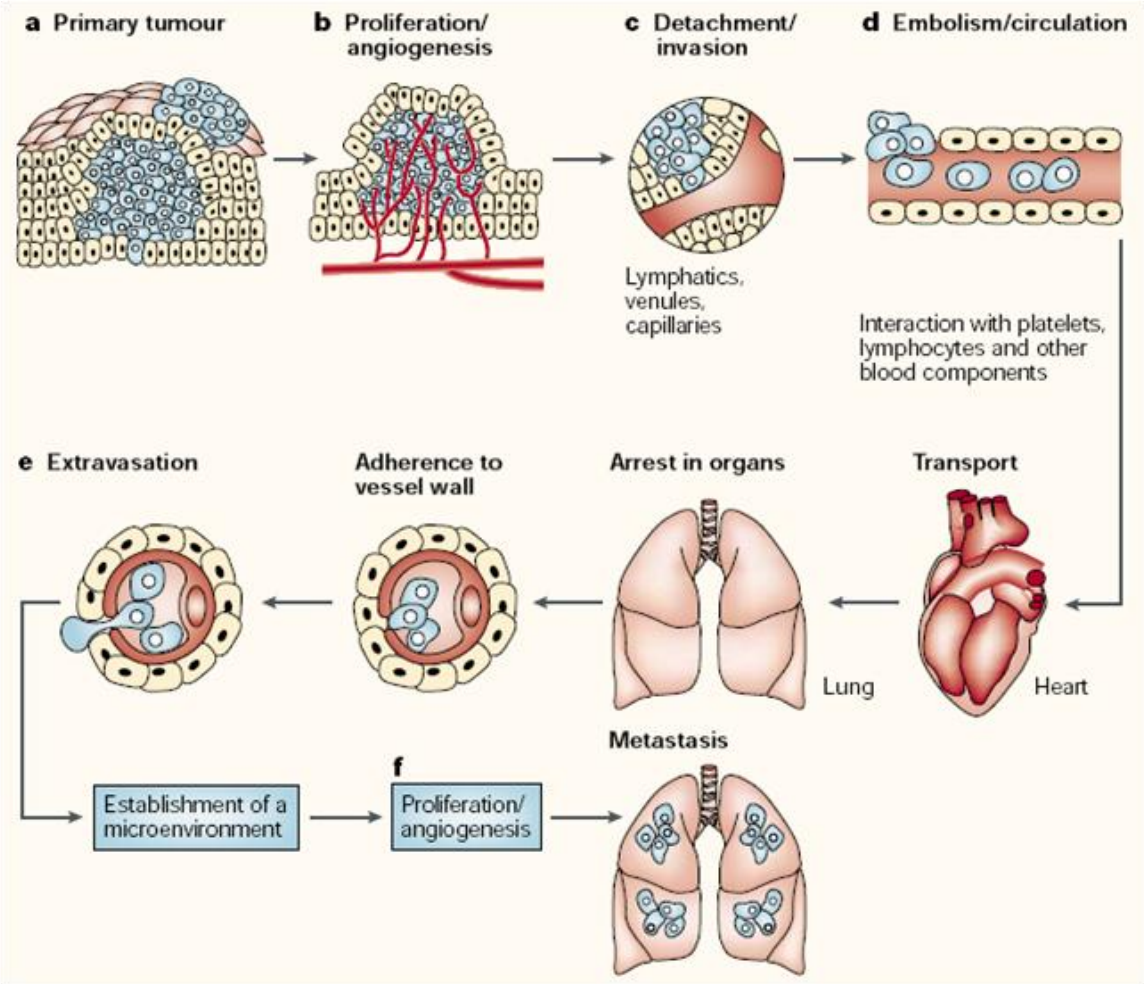

Figure 1.1 Major steps in the metastatic progression of cancer. (a) Cellular aberration and tumor growth. (b) Formation of blood vessels to sustain and replenish nutrients to the tumor. (c-d) Intravastion of tumor cells into the stroma tissue and dissemination through the circulation. (e-f) Tumor arrest and extravastion to form secondary metastases. (Fidler 2003)

As shown in figure 1.1a, the disease establishes with a local aberration of cellular functions at the genetic level, leading to malignant transformation and tumor growth. Subsequently, cell proliferation results in increase tumor mass and extensive vascularization supplies continual nutrients to maintain growth. The invasion or intravasation of tumor cells into the host stroma provides entry into the circulation where cancer cells become free to colonize a secondary site as shown in figure 1.1f. This cycle

occurs repeatedly which translates into an aggravation of the disease for the patient. Important events in the biological cascade of cancer metastasis are the uncontrolled cell proliferation, angiogenesis and tumor dissemination into the circulation. These processes sustain the growth and allow the progression of the disease. An estimated 90% of deaths from solid tumors are a direct result of metastasis (Gupta and Massague 2006). Therefore effective means to combat the disease are through early detection before metastasis has occurred or to prevent the spread of the tumor cells to distant sites of the body.

Technological advances have brought significant improvements in diagnostic methods, surgical techniques, general patient care and enhanced therapeutic treatments (Spinney 2006). For instance, the use of nano-particles achieved the targeted delivery of anti-cancer drugs directly to tumor cells, aiming to avoid debilitating outcomes with conventional chemotherapeutic treatments (MacDiarmid, Mugridge et al. 2007). The development of better imaging techniques such as the positron-emission tomography (PET) scan have proved useful in patients with non-small cell lung cancer (NSCLC) as compared to standard approaches using computed tomography (CT), ultrasonography and bone scanning (Pieterman, van Putten et al. 2000). As technology develops, it will increasingly have a broader impact in biology and healthcare, bringing more sensitive instruments for various clinical applications. This in turn hopes to improve the quality of life for patients. The need for better techniques in cancer detection cannot be overemphasized, given the increasing trend of people suffering or dying from the disease. New devices which are more sensitive and convenient in the clinical setting are necessary

to better detect tumors in the body so that they can be effectively eliminated before acquiring the ability to metastasize.

1.1.1 Circulating Tumor Cells

Cancer cells that enter the blood circulation are termed as circulating tumor cells (CTCs), with documented evidence of the presence of CTCs over a century ago (Ashworth 1869) during the examination of blood samples from a deceased patient. In more recent evaluations, CTCs are found in patients with different metastatic carcinomas (Allard, Matera et al. 2004; Steen, Nemunaitis et al. 2008) and clinical studies supported the potential use of the number of CTCs in peripheral blood as prognostic indicators for survival in metastatic breast, prostate and colon cancers (Cristofanilli, Hayes et al. 2005; Slade and Coombes 2007; de Bono, Scher et al. 2008; Helo, Cronin et al. 2009). Thus, analyzing the blood specimens of patients which are routinely taken can be useful and is also less invasive as compared with traditional biopsies. Evidence from various clinical investigations have also showed that CTC count in blood is directly linked to disease progression, overall survival (Cristofanilli, Budd et al. 2004; Nole, Munzone et al. 2008) and an indication of treatment efficacy (Reuben, Krishnamurthy et al. 2008; Serrano, Sanchez-Rovira et al. 2009). Comparing to invasive biopsies, the enumeration of CTCs in peripheral blood provides a promising alternative source of tumour tissue for the detection, characterisation and monitoring of non-blood-related cancers. Thus, isolating, quantifying and studying these cells obtained from peripheral blood are of much interest.

Research into tumor cell dissemination through the circulatory system has shown it to be an inefficient process and most of the tumor cells are destroyed before distant implantation can occur (Weiss 1990; Brodland and Zitelli 1992; Weiss 1992). As a result, the frequency of CTCs in peripheral blood of cancer patients is of very low concentration and varying in quantity from patient to patient (Zieglschmid, Hollmann et al. 2005; Losanoff, Zhu et al. 2008). The rarity of CTCs in peripheral blood presents a technical challenge to detect them (Pantel, Cote et al. 1999). Tumor cell count can be as low as 1 cancer cell to 1 ml of blood which contains approximately 4.8 – 5.4 billion erythrocytes; 7.4 million leukocytes and 280 million thrombocytes (Fournier 1998). Several different enrichment methodologies have been employed to isolate CTCs, most notably using biochemical means. Using anti-bodies targeted against epithelial specific antigens such as Epithelial Cell Adhesion Molecule (EpCAM), CTCs have been isolated using magnetic separation or flow based assays (Nagrath, Sequist et al. 2007; Riethdorf, Fritsche et al. 2007). Additional immunofluorescence staining or molecular based techniques are utilized to confirm the presence of CTCs in the isolated cell population, allowing them to be distinguished from hematopoietic cells. The procedure is demonstrated in various clinical settings but studies have established that the effectiveness is highly dependent on the specificity of the anti-body used (Sieuwerts, Kraan et al. 2009). Alternative methodologies such as a direct visualization assay (Kahn, Presta et al. 2004), fluorescent activated cell sorter (FACS) (Moreno, O'Hara et al. 2001) and fibre-optic array scanning technology (FAST) cytometer (Krivacic, Ladanyi et al. 2004) have also been used to detect CTCs in blood samples. Complex procedures, tedious inspections and long

processing time are the limiting factors associated with most existing techniques. Furthermore, viability of the isolated cells is lost during the process as fixations of the samples are required by most existing techniques. The understanding of the molecular and biological characteristics of CTCs and their connections to the metastatic process is in its infancy but these tumor cells hold important information about the disease (Pantel and Alix-Panabieres 2007).

There is much to appreciate about the conditions of CTCs whilst in circulation (Pantel, Brakenhoff et al. 2008) and having viable cells after isolation will allow studies to be carried out on CTC sub-populations. This may provide valuable insights into the metastatic process which will influence therapeutic decisions. Thus a sensitive enrichment method is crucial to aid in further examination of CTCs which can be clinically beneficial. Taken together, the enumeration of CTCs in peripheral blood is a promising and attractive complementary technique for the detection, investigation and monitoring of cancers.

1.1.2 Microfluidics

Biological cells, typically in the range of several microns to tens of microns, are extremely hard to handle for its small size. Precise control and instrumentation are required to work at such resolutions to correctly position the cell to the desired location for measurements to be taken (Van Vliet, Bao et al. 2003). Traditional bench-top tools in

cell and molecular biology are not sufficient to address the needs for sensitive and accurate measurements of rare cell events such as the isolation and enumeration of CTCs. The advent of various breakthroughs in micro and nano technology has aided the development of numerous manipulation and analytical methods for various qualitative and quantitative analyses. Techniques that are built upon engineering principles such as microelectronics as well as cell and nuclear mechanics have enabled the handling of micron and sub micron size objects or samples accurately. These methodologies also offer a high throughput analysis using small sample volumes (Bashir 2004; Whitesides 2006) and make these technologies suitable to handle the challenges involved in single cell and nucleus manipulations, and analyze the molecular components such as DNA and RNA (Thorsen, Maerkl et al. 2002; Hong and Quake 2003).

Microfluidics involves the miniaturization of systems for the handling and manipulation of small quantities of fluids. With microchannels in the dimensions of a few to hundreds of micrometers, it is well suited for single cell handling which is of comparable dimensions. The small size in microfluidic devices ensures laminar flow characteristics (low Reynolds number) which make the fluid flow predictable. The flow characteristics of such systems will further aid in the precise control of cells in the enclosed environment. A vast number of applications are being developed based on the technology which includes analytical systems in biochemistry, biomedical devices for disease detection and tools used in systems biology (Whitesides, Ostuni et al. 2001; Smith and Figeys 2006; Martini, Hellmich et al. 2007; Ohno, Tachikawa et al. 2008). Besides being suitable to handle single cells analyses, other motivations for using microfluidic platforms are

abundant. It provides a quick means to test out designs due to the fast turnover time and offers the ability to integrate several devices with various functions to form a complete integrated laboratory on chip (Melin and Quake 2007). Furthermore, the miniaturized platform allows for minimal use of expensive reagents compared to similar conventional biological bench-top methods, thereby saving cost. The technology fundamentally introduces myriad possibilities to enhance and bring about new capabilities in a variety of analyses (Sorger 2008). Hence, microfluidic devices can be especially useful in investigating rare cell events like the detection of CTCs in peripheral blood.

1.2 Motivations, Hypothesis and Objectives

According to the American Cancer Society, about a third of patients (excluding non-melanoma skin cancers) have metastases that are detected at the time when their cancer is first diagnosed. Another third of patients have metastases that are too small to be detected via the usual diagnostic tests. There is an inverse exponential relation for early detection with survival rate, and the disease can be fully cured if diagnosed early (Allard, Matera et al. 2004; Cristofanilli, Budd et al. 2004; Budd, Cristofanilli et al. 2006). Furthermore, for a patient with a malignant tumor, the surgical removal may bring immediate relief to the pain and suffering but leave the person with an uncertain future. The potential of remnant cancer cells resurgence in the body is unpredictable and there are no easy approaches to ascertain when it will happen again. Current methodologies that aid in the early detection of the disease cancer include tumor markers (such as PSA, CA 27.29, CA 15-3 and CEA)

and various imaging techniques. Tumor markers have little diagnostic value though they present well in prognosis (Zieglschmid, Hollmann et al. 2005; Elshimali and Grody 2006; Pantel and Riethdorf 2009), and imaging is difficult with newly formed and small micrometastases (Gilbey, Burnett et al. 2004). The detection of circulating tumor cells in peripheral blood is proposed as an alternative method in diagnosis and prognosis.

The clinical relevance of assessing the quantity of CTCs in peripheral blood is to establish the direct association with cancer progression (Racila, Euhus et al. 1998; Allard, Matera et al. 2004; Cristofanilli, Budd et al. 2004; Kahn, Presta et al. 2004; Cristofanilli, Hayes et al. 2005; Budd, Cristofanilli et al. 2006; Hayes, Cristofanilli et al. 2006; Cristofanilli, Broglio et al. 2007; Nole, Munzone et al. 2007). For instance, Kahn et al. reported a correlation of disease stage and progression with the number of CTCs in peripheral blood on 123 patients (Kahn, Presta et al. 2004). Cristofanli et al. studied 177 women with metastatic breast cancer and showed that patients with 5 or more CTCs in 7.5 ml of blood had an overall survival of less than10 months (Cristofanilli, Budd et al. 2004). Subsequently in a further report, they measured treatment efficacy through monitoring CTCs counts in blood (Cristofanilli, Hayes et al. 2005). The extraction of blood samples remain as one of the most commonly extracted body fluid in any health test which will allow ease of access to conduct CTC tests. Hence, a careful analysis of constituents in peripheral blood will assist in early detection of cancer.

Leading technologies in CTC enrichment from blood specimen uses affinity based techniques which employ antibodies that are absent in blood cells. These methods face

various drawbacks such as the need for pre sample preparation and more importantly the specificity of the antibody selected for enrichment. Additional preparatory steps are likely to incur CTC losses while the lack of a universal biomarker for CTC enrichment limits the detection of CTCs for different cancer types (Allard, Matera et al. 2004). The technique is also laborious, complicated and potential important information about the subpopulations of these cells may also be lost (Sieuwerts, Kraan et al. 2009). Furthermore, the isolated cells are no longer viable after processing of the blood samples which limits the downstream applications that can be done on CTC sub populations which hold important information about the metastatic process.

Past studies have revealed that the shear modulus, stiffness, size and deformability of cancer cells (Weiss and Dimitrov 1986; Weiss 1990) are distinctively different from blood constituents (Shelby, White et al. 2003; Mohamed, McCurdy et al. 2004). Fundamental cell rheological properties of cancerous cells such as deformability and flow characteristics were extensively studied (Lekka, Laidler et al. 1999; Leinung, Wurl et al. 2000; Ito, Nakanishi et al. 2002) and are attractive for CTCs enrichment. No functional modifications will be required as isolation is solely dependent on the biorheological properties differences of cancer cells and blood constituents. In addition, it bypasses the use of a selection antibody during the CTCs enrichment process. Without the need for functional modifications, it will simplify device preparation and blood processing.

It is hypothesized that an efficient isolation of CTCs from peripheral blood can be achieved by utilizing the physical characteristics of tumor cells. From a mechanistic

purview, the separation and enrichment of tumor cells from blood is versatile for different cancer types, though significant molecular heterogeneity exists. The scope and objectives of the study will include designing a microfluidic device that exploits the differences in cell size and deformability of cancer cells to blood cells for the isolation and detection of CTCs. The microdevice is required to be biocompatible, and allow direct processing of blood to minimize intermediary steps so as not to compromise the CTC yield. In addition, the platform has to be able to handle large blood sample volumes and yet be gentle to isolated cells to maintain the integrity of CTCs. With the microdevice, the efficacy for separation and detection of CTCs will be studied. The system will be assessed based on its efficiency, sensitivity and isolation purity of tumor cells from blood. The study will also encompass the use of tumor cells from various cancer origins to ascertain the technique versatility. With clinical trials using peripheral blood specimens from cancer patients, it will test the applicability of the system on actual clinical samples and investigate various characteristics of CTCs.

Chapter 2 Literature Review

The leading cause of death in patients with carcinomas are due to metastatic lesions and less likely of the primary tumor itself (Pantel and Brakenhoff 2004; Gupta and Massague 2006). Even after curative resections, the probable resurgence of the disease poses an uncertainty that affects the emotional aspect of the patients. Furthermore, surgical operations are not entirely restorative and it was reported that 20-50% of patients with "localized" colorectal tumors after surgical removal die of metastasis (Cohen, Kelsen et al. 1997; Ratto, Sofo et al. 1998; Riethdorf, Wikman et al. 2008; Sergeant, Penninckx et al. 2008). The need for better diagnostic, prognostic and monitoring apparatus for the disease cannot be over emphasized.

Technology development has bring about new tools in the field of biomedical engineering and microfluidic devices attracted great attention for its suitability to handle the various challenges involved (Whitesides 2003; Toner and Irimia 2005; Whitesides 2006). Microfluidics is still in its infancy and represents a revolution in laboratory innovation, bringing the benefits of miniaturization, integration and automation for numerous research applications. It can be considered an integrative science with a combination of engineering, chemistry and biology (Gomez 2008). This technology has been the motivation for various biochemical applications in point of care diagnostics, bioterrorism detection and drug discovery. For instance, the methodology has been applied in single cell analysis which will allow for greater discrimination of different cell types (Wheeler, Throndset et al. 2003; Li and Li 2005), thereby producing more sensitive

responses to diseases and treatment monitoring. The technology has also been applied to cell sorting, and produced systems with the capabilities of high throughput and rare cell recovery (Huang, Cox et al. 2004; Davis, Inglis et al. 2006; Nagrath, Sequist et al. 2007; Pamme 2007; Tan, Yobas et al. 2009).

For the purpose of the discussion, the clinical significance of CTCs will be reviewed, showing its association to aid in studying cancer. Competing technologies for the detection of CTCs will also be identified and compared. Lastly, the chapter will examine current microfluidic systems used in cell sorting and single cell analysis which are relevant to the current proposed microsystem to enrich CTCs from peripheral blood.

2.1 Clinical Significance of CTCs

The detection of CTCs dates back to 1869, which was first reported by Ashworth (Ashworth 1869) who observed the presence of tumor cells in blood taken off from the saphena vein of a deceased patient. Interest on these cells in circulation amass over the years to address how these tumor cells traverse and survive in the blood circulation (Weiss and Ward 1983; Weiss and Dimitrov 1984; Weiss and Dimitrov 1986; Weiss and Schmid-Schonbein 1989; Weiss 1990), their clinical significance to patients' overall survival rate (Pool E.H. and G.R. 1934; Roberts, Jonasson et al. 1961; Cristofanilli, Budd et al. 2004) and the characteristics of these cells (Paget 1889; Ashida, Okuda et al. 2000). The use of CTCs as a tool for monitoring and understanding tumor cells in circulation is

rekindled in recent years due to the availability of new and emerging technologies, and is progressing rapidly to address various important problems in metastasis (Pantel and Alix-Panabieres 2007; Pantel, Brakenhoff et al. 2008). These studies outline the importance of understanding the cancer cell biology for CTCs and its survival mechanism for this diverse population of tumor cells.

Several reports demonstrated important connections between the presence of CTCs in peripheral blood and the disease. Mostly notably, CTCs were detected in many of the cancers at the early stage, indicating dissemination of neoplastic cells into the bloodstream occur at the initial stages of the disease (Loberg, Fridman et al. 2004; Riethdorf, Wikman et al. 2008). The possibility for CTCs to be isolated and detected during the early phases of the disease may provide values in prognosis and aid to design regimens for more effective therapeutic treatments. A summary of various studies with different cancer types are presented in tables 2.1, 2.2 and 2.3.

2.1.1 Breast Cancer

Numerous studies have been put forward on the detection of CTCs from the peripheral blood of breast cancer patients, its clinical relevance to disease progression and overall survival, and a measure of treatment efficacy (Schlimok, Funke et al. 1987; Harbeck, Untch et al. 1994; Cristofanilli, Budd et al. 2004). Breast cancer is the most widespread cancer among women in Singapore and demands attention for its prevalence. Table 2.1

summarizes various studies utilizing different enrichment schemes for the detection of CTCs from breast cancer patients. The most commonly used techniques for detecting CTCs after enrichment from peripheral blood are immunofluorescence staining for specific markers and RT-PCR for different oncogenes of interest. As shown in table 2.1, in order to detect breast cancer CTCs, a variety of molecular markers are employed which include CK2, CK18, CK19, EMA, MUC5B and CEA. The detection rates also vary in different investigations even with trials using the same molecular markers and are highly indicative of the heterogeneous nature of the disease. Positive detection rates of tumor cells range from 18% to 83% of peripheral blood samples from cancer patients at various stages of the disease.

Schlimok et al. (Schlimok, Funke et al. 1987) and Cote et al. (Cote, Rosen et al. 1991) enriched CTCs from peripheral blood using density centrifugation from a patient pool of 155 and 49 patients, respectively. Patients who participated in the tests were from various stages of systemic therapy and were tested for keratins from the enriched cell populations. From the studies, it was deduced that the presence of CTCs in peripheral blood was an indication to distant metastases and was positively correlated to early recurrence of the disease. The clinical implications of the results show that monitoring the presence of these tumor cells will aid to provide a measure to disease relapse and possibly introduce new treatment regimens before further disease progression occurs. The results from various other tests (Harbeck, Untch et al. 1994; Cristofanilli, Budd et al. 2004; Becker, Becker-Pergola et al. 2006) further confirms the CTCs' clinical value which present correlations of the quantity of CTCs in peripheral blood to overall and disease free

survival, and the effects of chemotherapeutic exposures to cancer patients. Becker et al. (Becker, Becker-Pergola et al. 2006) in their studies showed a reduction of CTCs after chemotherapy which proves to be useful and sensitive to gauge treatment efficacy. Given the heterogeneity of the disease, Berois et al. (Berois, Varangot et al. 2003) investigated a series of molecular markers by RT-PCR. CEA and CK19 were shown to be significant prognostic indicators for patients with early disease. In short, CTCs in breast cancer had been detected as early as during primary diagnosis and also described as potential measures of chemotherapeutic treatments. The persistence of CTCs in circulation is likely to demonstrate the link to the disease and further evidences from molecular analyses will elucidate the characteristics of CTCs to design targets for them.

2.1.2 Colorectal Cancer

The detection of CTCs in colorectal cancer patients has yielded significant impact to demonstrate its clinical benefits. Most studies were performed with cytokeratin anti-bodies which are illustrated in table 2.1. A variety of methodologies have also been employed which showed clinical correlation to patients at different stages of the disease. For instance, Silly et al. (Silly, Samonigg et al. 1992) used 5 ml of blood extracted from the patients who participated in the study and showed that there were a spike in tumor cell detection directly after surgical operations. CTCs were also discovered at early stages of the disease though the numbers were small. A total of 19 patients were enlisted for this trial and had a 79% detection rate using CK18 as the detection marker. In a similar trial

that examines the effects of surgical procedures, O'Sullivan et al. (O'Sullivan, Collins et al. 1997) predicted a high disease recurrence with the presence of CTCs after the operation to resect the tumor. Flow cytometry was used to detect CTCs in the samples using CK18 as the detection marker. Patients involved in the study were distributed over different disease stages and yielding a 27% detection rate from the sample population.

Broll et al. (Broll, Lembcke et al. 1996) studied the results from 34 patients using density centrifugation to enrich CTCs from 8 ml of blood and showed that there was a strong relationship between the patients and the stage of their disease. The results were promising given patients from different stages showed a strong link to CTC detection. A panel of markers was also tested specifically for colorectal cancer and had varying detection rates which could be specific to the etiology of cancer. A 74% detection rate was achieved and clearly effective to associate the severity of cancer to specific patient's state of health. Cohen et al. in 2 separate investigations (Cohen, Garin-Chesa et al. 1998; Cohen, Punt et al. 2009) showed the importance of detecting CTCs for colorectal cancer patients. In an earlier study with smeared samples, a significant decline in CTC count was observed after the tumor was resected. In more recent analyses using the CellSearch system, CTC count was demonstrated to be strongly linked to overall survival of patients with a sample size of 397 specimens. Progression free survival was also shorter for patients with unfavorable CTCs count and can be used as supportive evidence for future evaluations of CTCs in specific patient subgroups as a marker of outcome and treatment effects.

Table 2.1 Detection of CTCs and the clinical significance for breast and colorectal carcinomas

Cancer Type	Method of Enrichment	Specimen Volume	Detection Markers	Stage	Detection Rate (sample size)	Correlation to disease	Reference
Breast Cancer	Ficoll	6.1ml	CK2,CK18	T1-4	18% (155)	Detected distant metastasis	(Schlimok, Funke et al. 1987)
	Ficoll	NA	Cell surface antigens; pan-CK	>T1	37% (49)	Showed early recurrence	(Cote, Rosen et al. 1991)
	Lymphoprep	4-6ml	EMA; Pan-CK	M0,T1-4	38% (100)	Demonstrated relapse free survival and overall survival	(Harbeck, Untch et al. 1994)
	CellSearch	7.5ml	pan-CK	>T2	61% (177)	Demonstrated progression free survival and overall survival	(Cristofanilli, Budd et al. 2004)
	Biocoll	10-20ml	pan-CK	T1-4	83% (112)	Chemotherapy response. 24% detection rate after treatment.	(Becker, Becker-Pergola et al. 2006)
	Buffer Coat	5ml	MUC5B, CK19, CEA	T1-4	41% (46)	Detection rate with different markers. MUC5B (19%), CK19 (41%), CEA (17%)	(Berois, Varangot et al. 2003)
Colorectal Cancer	Ficoll	5ml	CK18	I-IV	79% (19)	Different detection rate in different stages. M1 (16%), Post operative (71%)	(Silly, Samonigg et al. 1992) (Lindemann, Schlimok et al. 1992; Panaro, Lou et al. 2005)
	Flow Cytometry	NA	CK18	I-IV	27% (48)	Fewer metastatic cells postoperative Recurrence high with CTC present postop	(O'Sullivan, Collins et al. 1997)
	Ficoll	8ml	Pan-CK; CK18; CEA; 17-1-A	I-IV	74% (34)	Correlated to stage of disease Detection rate for markers: CEA (30%), 17-1a (26%), pan-CK (67%), CK18 (52%)	(Broll, Lembcke et al. 1996)
	Smear	NA	A33, CK18, pan-CK	M1	34% (80)	Showed significant decline post operation: resected: 9%; non resected: 34%	(Cohen, Garin-Chesa et al. 1998; Hou, Bhagat et al. 2010)
	CellSearch	7.5ml	pan-CK	IV	NA (397)	Important prognostic factor for overall survival and progression free sruvival	(Cohen, Punt et al. 2009)

* CEA: Carcinoembryonic antigen; CK: Cytokeratin; EMA: Epithelial membrane antigen; MUC5B: Mucin-5B

2.1.3 Lung Cancer

Table 2.2 summarizes 5 different studies conducted on lung cancer patients to investigate the significance of CTCs for this particular cancer type. Different methods of CTC isolation had been employed with specimen volume used in the tests ranging from 0.5 ml to 20 ml of blood. A variety of markers were also tested which is clearly indicative of the diverse nature of the disease and showed a high success rate to determine the molecular characteristics of lung cancer. For instance, Maheswaran et al. (Maheswaran, Sequist et al. 2008) demonstrated the active monitoring of changes in genotypes of epithelial tumor cells in circulation. EGFR mutations which are responsible for resistance to certain drug treatments are identified in patients with NSCLC. By actively monitoring the changes of secondary mutations in the tumor cells, better administering of drugs can be devised.

In other tests with lung cancer patients, there were direct correlations to tumor size and grades. Pantel et al. (Pantel, Izbicki et al. 1993) provided affirmative evidence of CTC detection with the severity of cancer linking tumor size and grading to the detection of CTCs. A sample population of 82 specimens was tested with 0.5 to 5 ml of blood volume using density centrifugation. Patients were in stage I to III of the disease. The results also showed that the disease recurrence is also linked to the amount of CTCs detected. In another test with EpCAM as the detection marker, there were however no significant conclusions drawn with clinical outcome with CTC detection. Brunsvig et al. (Brunsvig, Flatmark et al. 2008) tested 196 specimens from patients with stage I-IV lung cancer and denoted no significant correlation. The results could be due to the unsuitability of the

detection marker that was used in the tests or the heterogeneity of the disease. The former might be a stronger reason for the discrepancy as studies which utilized cytokeratins as detection markers registered a strong link to the clinical outcome of lung cancer patients. Kasimir et al. and Yasumoto et al. (Kasimir-Bauer, Schleucher et al. 2003; Yasumoto, Osaki et al. 2003) in two separate studies showed that the presence of CTCs significantly related to reduced overall survival in lung cancer patients and is correlated to the tumor size. Patient sample sizes were 80 and 351, respectively in each of the investigation and yielded a detection rate of 23% and 32%, correspondingly. The use of CTCs in patients with lung cancer is thus promising to aid in active disease monitoring and prediction of overall survival.

2.1.4 Prostate Cancer

There is evidence that detection of CTCs in peripheral blood of prostate cancer patients may represent a prognostic parameter. Different molecular markers have been proposed such as cytokeratins, PSA and EpCAM, which has shown to be effective to a certain extent. Detection of CTCs in prostate cancer patients are found in early stages of the disease as illustrated in table 2.2 and genotyping of the cells are now possible with new techniques available. Oberneder et al. (Oberneder, Riesenberg et al. 1994) for instance correlated the presence of CTCs to tumor size, distant metastases and tumor differentiation. A total of 84 specimens were analyzed with a detection rate of 33%. Samples were taken from patients with early stages of the disease and enriched using

density centrifugation with 6 ml of sample volume. CK18 was used as the detection marker and the results were promising in identifying patients with critical conditions. Melchior et al. (Melchior, Corey et al. 1997) used PSA, which is a common serum antigen tested in clinical practice for prostate cancer. PSA is usually low in normal people and a sudden elevation may suggest the presence of prostate cancer. 16% of the prostate cancer patients with organ confined tumors were found to be positive for PSA from CTCs using RT-PCR. A total of 71 participants were enlisted, showing an approximate 20% detection rate. Patients with advance stage disease showed 71% positive responses in peripheral blood. The study also demonstrated a direct comparison with samples from the bone marrow and presented evidence that specimens from the bone marrow had a significantly higher rate of detection. This is suggestive of a more sensitive reading with bone marrow specimens than peripheral blood.

On the other hand, Pfitzenmaier et al. (Pfitzenmaier, Ellis et al. 2007) concluded there were no specified correlations to the disease status using EpCAM as the detection marker. However, a detection rate of 92% was achieved for certain subgroups of cancer patients that were tested, showing a strong positive outcome. The tests also claimed to achieve the isolation of viable cells via an immuno-magnetic separation. In another interesting study, Leversha et al. (Leversha, Han et al. 2009) successfully performed fluorescence in situ hybridization (FISH) on isolated CTCs using the CellSearch system. FISH probes used included AR, MYC and 8p which were shown to be present in men with progressive castration-resistant disease. This is beneficial to aid in understanding disease genotypes and active monitoring for secondary mutations so that treatment regimens can be tailored.

Table 2.2 Detection of CTCs and the clinical significance for lung and prostate carcinomas

Cancer Type	Method of Enrichment	Specimen Volume	Detection Markers	Stage	Detection Rate (sample size)	Correlation to disease	Reference
Lung Cancer	Ficoll	0.5-5.0ml	CK18	I-III	22% (82)	Correlated to tumor size and grade. Showed disease recurrence with CTC detection	(Pantel, Izbicki et al. 1993)
	Lymphoprep + immuno-magnetic separation	10-20ml	EpCAM	I-IV	55% (196)	No significant correlation to clinical outcome	(Brunsvig, Flatmark et al. 2008)
	Ficoll + immuno-magnetic separation	10ml	pan-CK	I-IV	23% (80)	Presence of CK+ cells significantly correlated with reduced overall survival	(Kasimir-Bauer, Schleucher et al. 2003)
	Ficoll	5ml	CK18	I-III	32% (351)	Correlated to tumor size and overall survival for stage II and III patients	(Yasumoto, Osaki et al. 2003)
	CTC Chip	1-5ml	Pan-CK; EGFR	NA	100% (23)	Monitoring changes in epithelial tumor genotypes during treatment Genotyping CTCs had a sensitivity of 92%, whereas plasma genotyping had 33%	(Maheswaran, Sequist et al. 2008)
Prostate Cancer	Ficoll	6ml	CK18	N0M0	33% (84)	Correlated to tumor size, distant metastases and tumor differentiation	(Oberneder, Riesenberg et al. 1994)
	Ficoll	5ml	PSA	pT1-3 M0	20% (71)	CTCs preferential in the bone marrow than peripheral blood	(Melchior, Corey et al. 1997)
	MACS	10ml	EpCAM	NA	46-92% (292)	Viable cells can be acquired but no specific correlation was performed	(Pfitzenmaier, Ellis et al. 2007)
	CellSearch	7.5ml	pan-CK, FISH probes (AR, MYC, and 8p.)	Late Stage	NA (77)	Performing FISH in CTCs in men with progressive castration-resistant disease to analyze disease genotypes	(Panaro, Lou et al. 2005; Leversha, Han et al. 2009)

* EGFR: Epidermal growth factor; PSA: Prostate specific antigen; AR: Androgen receptor

2.1.5 Renal Cancer

Renal cell carcinoma typically has poor prognosis as early detection is difficult and for the lack of tumor specific markers in the disease (Loberg, Fridman et al. 2004). The detection of CTCs may therefore aid in the clinical setting to provide a measure for early detection or monitoring purposes. It is also valuable to rely on CTCs to detect specific mutations linked to RCC which can be used as a means of genotyping the disease. As shown in table 2.3, Ohlmann et al. (Ohlmann, Ozgur et al. 2006) showed that the expression of MN/CA9 was significantly present in CTCs from renal cancer patients. The sample size of 24 yielded a positive detection rate of 67%. 8-10 ml of blood were drawn from each patient and enriched for CTCs using centrifugation. There were however no direct correlation to clinical outcome with the presence of CTCs in the study. On the other hand, Bluemke et al. (Bluemke, Bilkenroth et al. 2009) demonstrated significant links of CTCs to lymph node status and showed CTCs can be a strong prognostic factor in RCC. 16 ml of blood were used from each patient and enriched using centrifugation and a negative depletion technique that removed WBCs from the buffy coat. CK8/18 were used as the detection marker for CTCs. An interesting observation from this study found considerable quantity of cytokeratin negative large cells which appeared to have morphology and characteristics of tumor cells. This is indicative of the presence of CTC subgroups which were not identified with standard markers.

Using the CellSearch system, Basso et al. (Basso, Rossi et al. 2009) and Zovato et al. (Zovato, Opocher et al. 2009) demonstrated the detection rate of 80% and 71% with a

sample size of 20 and 21, respectively. It was also found that the baseline CTC count do not significantly relate to the extension of the disease nor to sunitinib (Tryosine Kinase Inhibitor) response. There were however interesting observations about the state of CTCs in the samples which showed that 50% of sporadic RCC patients and 66% of VHL patients had 100% apoptotic cell population. In addition, few studies have focused also on the genotyping aspects of RCC. For instance, Ashida et al. (Ashida, Okuda et al. 2000) reported the detection of the VHL tumor suppressor gene mutations in CTCs which were also detected in the tumors of RCC patients. This is direct evidence of tumor shedding into the blood circulation with CTCs retaining the characteristics of the primary tumor. The clinical implications of the study showed the possibility of tracing the characteristics of the tumor based on the cancer cells that were released into the blood circulation.

2.1.6 Gastric Cancer

Although recent technological advances and awareness to a healthy diet have brought about an improvement in clinical outcome of patients with gastric cancer, the prognosis of patients in their advanced stages remain bleak. This is largely because of the high incidences of metastases and disease resurgence. Early detection is the key component to reduce the mortality rate. The use of CTCs in the clinical setting may provide a convenient technique as blood samples are readily available. With a suitable biomarker, an accurate measure of the disease as well as a high detection rate can be achieved.

For instance, Koga et al. (Koga, Tokunaga et al. 2008) tested a variety of different common targets in gastric cancer. The density centrifugation technique was applied to enrich the tumor cell population from 10 ml of blood for the trials. mRNA sequences for CK18, CK19, CK20 and CEA were used on the isolated cell populations to test their prevalence. The results showed that the CK19 and CK20 expressions were significantly increased in patients with a non-curative operation or recurrence of gastric cancer as compared to healthy volunteers. Furthermore, the five year survival rate for patients' samples who expressed CK19 above the cutoff rate (results taken from healthy volunteers) was 50% and for CK20 was 51.9%. CK19 was proposed to be a more suitable marker than CEA, CK18 and CK20. This could be clinically beneficial for prognosis or to design a postoperative strategy of adjuvant treatment.

In another investigation, Mimori et al. (Mimori, Fukagawa et al. 2008) showed that MT1-MMP was useful to detect CTCs in the sample population of 185 specimens. A 100% detection rate was achieved in the trials with patients from stages I-IV. It was further deduced that MT1-MMP from CTCs in peripheral blood of cancer patients was an independent marker for determining cancer recurrence and distant metastases. These can be clinically valuable to make judgments about the disease and also in early detection of gastric cancer. In other tests with gastric cancer patients, Allard et al. (Allard, Matera et al. 2004) demonstrated the isolation of intact cancer cells using the CellSearch system with an average of 24 recovered tumor cells from the tests. A 31% detection rate was achieved using pan-cytokeratin as the detection marker in a sample size of 13 specimens.

Table 2.3 Detection of CTCs and the clinical significance for renal cell and gastric carcinomas

Cancer Type	Method of Enrichment	Specimen Volume	Detection Markers	Stage	Detection Rate (sample size)	Correlation to disease	Reference
Renal Cancer	Ficoll	8-10ml	MN/CA9	pT1-3	67% (24)	Use of MN/CA9 in the detection of CTCs No direct correlation of CTCs to clinical outcome	(Ohlmann, Ozgur et al. 2006)
	Ficoll + MACS	16ml	CK8/18	NA	41% (154)	CTCs correlated to lymph node status and a strong prognostic marker	(Bluemke, Bilkenroth et al. 2009)
	CellSearch	7.5ml	pan-CK	NA	80% (20)	Baseline count does not correlate to extension of disease nor to sunitinib treatment	(Basso, Rossi et al. 2009)
	CellSearch	7.5ml	pan-CK	NA	71% (21)	Apoptotic cell population found in CTCs from sporadic RCC patients (50%) and VHL patients (66%)	(Zovato, Opocher et al. 2009)
	Ficoll	10ml	VHL	I-IV	75% (20)	Mutations of the VHL tumor suppressor gene detected in CTCs which are also found in the tumors of RCC patients	(Wilding, Kricka et al. 1998; Ashida, Okuda et al. 2000)
Gastric Cancer	Ficoll	10ml	CK18; CK19; CK20; CEA	Late Stage	15.5% (69)	Detection rate with different markers. CK19 (11.6%); CK20 (15.5%). 5 year survival rate for CK19 positive patients (50%); CK20 (51.9%)	(Koga, Tokunaga et al. 2008)
	NIL	1.0ml	MT1-MMP	I-IV	100% (185)	MT1-MMP in peripheral blood was an independent factor for determining recurrence and distant metastasis	(Mimori, Fukagawa et al. 2008)
	CellSearch	7.5ml	pan-CK	NA	31% (13)	Mean cell count of 24 cells were retrieved	(Allard, Matera et al. 2004)

*VHL: von Hippel-Lindau

2.2 Prior Art in CTC Detection

The isolation, quantification and molecular categorization of CTCs is extremely challenging as they exist as rare events in the presence of billions of blood cells. Furthermore, given the sheer size of these cells, handling them using conventional bench top techniques are difficult. Several methods are proposed in the processing of peripheral blood for the detection of CTCs and a summary is outline in table 2.4. A more detailed analysis for two of the leading detection methodologies are presented in the subsequent discussion.

The CellSearch system (Veridex LLC, Raritan, NJ, USA) is currently the only setup in the market approved by the US Food and Drug Administration (FDA) for the clinical use of CTCs in breast, colorectal and prostate cancer. It consists of a CellPrep system, the CellSearch Epithelial Cell Kit, and the CellSpotter Analyzer. Blood specimens are also extracted into their proprietary CellSave Preservative Tube which is an evacuated blood draw tube containing EDTA as the anti-coagulant together with the presence of a cellular preservative. Requirements for blood specimen storage are straightforward, keeping them in room temperature prior to use and to be processed within 72 hrs of blood collection. The CellPrep machine is for the purpose of sample preparation and is semi-automated to ease operations. The CellSearch Epithelial Cell Kit is a set of standard reagents used for CTC enrichment and detection. It consists of ferro-fluids coated with epithelial cell specific EpCAM antibodies for immuno-magnetically separation of CTCs from peripheral blood; a mixture of two phycoerythrin-conjugated antibodies that bind to

cytokeratins 8, 18, and 19 which are supposed to be present in epithelial tumor cells and not in blood cells; anti-bodies for CD45 conjugated to allophycocyanin as a negative stain to identify WBCs; and DAPI to label the nucleus of the cells.

The kit also comes with standard buffers for washing procedures, permeabilizing of the cells and blocking to prevent non specific bindings. Briefly, 6 ml of buffer was added into 7.5 ml of blood, centrifuged for 10 minutes at 800g, and placed on the CellPrep system. The plasma and buffer layer were then automatically removed by the system and ferro-fluids from the CellSearch Epithelial Cell kit were added followed by an incubation period. The bounded cells were the separated by means of the affinity of ferromagnetic beads attached to cells to be attracted to a magnetic field and the rest of the effluence were aspirated. The staining agents used to identify CTCs for immunofluorescence were added together with the permeabilization buffer and set for another incubation cycle to molecular interactions to complete. After the incubation period, the magnetic field was applied again so that cells were immobilized and excess reagents could be washed away.

For the final procedure before detection, the isolated cells were resuspended in the MagNest Cell Presentation Device, where it contained a magnet that orient the labeled cells onto the same focal plane for analysis using the CellSpotter Analyzer. The CellSpotter Analyzer is a four-color semi-automated fluorescence microscope which captures images from the MagNest and presents them to the user for manual identification. Criteria used to confirm the presence of CTCs included round to oval morphology, a visible nucleus (DAPI positive), positive staining for cytokeratin, and

negative staining for CD45. As illustrated in table 2.4, the system had a proof of concept using specimens from numerous cancer patients suffering from a variety of different cancers (Allard, Matera et al. 2004) and were successful in providing standardized tests for reproducible measurements. The specificity of the technique was high and had negative responses from healthy volunteers. Recent development effectively integrated additional features for the molecular characterization of CTCs to determine the genotype analysis of the disease (Leversha, Han et al. 2009). The system thus has potential to be clinically relevant for monitoring and prognostication of cancer.

Figure 2.1 shows the experimental setup for the CTC-chip which is also used to isolate and detect CTCs from whole blood. It consisted of an array of microposts as shown in figure 2.1d which had been chemically treated to be functional with EpCAM antibodies. The arrays of microposts were optimally positioned to enhance the interaction of tumor cells to micropost surface, and the microscale of the setup ensured a high surface area to volume ratio to maximize capture efficiency. The flow velocity was the controlling parameter for the efficacy of the system and to establish flow through the chip, pneumatic lines were added to drive sample fluid across the system.

In brief, for device preparation, the microchips made out of silicon were purged with nitrogen and sealed using pressure sensitive adhesive tape (3M, St Paul, USA). The silicon chip was then placed in a custom made plastic manifold with inlet and outlet ports for fluid handling. The system was made leak resistant by mechanically locking the microchip in the manifold with screws that ensures all the parts were tightly in place.

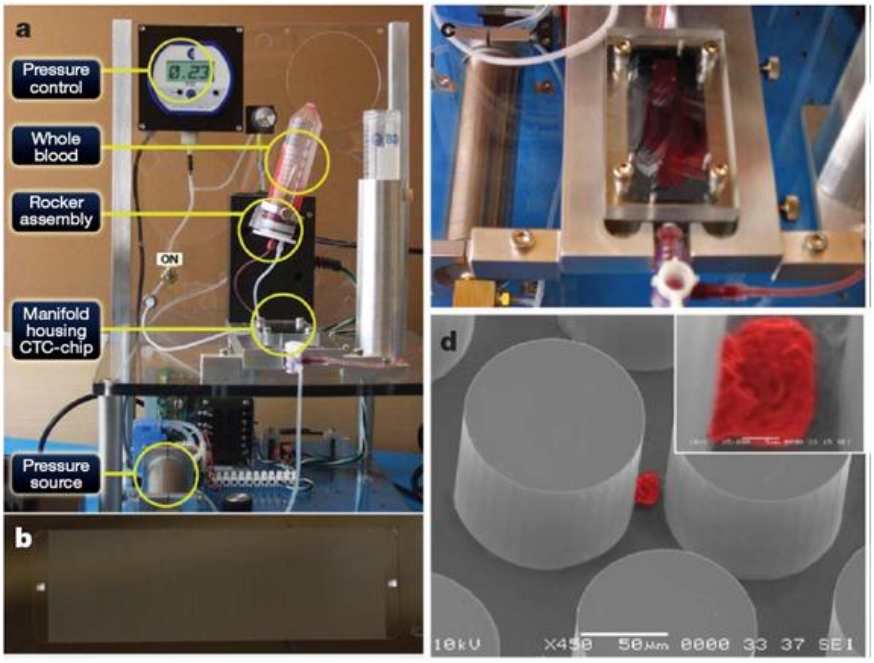

Figure 2.1 Isolation of CTCs using a microfluidic device. (a) Experimental setup with the sample continually mixed on a rocker, and pumped through the chip using a pneumatic pressure-regulated pump. (b) Overview of the CTC-chip with microposts etched in silicon. (c) Whole blood flowing through the microfluidic device. (d) Scanning electron microscope image of a captured NCI-H1650 lung cancer cell spiked into blood (pseudo coloured red). The inset shows a high magnification view of the cell. (Nagrath, Sequist et al. 2007)

Standard luer lock fittings were added to the inlet and outlet ports to facilitate sample entry and effluence removal.

For blood delivery into the system, a pneumatic driving setup consisting of manual pressure regulators, digital gauges and a blood tube rocking mechanism were designed in-house. Prior to running the samples, the device was purged with 3 ml of buffer that removed trapped air bubbles in the system. The sample was then allowed to mix on the rocker for at least 5 min before running the experiment. At the start of blood processing, the pneumatic pump was turned on and adjusted to the required settings for the desired

flowrate. After the processing of blood, the microchip was flushed with 10 ml of PBS at 10 ml/h to remove cells that were non specifically bounded.

Identification and enumeration of CTCs were then performed in situ with immunofluorescence staining for cytokeratin, CD45 and DAPI. The microchip was scanned automatically in a 1mm × 1mm grid format using the programmable stage and Qcapture Pro software (Media Cybernetics, Bethesda, MD, USA). Enumeration for CTCs were then performed with careful evaluation of the images at 100X magnification by examining the staining results, morphological characteristics such as cell size and shape to exclude possibilities of non specific cells that were attached and/or debris present in the blood specimen. The results were evaluated by 2 different operators independently to reduce inter-operator variability. As illustrated in table 2.4, the proof of concept were shown with patients samples from lung, prostate, pancreatic, breast and colorectal cancer, and achieving a high sensitivity and tumor cell yield from these samples. The system was further proven to be gentle to isolated cells and the use of whole blood directly aid to ease operational needs.

With the enabling technologies available, the isolation of CTCs which is clinically beneficial will be enhanced. Table 2.4 summarizes the main points about current techniques employed in the detection of CTCs but is by no means exhaustive for all the existing techniques. As noted in table 2.4, the capture target using different techniques are dissimilar but have yielded significant results with clinical samples. These technologies are also likely to complement each other to fill in the short comings

associated with certain techniques. Ikonisys (table 2.4) for instance uses a combination of centrifugation and filtration which is likely to reduce noise levels (non specific cells) in the isolated cells. Affinity based techniques using EpCAM is hotly debated as the marker is shown in certain cases to be less expressed in various tumor cells (Sieuwerts, Kraan et al. 2009), which will result in the loss of these cells and consequently presents an underestimate of CTCs in blood. Nonetheless, the development of techniques for CTCs isolation is still new and with more studies done on these tumor cells, better methodologies can be devised which will be clinically beneficial. The long term goal is thus to incorporate the tests as standard measures to enhance the quality of life for cancer patients.

Table 2.4 Comparison of current methods to detect CTCs (Stebbing and Jiao 2009)

	Methodology	Capture target	Confirmatory markers	Instrumentation	Proof of concept data	Other applications	Strengths	Weaknesses
CellSearch	Automated magnetic separation & flouresent antibodies with automated image analysis	EpCam Ferrofluid bound	CK8, CK18, CK19 DAPI CD45 (Exclusion)	Sample Preparation: AutoPrep Image Analysis: CTAII	Tumours of epithelial origin including lung and ovarian	Kits for EGFR, HER2, expression evaluated in 4th channel. Profiling kit for molecular characterization including FISH	Standardization and reproducibility. Only FDA approved system for CTC enumeration.	Approved only for enumeration of CTCs in metastatic cancer. Leucocyte contamination makes molecular characterization difficult
Genetix	Manual Magnetic Separation & Fluorescent Antibodies with automated image analysis	Cytokeratin and/or EpCAM immunomagnetic purification	CK8, CK18, CK19 DAPI CD45 (Exclusion)	Sample Prep: Manual Image Analysis: Ariol SL 50	Proof of Concept (POC) data for breast cancer	Potential for IHC and FISH assays based on the Ariol system capabilities	Smaller magnetic beads allow for capture using intracellular markers and integrates IHC and FISH. Data show higher sensitivity by capturing cells with Cytokeratin instead of EpCam	Lack of standardization & reproducibility. Capturing platform not automated
Ikonisys	Density Gradient Separation or filtration, with automated image analysis	Centrifugation and/or filtration	EpCam CK7/8	Sample Prep: Manual Image Analysis: Ikoniscope	POC data for prostate, colorectal and ovarian cancer	FISH assay for chromosomes 7 and 8 aneuploidy evaluated	Ikoniscope imaging system well developed.	Enrichment methodology not well developed
Adnagen	Immuno Magnetic Separation then RT-PCR	EpCam & MUC1 immunomagnetic separation	Multiplexing PCR up to 5 genes.	Sample Prep: Manual PCR: ThermalCycler	RUO detection kits available for colon, prostate and breast cancer	No additional characterization possible	Sensitive due to use of PCR	Limited characterization possible: after RT-PCR, no further characterization possible
CTC-Chip	Micro Fluidic with EpCam bound posts.	EpCAM coated microposts	Cytokeratin+ and phenotypic morphological characteristics. Cyt+, DAPI+, CD45- evaluated in limited number of patients	Fluorescence microscopy: Instrumentation under development	POC data for lung, prostate, pancreatic, breast and colon cancer	EGFR mutations evaluated	Microfluidics is 'gentler' on cells. Whole blood samples do not require processing. Mutation analysis allows monitoring of the emergence of mutations	Data reported uses different criteria. Imaging system not well developed
MagSweep	Immuno Magnetic Seperation	EpCAM coated magnetic beads. Cells are pooled using a magnetic rod	EpCam	Sample Prep: Manual Image Analysis: Fluorescent Microscope	POC data for breast cancer	Data using Fluidigm to look at single cell mRNA	Claim higher purity	Early stage development
Cyntellect	Fluorescent label of CTC followed by laser lysis of tumour cell	CTC identification markers not specified	CTC identification markers not specified	SCIP: Single cell identification platform.	POC data for K-Ras mutation at the single cell level	Nucleic acid isolation permits mRNA and DNA analyses	Highly specific nucleic acid purification	Early stage of development
Maintrac	CTC testing service. Imunomagnetic enrichment and scanning laser cytometry	Ammonium Chloride Lysis. EpCam & CD45 labeling	Viability assessment	Sample Prep: Manual Cellullar Analysis: Laser Scanning Cytometer	Data for breast cancer	Claim applicable in solid epithelial tumours (eg. breast, colon, prostate cancer, sarcomas etc)	CTC testing Service for centers without CTC testing capability	Only 2 Maintrac machines. Too many CTCs obtained

2.3 Microfluidics for Cell Sorting using Physical Methodologies

Effective methods for the manipulating, isolating and sorting of cells are essential for the development of microfluidic-based point of care diagnostic platforms. Cells are extremely heterogeneous, differing in their genetic makeup, behavioral characteristics and functions. The benefits of such technologies enable high speed processing with enhanced sensitivity, allowing for rare cell recovery and better discrimination of cell types in a mixed cell population. Microfluidic systems are well positioned to tackle the challenges involved, given the compatibility with biological species, similar dimensions to cells and accuracy in manipulation with flow control. The proposed system for the

Table 2.5 Cell sorting using physical techniques with microfluidic devices

Methodology	Capture Target	Reference
Pillar structures that deflect particles and cells based on size	Sorted beads of different sizes and fractionation of blood in a continuously mode	(Huang, Cox et al. 2004; Davis, Inglis et al. 2006; Inglis, Davis et al. 2006)
Side diffusive filter system in a microchannel	Leukapheresis, for the enrichment of leukocytes in a blood sample	(Sethu, Sin et al. 2006)
Direct filter structures in the flow path of flow that passively selects fetal cells in the sample	Isolation of fetal cells from maternal circulation	(Mohamed, Turner et al. 2007)
Weir structures that have a gap at the top of the pillars to selectively allow cells to pass based on deformability	Separation of leukocytes from blood and allowed further molecular analysis to be carried out	(Wilding, Kricka et al. 1998; Panaro, Lou et al. 2005)
Step weir structures that differentiate samples based on physical means and the gap distance from the top of the chamber	Size separations of mixtures of 0.5 and 1.0 microm carboxylated polystyrene beads as well as of binary mixtures of Staphylococcus aureus and Saccharomyces cerevisiae cells and of S. cerevisiae and Escherichia coli cells are demonstrated.	(Vankrunkelsven, Clicq et al. 2004)
Inertia flow separation based on the migration of particles across stream lines due to the inertial aspect of the flow	Massive parallelization of continuous pathogenic cell separation from diluted blood	(Mach and Di Carlo 2010)

isolation of CTCs from the peripheral blood of cancer patients works on the physical characteristics of cancer cells from blood cells, and the section aims to review various physical separation microfluidic technologies. Table 2.5 highlights various examples of microfluidic systems utilizing physical separation to effectively discriminate against different cell types.

2.3.1 Pillar structures

The use of pillared structures is attractive for size and deformability based cell sorting. Huang et al. describe a method of continuous separation based on a "deterministic lateral displacement" of micron sized particles with a resolution less than 20 nm (Huang, Cox et al. 2004). The layout of the microfluidic device consists of arrays of pillar structures within the main flow channel.

Using the technology, Davis et al. successfully fractionated blood components by tailoring the design of the microfluidic devices to the sizes of the blood cells (Davis, Inglis et al. 2006). In the approach, the selection mechanism is based on the size of the cells as they interact with the obstacles (figure 2.2a). Taking advantage of the laminar characteristics of the flow profile, sorting of the cells is achieved during the asymmetric bifurcation of the flow around the pillars. The effectiveness of the separation is controlled by the critical hydrodynamic diameter (Inglis, Davis et al. 2006) which is related to the size of the gaps, positions of the pillar arrays and the dimensions of the cells. Sizes of

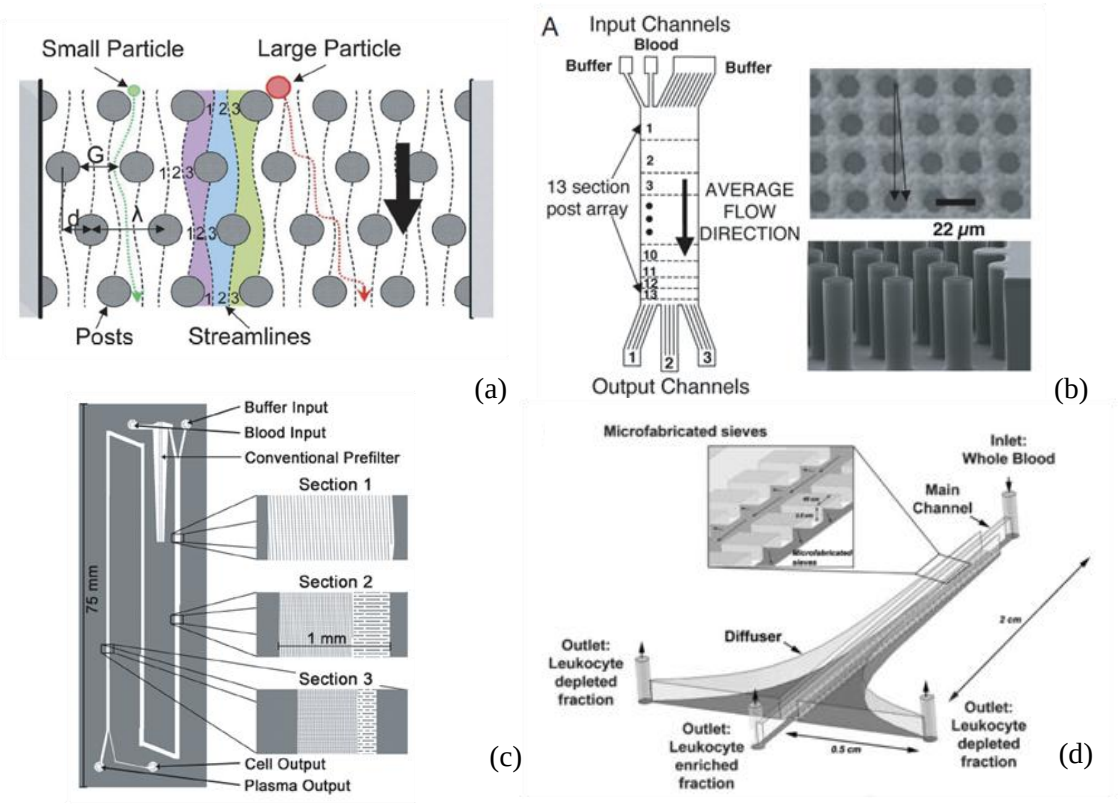

Figure 2.2 Cell separation using lateral displacement in a laminar flow. (a) Schematic of design and separation principle. Particles that are smaller than the critical diameter (green particle) follow initial designated streamlines while the larger particle (red particle) is displaced to the right during the interactions with the obstacles. (b) Fractionating device that separates blood cells. (c) Plasma separation device for the removal of all cells from whole blood (Davis, Inglis et al. 2006). (d) Design of microfluidic diffusive filter for leukocyte enrichment (Sethu, Sin et al. 2006).

cells smaller than the critical hydrodynamic diameter maintains an average downward flow direction following the streamlines around the pillar obstacles. Above the critical diameter, cells are laterally displaced into the adjacent streamlines in a particular direction controlled by the placement of the pillars.

The advantage of the system lies in its simplicity and reliability. It does not require the presence of any molecular tags nor complex preparatory procedures and the system

maintains clog free throughout various sample processing (Davis, Inglis et al. 2006). In addition, the microfluidic device is capable of sorting multiple sizes of cells in a single pass as shown in figures 2.2b and 2.2c for the fractionation of whole blood.

Besides utilizing the characteristics of the laminar flow, pillar structures are ideal as filters for cell sorting. By tailoring the dimensions in between pillars, selection of cells based on their size and deformability can be achieved. The technique has been demonstrated to be effective in isolating circulating tumor cells (CTCs) from blood (Mohamed, Murray et al. 2009; Tan, Yobas et al. 2009) and also in leukapheresis (Sethu, Sin et al. 2006). Sethu et al. showed the ability to enrich leukocytes from whole blood without clogging the device and offers the possibility for the leukocyte depleted blood to be returned to the donor (figure 2.2d) (Sethu, Sin et al. 2006). The design features pillar structures with 2.5μm gaps alongside the central channel that permits passage of erythrocytes in a continuous separation while acting as barriers to leukocytes.

With a similar methodology, CTCs which are generally larger and stiffer than blood constituents are impeded with different gap sizes (Mohamed, Murray et al. 2009; Tan, Yobas et al. 2009). The technique which is simple and straightforward is attractive for cell sorting in various applications. However, such physical systems that separate cells passively by geometrical and rheological differences are likely not universal. The gap sizes between pillar structures will need to be modified to suit the target sample.

2.3.2 Weir Structures

Cell sorting using mechanical filtration techniques such as weir structures in microfluidic designs are straightforward and simple to operate. The mechanism at which separation is achieved is primarily by the sizes of components in a heterogeneous sample. Gaps are created in between weirs and the top cover, which performs as a filter to permit smaller cells to go through while impeding larger cells. Wildings et al. use a series of such weir structures to isolate leukocytes from blood (Wilding, Kricka et al. 1998) as shown in figure 2.3a. The weir-type filter features a 3.5 µm gap between the silicon structure and the Pyrex top cover, which effectively allows the passage of biconcave shaped erythrocytes of 7.6 - 8.2 µm diameters and 2 µm thicknesses. The major drawback of a direct filtration system is the clogging issues that may interfere with the separation

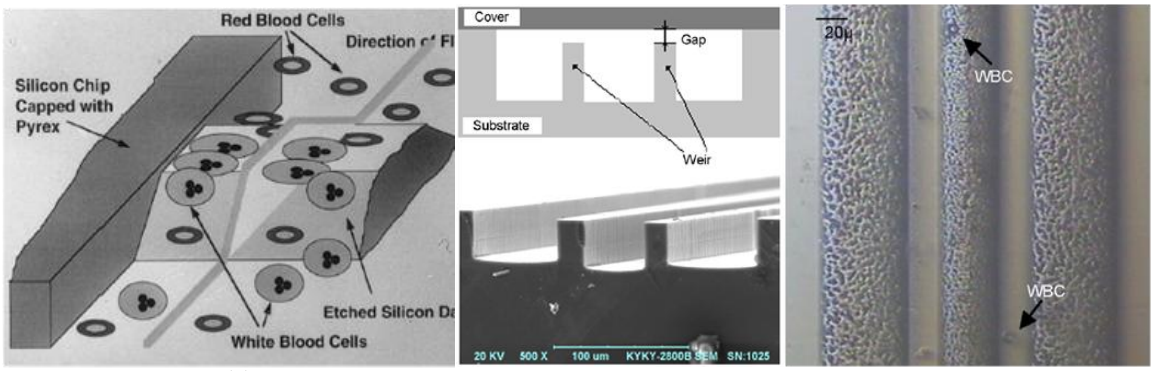

(a) (b) (c)

Figure 2.3 Physical based separation using weir structures. (a) Impediment of white blood cells due to the size of the cells comparing with red blood cells (Wilding, Kricka et al. 1998). (b) Weir structures alongside the main flow channel which effectively prevents clogging when dealing with larger sample volume. (c) The weir type device after filtration of blood showing the clear separation of white blood cells (Chen, Cui et al. 2008).

process due to the processing of large sample volumes. Weir filters that are perpendicular to the flow cause cell buildup over time, leading to obstructions. Chen et al. produce microfluidic devices by setting weirs structures alongside to the main flow (Chen, Cui et al. 2008) to address the cell clogging issue as depicted in figure 2.3b. The device consists of 3 parallel micro channels, separated by weir filtration blocks along the main flow direction. With a 3.5 µm gap, the device allows erythrocytes and other smaller cells to cross from the main channel into the side flow, which effectively restricts only the leukocytes in the main channel (figure 2.3c). However, such mechanical filtration systems that separate cells by geometrical differences are likely not universal and will require variations in design when the target sample changes. Furthermore, reported studies show limited efficiency in the target cell isolation (Wilding, Kricka et al. 1998; Chen, Cui et al. 2008) though the amount is sufficient for further downstream analysis to be carried out.

Nonetheless, physical cell separation represents a simple yet straightforward means for an effective separation. The use will be extended in the current study to address rare cell events to detect CTCs from metastatic cancer patients.

2.3.3 Inertia Flow Separation

The use of inertia forces in separation is an important technique given the simplicity of the procedure and is generally label free during separation. In a laminar flow as in the

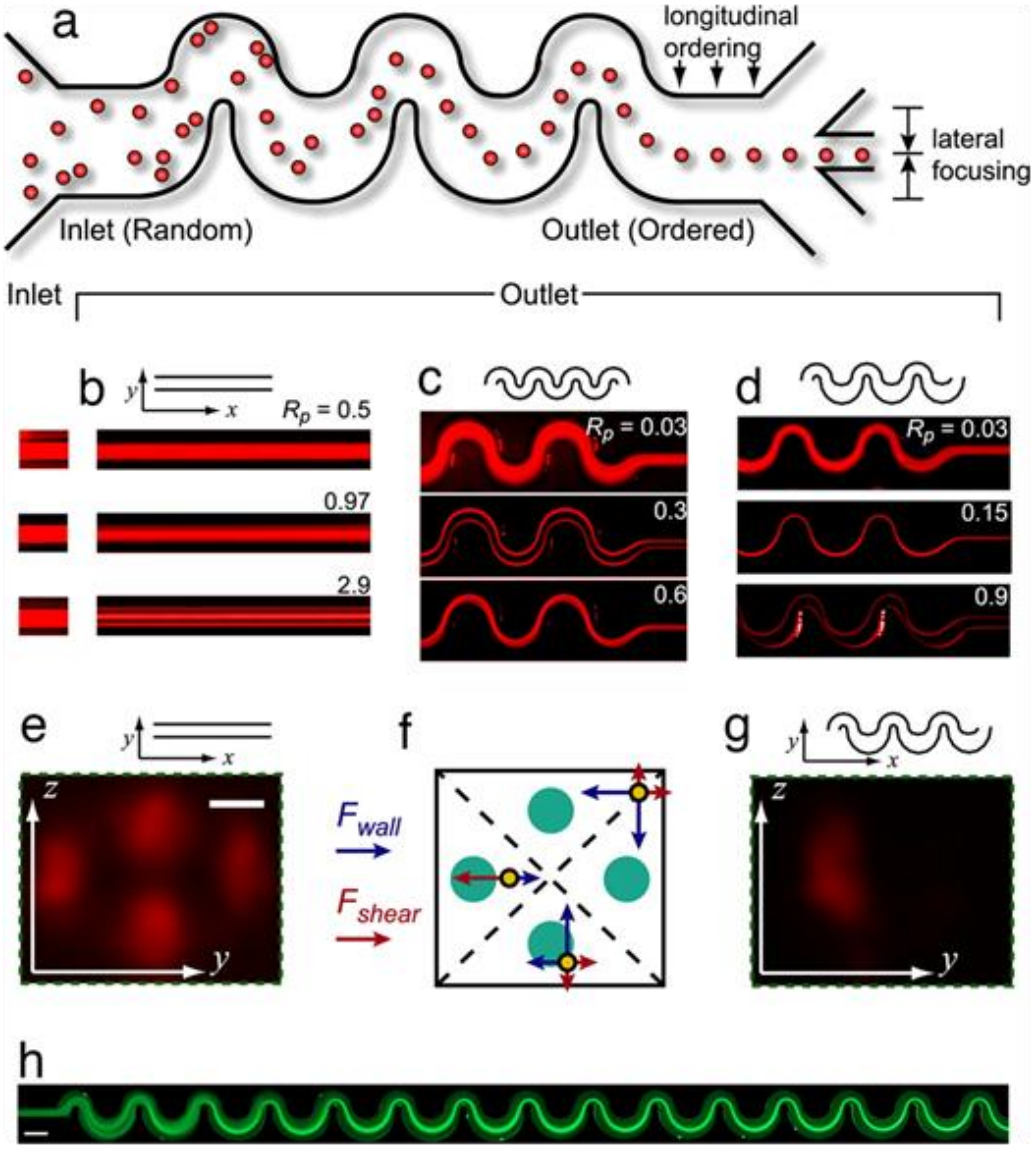

Figure 2.4 Inertial forces that achieves self-ordering of articles. (a) Schematic of the ordering process. Precise ordering of initially scattered particles is observed both longitudinally along the direction of flow and laterally across the channel. (b) Top-down views of fluorescent streak where flow is from left to right. Particles are initially uniformly distributed within the fluid and focusing of particles into four single streamlines is observed. (c) For a symmetric curving channel the symmetry of the system reduces focusing to two streams. Above a critical Dean number (De) focusing is perturbed. (d) For an asymmetric curving system, focusing down to a single stream is favored. Focusing is again more complex as De increases. (e) A confocal cross-section of the rectangular channel shown in b shows focusing of particles to the four channel faces. (Scale bar, 10 μm.) (f) Schematic diagram showing the force balance between the shear-gradient (F shear, red arrows) and wall-induced lift (F wall, blue arrows) for particles in three positions. (g) Confocal cross-section for an asymmetric channel. (h) Starting at the inlet on the left, a random inlet distribution of fluorescent microparticles is focused to a tight streamline on the right after a short distance. (Scale bar, 160 μm.) (Di Carlo, Irimia et al. 2007)

case of fluid traversing in a microfluidic channel, it is generally accepted that in the absence of an external force, particles tend to follow defined streamlines. Inertia forces become significant when the aspect ratio and geometries of the flow channels are altered as characterized by Di Carlo et. al (Di Carlo, Irimia et al. 2007). By making use of the inertia effects, particles can cross streamlines in a predictable manner, thus achieving an effective separation (Di Carlo, Irimia et al. 2007; Di Carlo, Edd et al. 2008; Di Carlo, Edd et al. 2009; Gossett and Di Carlo 2009; Russom, Gupta et al. 2009; Hou, Bhagat et al. 2010). A schematic of how a series of ordered particle can be obtained due to the inertia forces exerted of them in the flow is shown in figure 2.4. By further controlling the fluid flow parameters as shown in figure 2.4b, c and d, the effects of the focused flow can be enhanced to attain a more distinctive separation.

Using this phenomena in fluid flow, cell separation of pathogenic bacteria cells was retrieved from diluted blood specimens (Mach and Di Carlo 2010). A massive parallel microfluidic device was designed and achieves more than 80% removal of the bacteria cells after 2 passes. It allows a throughput of 400 million cells per minute and can process blood at 240 ml.hr. The technique is potentially useful in the field for its simplicity and portability for concentrating specimens in a robust manner.

Chapter 3 Methods and Materials

3.1 Microdevice Fabrication

Figure 3.1a highlights the fabrication steps involved in the manufacture of the microdevice. The microfluidic biochip was produced using soft lithography (Chang, di Tomaso et al. 2000) and the procedures are described as follows. The design of the microdevice was first printed on a photo mask (Infinite Graphics Inc., Minneapolis, MN, USA) which was drawn on a computer aided design (CAD) software Cadence (Cadence Design Systems, Inc., San Jose, CA, USA). SU8-2025 (Microchem Corporation, Newton, MA, USA), a negative photoresist was spin coated at 3200 rpm for 45 seconds on an 8 inch silicon substrate to achieve the thickness of 18-20 μm. Then it underwent an ultraviolet exposure of 120 mJ/cm^2 through the photo mask where the portions that were exposed become polymerized. Following that, the photoresist developer removed the unexposed region chemically. A final hard bake in the oven was performed to ensure a better adhesion of the photoresist to the substrate. The designs on the silicon substrate become the master molds (figure 3.1b) which could then be used for replica molding of the microdevice.

Polydimethylsiloxane (PDMS, Sylgard 184, Dow Corning, Midland, MI, USA) mixed according to manufacturer's recommendation (10:1) was degassed and poured over the master mold. The mixture was then subjected to the curing conditions of 80°C for 2 hours in an oven. Fluidic ports were created using punches on the patterned PDMS shown in

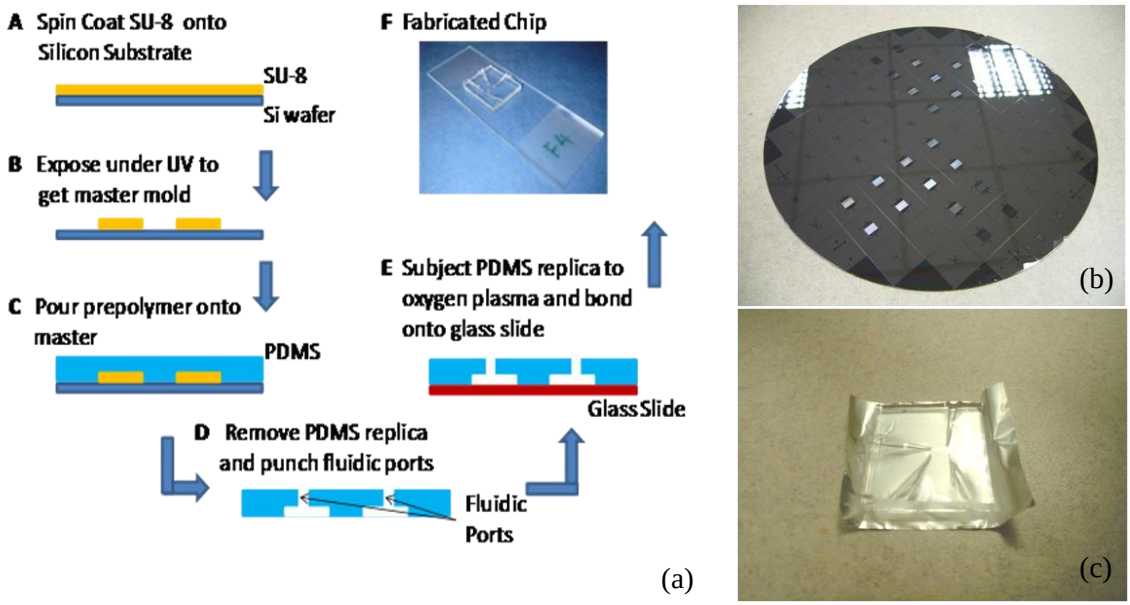

Figure 3.1 Major steps in the fabrication of the microdevice. (a) Device fabrication using soft lithography procedures. (b) Master mold on a pre cut 8 inch wafer. (c) Microdevice removed from the master mold.

figure 3.1c after the removal from the master mold. The PDMS block together with a glass slide was then subjected to oxygen plasma treatment and bonded irreversible. A power setting of 70W, exposed to plasma for 65s with oxygen flowrate of 60 sccm were used. The bonded microdevice underwent a final heat sterilization cycle at 150 ºC overnight. Prior to use, tubings were finally inserted directly into the fluidic ports of the finished microdevice to allow blood samples to be introduced.

3.2 Experimental Setup and Apparatus Preparation

The experimental setup which is integrated onto an inverted microscope (Leica Microsystems GmbH, Germany) is illustrated in figure 3.2. The compatibility with

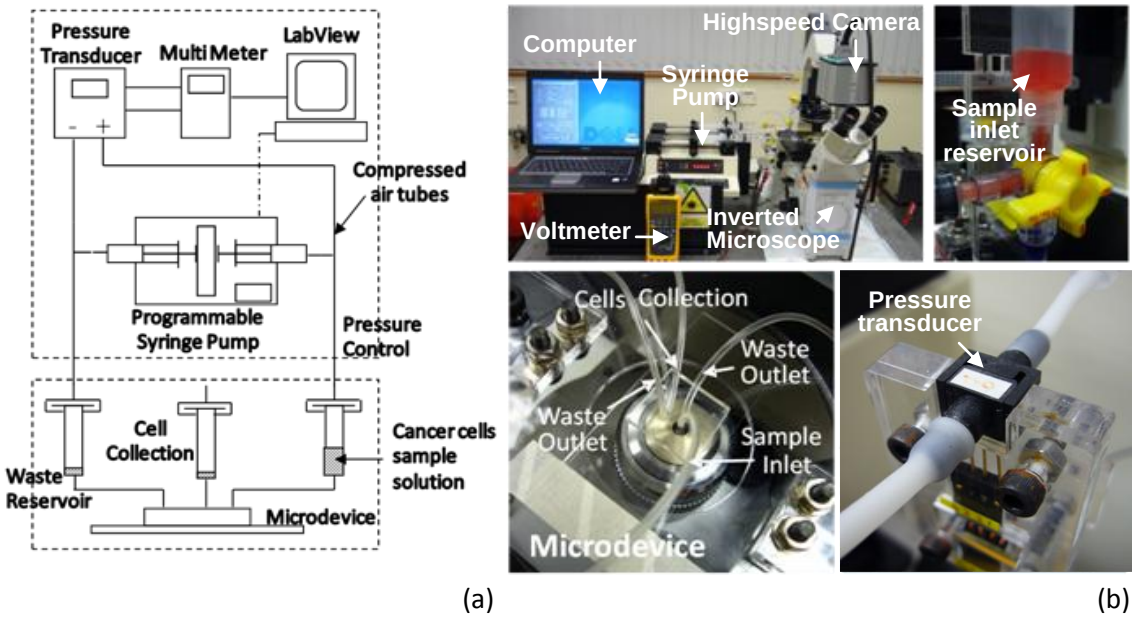

Figure 3.2 Experimental apparatus and setup. (a) Schematic of the entire setup showing the pressure control component and the microdevice system. (b) Entire CTCs isolation setup which is integrated onto an inverted microscope to allow real time visualization and compactness to reduce dead volume.

existing laboratory microscope meant that real time visualization of the isolation process can be achieved. Predetermined pressure differentials were used to drive the samples across the microdevice using manual pressure regulators in the initial design layout (Tan, Yobas et al. 2009). The platform was upgraded as depicted in figure 3.2a to use compressed air from two large syringes to produce pressured lines. A program written in NI Labview (National Instruments, Austin, TX, USA) controlled the programmable syringe pump (Harvard Apparatus, Holliston, MA, USA) and made minute adjustments every 100 ms in response to pressure drop. The differential pressure was measured by a pressure transducer (Honeywell, Morristown, NJ, USA) which was feedback to the computer via a voltmeter to precisely control the pressure settings into the microdevice. This allowed semi-automation in the blood processing and also made the entire system

easily portable without requiring external pressure sources. The control of the pressure differential is critical as the efficacy of CTC separation is highly dependent on the applied pressure conditions. With the semi-automated system, the refresh rate of 100 ms ensured the operating pressure differential is tightly controlled.

For apparatus preparation prior to samples processing, the microfluidic system was flushed with 5mM EDTA (Sigma, St. Louis MO, USA) buffer through the sample inlet as shown in figure 3.2b for 10 minutes at 120 µl/min. No other preparatory steps were required for the sample.

The device was mounted on an inverted microscope, with custom made fixtures as depicted in figure 3.3 to hold liquid reservoirs as close as possible to the microfluidic device to minimize sample/reagent wastage in the tubings during processing. The setup also allowed multiplexing of the microdevices to concurrently process more samples at the same time (figure 3.3b and 3.3c). The fixtures which are shown in figure 3.3a is made of acrylic and fabricated using a laser cutter from the Institute of Microelectronics, A*STAR. Dimensions of the fixtures are designed to be compatible to the existing Leica microscope and could be easily modified to suit other microscope systems by changing the size of the base and the locking screw locations.

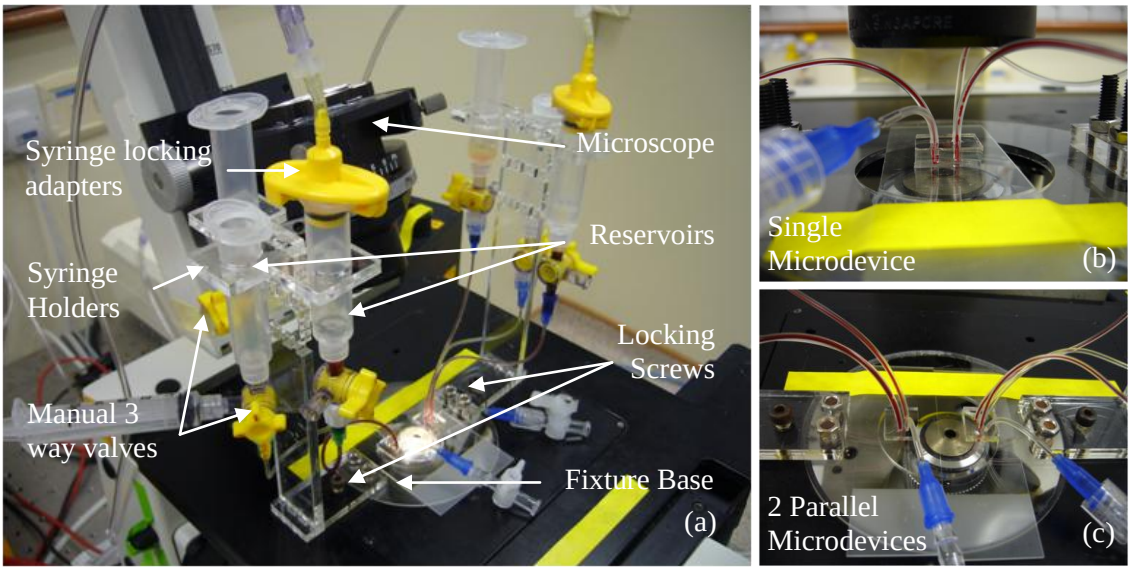

Figure 3.3 Custom made fixtures for holding tubings and reservoirs for the microdevice. The fixtures is made of acrylic and fabricated according to dimensions using a laser cutter to fit the Leica inverted microscope. (a) Overview of the setup. (b) Single unit processing. (c) Dual units processing.

The complete experimental setup is shown in figure 3.2b and 3.3, and cell enumeration was done manually and immediately after cell isolation. Image capturing of the cell isolation process was taken using a high speed camera (Photron, San Diego, CA, USA).

3.3 Computational Fluids Dynamics (CFD) Analysis

A 3D computational model of the microdevice was developed to better understand the flow characteristics as well as to help in initial optimization of the design as shown in figure 3.4. A simplified model of the microdevice due to symmetry of the uniform array

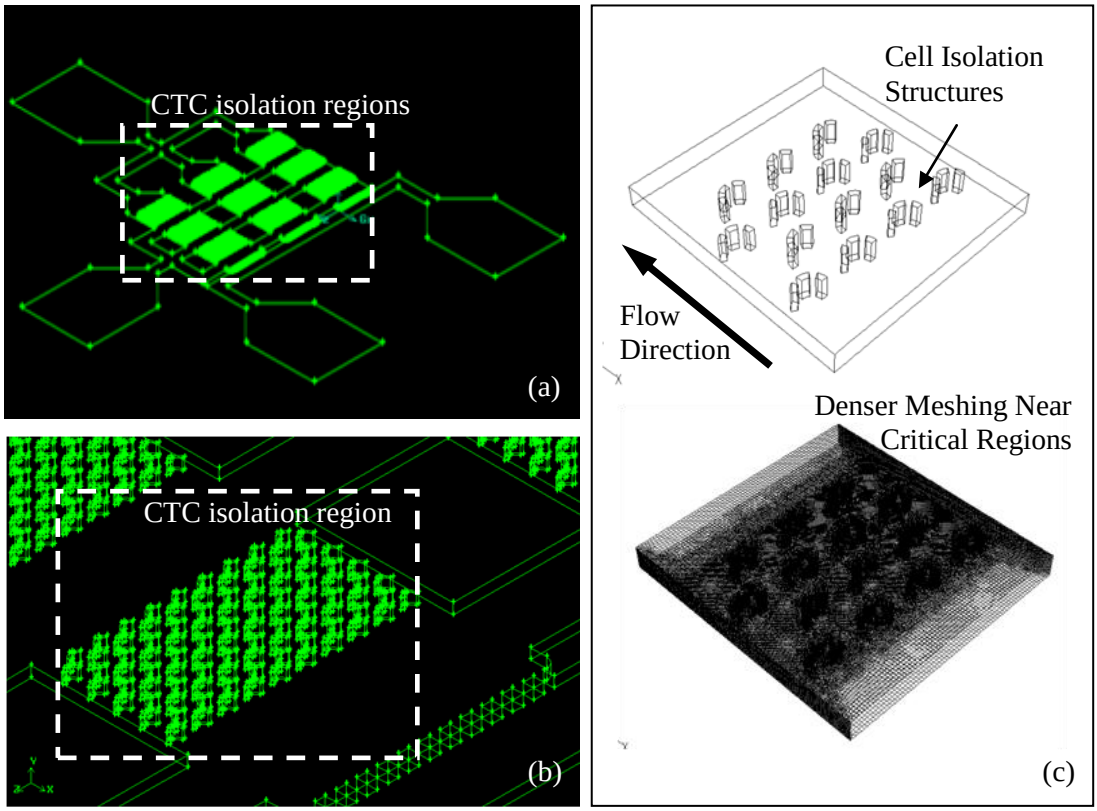

Figure 3.4 Isometric views of the computational models for the optimization of the microdevice isolation structures. (a) Overview of the device layout generated from Gambit. (b) Closeup view of the cell isolation structure compartment. (c) Simplified model for the analyses of shear stresses around isolated cells, flow profile around the isolation structures and optimization of structure positions.

was created using Gambit (Ansys Inc., Lebanon, NH, USA) and simulated using Fluent (Ansys Inc., Lebanon, NH, USA) as illustrated in figure 3.4c. The model consisted of fourteen isolation structures. An optimized mesh density of 579, 820 was used. Mesh independence was ascertained by increasing the mesh density and observing the difference in velocities to be less than 1%. Adopting a no-slip wall boundary condition and fluid properties of pure H_20 (density at 998.2 kg/m3 and viscosity 0.001003 kg/ms), the study was carried out by analyzing the velocity profiles, particle flow paths and shear

stresses at the isolation structures under different initial conditions. Boundary conditions at the inlets were determined experimentally by measuring the flow rates through the device at various operating pressures. The simulated operating pressures range from 2kPa to 20kPa. Free stream was assumed at the outlet.

This is crucial to ensure minimal damage to the isolated cells. The shear stresses and flow patterns in the microdevice at various operating conditions were extracted from the computational analysis to aid in optimizing the design and determining the operating conditions for the microdevice.

3.4 Blood Collection

Informed consent from healthy volunteers and cancer patients were taken before blood extraction, as approved by the institutional review board. Blood samples from healthy patients served as controls and were also used in spiking experiments for the characterization of the microdevice. Samples were stored in EDTA tubes (BD, Franklin Lakes, NJ, USA) prior to use and discarded after the experiment. From cancer patients, 9-10 ml of blood was extracted each time with the first 0.5-1.0 ml of blood discarded to prevent false positive responses. A total of 10 healthy volunteers and 39 cancer patients participated in the study.

3.5 Cell Culture

The cell lines of human breast adenocarcinomas (MCF-7 and MDA-MB-231), colorectal adenocarcinoma (HT29), gastric carcinomas (AGS and N87), hepatocellular (HepG2 and HuH-7) adenocarcinomas, tongue squamous carcinoma (CAL27) and pharynx squamous carcinoma (FADU) were used to characterize the efficacy of the microfluidic chip. Culturing of cells was done in 25 cm^2 tissue culture flasks (Greiner Bio-One, Frickenhausen Germany). AGS and N87 were maintained using RPMI 1640 (Sigma, St. Louis, MO, USA) while the rest used Dubelcco's Modified Eagle Medium (DMEM) (Sigma, St. Louis, MO, USA). Both culture media were supplemented with 10% fetal bovine serum (FBS) (Hyclone, Logan, UT, USA) and 1% penicillin G / streptomycin / amphotericin (Gibco, Carlsbad, CA, USA).

The culturing media were continually changed every 2 days during the maintenance of the cancer cell lines, keeping the cells with fresh media which supported their growth. Upon close to 95% confluence in the flask, the cells were sub-cultured and the protocols are as follows. Cells were washed with 1×phosphate buffered saline (PBS) to remove traces of media in the culturing flask and 2.5 ml of trypsin-EDTA (Gibco, Carlsbad, CA, USA) was added. Trypsin-EDTA aided to release the cells from the culture flask surface so that these adherent cells become suspended. The culture flask was then placed back into the incubator for 5 minutes for the release of the cells.

Confirmation of cell detaching from the surface of the flask was done optically under the inverted microscope using phase contrast imaging at 10X magnification. An additional 2.5 ml of fresh media was added into the suspended cells mixture to neutralize the effects of trypsin-EDTA. The cell suspension was then spun down into a pellet using centrifugation at the operation parameters of 1200 rpm for 5 minutes. The supernatant was removed and fresh media of 1 ml was added to resuspend the cell pellet. Depending on the cell type, a minimum seeding number was replaced into a new flask based on the recommendations from the American Type Culture Collection **(**ATCC). The rest of the cells were used for experimentations.

3.6 Cell Size Measurements and Spiked Sample Preparation

The measurement of cell diameters is important for the study, as the separation technique uses the physical characteristics of cancer cells to enrich them from peripheral blood. For cell size measurements of the cancer cell lines, the diameter was taken as an average reading obtained from images of 100 suspended cells and determined using an image processing software (NIS-Elements AR, Nikon Corp., Singapore). For the preparation of sample solutions used in the various experiments, cancer cell counting was done with a disposable hemocytometer (iN Cyto, Republic of Korea) and serial diluted to achieve the desired concentration of 100 cells per milliliter in 1×PBS.

For a more detailed description, in each experiment involving cancer cell lines, cells were grown to confluence and resuspended in culture media. A portion of the suspended cells were taken as control in the experiment and cultured normally. The rest was diluted to a concentration of approximately 100 cells per milliliter and the sample solution was injected into the device for characterizing the isolation efficiency of cancer cells. For cell viability experiments, isolated cells were retrieved by reversing the pressure differential in the system which directed the isolated cells to dislodge and flow towards to the collection point. The collected solution was centrifuged at 1200 rpm for 5 minutes with the cell pellet resuspended later in culturing media DMEM. These were then reseeded in the T25 culture flask. Their proliferative rates were compared with normal cultures which acted as controls in the experiment over a period of 5 days under normal culturing conditions.

3.7 Immunofluorescence Staining to Identify CTCs

To ascertain the isolation purity, each of the cancer cell types were added into whole blood donated from healthy donors at a concentration of approximately 100 cells per milliliter. The sample solution was further diluted with 5mM EDTA in a 1:2 ratio to reduce the sample viscosity so that it could be processed easily. Isolated cells in the microdevice were immunofluorescently stained to distinguish between cancer cells and hematopoietic cells to allow the visual examination of the isolation purity of cancer cells in the microdevice.

For the control experiment, the pre-mixed sample of blood and cancer cells (200 μl) was incubated onto a 12 mm coverslip (polylysine coated) for 30 minutes. The sample was then stained for EpCAM (1:50, Santa Cruz Biotechnology Inc., Santa Cruz, CA, USA) to identify cancer cells, CD45 (1:50, Santa Cruz Biotechnology Inc. , Santa Cruz, CA, USA) for white blood cells and 4',6-diamidino-2-phenylindole (DAPI) to permit nuclei visualization.

For staining in the microdevice, a pressure differential of 5 kPa was used to induce fluid flow into the microdevice. The value of 5 kPa was chosen as it best preserves the state of the isolated cells in the microdevice as compared to using higher pressure differentials. Lower pressure conditions would increase the processing time. Captured cells were first fixed by flowing 4% paraformaldehyde (PFA) for 30 minutes, permeabilized by 0.1% Triton X-100 in 1× PBS for 10 minutes, followed by washing with 1×PBS for 15 minutes and adding 10% goat serum to block out non-specific bindings. To identify cancer cells, 0.2 ml of EpCAM antibodies were injected for 15 minutes, left to stand for another 45 minutes and followed by washing with PBS. The procedures of antibody injection and PBS wash were repeated for the secondary antibody (1:500, goat anti-mouse AlexaFluor 568, Invitrogen Corp., Carlsbad, CA, USA). For the identification of white blood cells, 0.2 ml of fluorescein isothiocyanate (FITC) conjugated with CD45 antibodies were injected for 15 minutes, left to stand for another 45 minutes and followed by washing with PBS. Staining was completed by flowing DAPI for 15 minutes at 5 kPa followed by washing with PBS.

For the identification of CTCs in metastatic lung and nasopharyngeal cancer patients, anti-cytokeratin antibodies (CAM5.2, BD Bioscience, San Jose, CA, USA) were used. For renal cell carcinoma (RCC) patients, anti-panCytokeratin antibodies (1:50, Santa Cruz Biotechnology Inc., Santa Cruz, CA, USA) were used. A positive CTC count was defined to be cytokeratin positive, CD45 negative and DAPI positive.

3.8 Experimental Tests with Low Cancer Cell Count

We attempted to ascertain the detection limit for the setup with low cell count in sample solutions. 1-3 cell(s) were suspended in 1ml of 1×PBS and passed through the device. Isolation of individual cells from suspended state after trypsinization was done by either manually pipetting or using the fluorescence activated cell sorter (FACS, BD FACSAria II Cell Sorter, Franklin Lakes, NJ, USA) to automatically sort the cells.

For each trial with different cancer cell lines, a sample size of 10 experiments was adopted. The study was conducted with cancer cells from diverse origins to ascertain the universality of the isolation and detection technique. The device was prepared normally as illustrated in section 3.2 and freshly trypsinized cells from cultures were used. For manual picking out of cells, a drop of suspended cancer cells (highly diluted) was observed under the microscope and picked up using a pipette. This was then transferred immediately into the inlet reservoir of the system and processed by the biochip. Manual

pipetting is preferred over serial dilution as errors associated with the latter technique are enormous when dealing with low concentration of cells. FACS is another alternative which provided a faster means to obtain small number of cells per sample. The sole issue of the automated technique is the errors involved to get a single cell per vial and the correct transfer of the sample to the reservoir. Potential significant errors in sample preparation were minimized by confirming the presence of cells under the microscope before transfer to the inlet reservoir.

3.9 Blood Processing Protocol

The average blood processing time for 2 ml of blood was approximately 3.5-4.0 hrs, inclusive of a washing step to remove blood residues from the system. Detailed step by step procedures for the clinical aspect are illustrated in figure 3.5. As stipulated in the instructions from the institutional review board, informed consent was taken under no forms of undue influence. Procedures for blood extraction were described earlier in section 3.4 and blood processing was performed preferably within 24 hrs. Depending on the requirements of the clinical collaborators, a cell count and/or extraction of CTCs were performed.

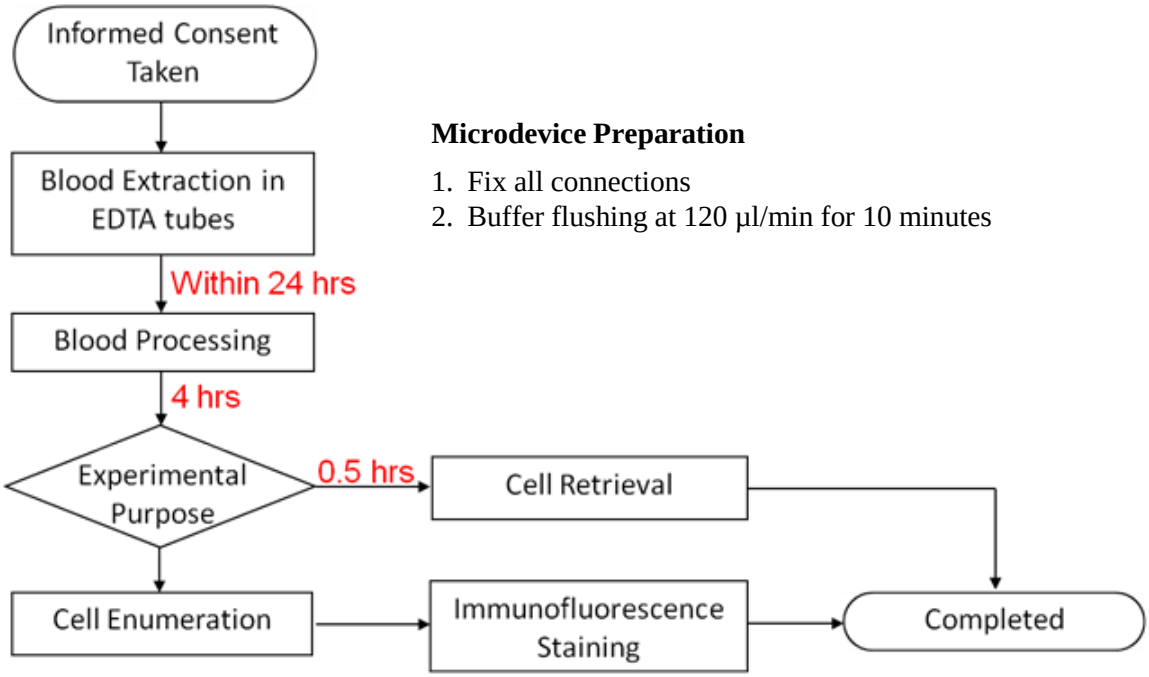

Microdevice Preparation

1. Fix all connections
2. Buffer flushing at 120 µl/min for 10 minutes

Figure 3.5 Flowchart that shows the sequence of events from requesting for informed consent to blood extraction to completing the blood processing for enumeration or recovery of isolated CTCs.

Chapter 4 Microdevice Design and Computational Fluid Dynamics Simulations

4.1 Microdevice Design

Figure 4.1 shows the experimental setup and the design of the microdevice. The microdevice is affixed to custom made fixtures as shown in figure 4.1a which aids to compact the system and allows it to be portable. In this way, the usage of reagents such as anti-bodies can be minimized, thereby saving cost. During processing, blood specimens are pressure driven into the microdevice as shown in figure 4.1b, and controlled by the computer, achieving a semi-automated operation. Blood enters the

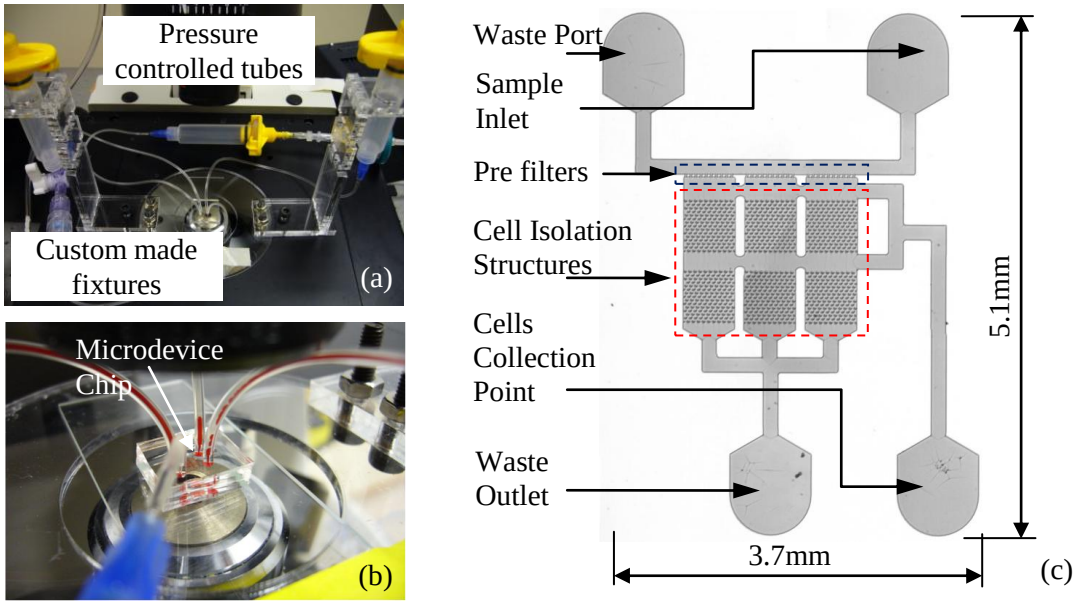

Figure 4.1 Microdevice setup and design layout. (a) Apparatus setup. (b) Microdevice chip (c) Detailed layout of the plan view of the microdevice.

microdevice via the sample inlet (figure 4.1c), pass the cell isolation region and out from the waste collection at the bottom. The cell collection and secondary waste ports are closed at this point to prevent specimens from entering and are only activated when required. A set of pre-filters shown in figure 4.1c before the isolation traps also serve to prevent large clumps or debris from clogging up the setup and are linked to the waste outlet to effectively remove debris. Clogging prevention is important to get a feasible system which is a major issue associated with devices that attempt to separate and isolate cells through direct physical means (Mohamed, McCurdy et al. 2004; Di Carlo, Wu et al. 2006; Pamme 2007). In addition, the microdevice allows for recovery of cells in the isolation traps through the cell collection point. A key advantage of using microfluidic devices lies in their laminar flow characteristics, making the profile predictable. The flow patterns inside the small enclosed volume can be easily controlled by changing the external conditions to guide the recovery of isolated cells.

The technique for the enrichment and isolation of CTCs utilizes the differences in physical characteristics of tumor cells and blood constituents. Physical parameters such as the size of cancer cells and their deformability are distinctively dissimilar (Weiss and Dimitrov 1986; Weiss 1990; Shelby, White et al. 2003; Mohamed, McCurdy et al. 2004). The design of each trap follows a crescent shape with gaps of 5μm in each of the traps as shown in figure 4.2 to ensure the exit of blood constituents due to their ability to traverse very small constrictions. Multiple arrays of these crescent-shaped isolation traps are created in the microchannel to isolate cancer cells while allowing blood constituents to sieve through (figure 4.2). In this way, larger white blood cells (WBCs) of comparable

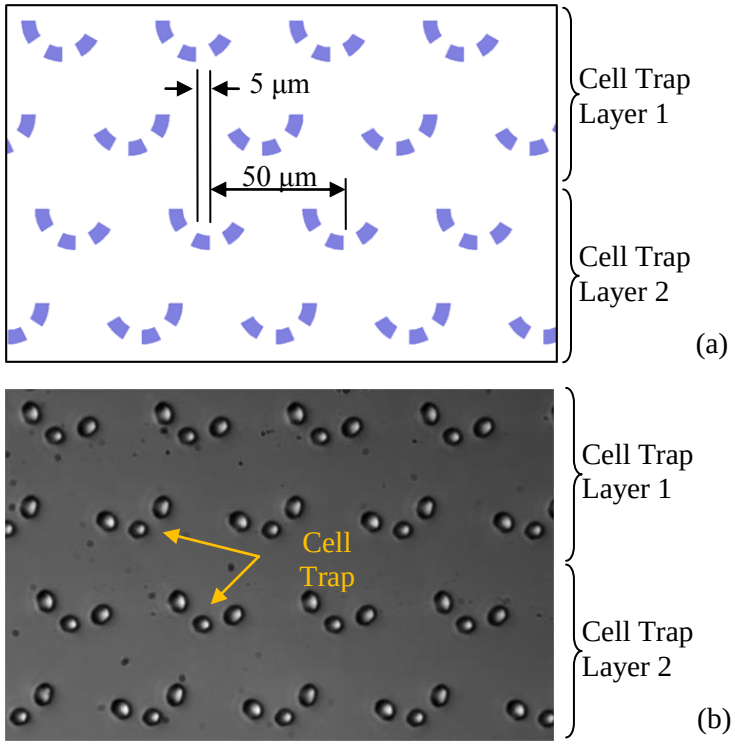

Figure 4.2 Design characteristics and view of fabricated device for CTCs trapping. (a) Cadence schematic drawing for design layout. (b) Corresponding fabricated PDMS structures

dimensions to but more deformable than cancer cells can be effectively removed and this will ensure high purity of trapped cancer cells. Each trap is positioned with a pitch of 50 µm which effectively prevents cells build-up in any particular region. In addition, each row of isolation structures is offset by 25 µm to enhance the hydrodynamic efficiency (figure 4.2). The crescent shape of the isolation trap which is alternated left and right also aid to prevent clogging and allow each structure to hold a single cell by directing incoming cells away, as the fluid resistance on the adjacent sides are smaller when the trap is occupied (further analyses are given in chapter 5).

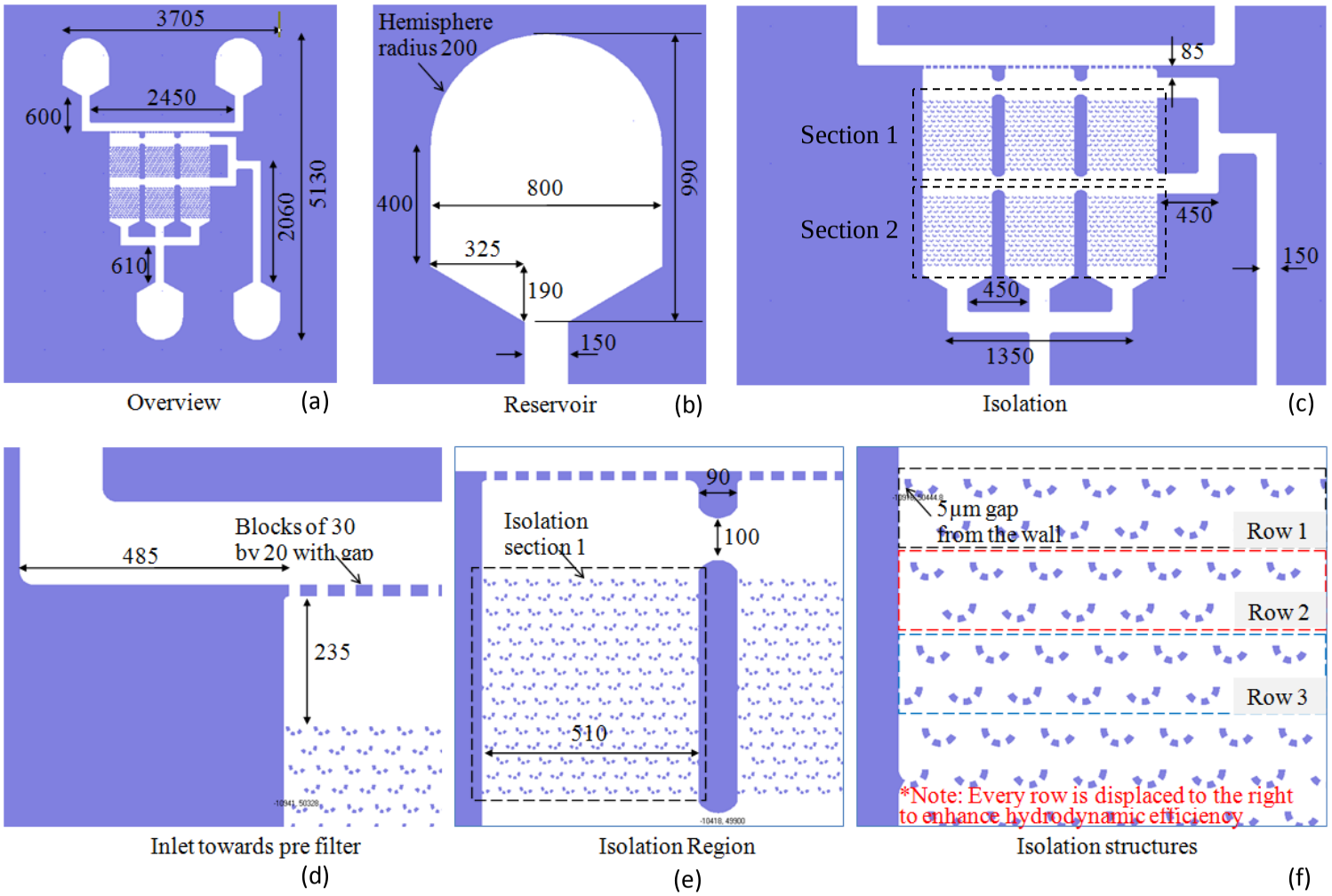

Figure 4.3 Schematic, dimensions and layout of the finalized microdevice design. (a) Overview of the microfluidic chip. (b) Fluidic connections. (c) Overview of the cell isolation region. (d) Prefilter designs and channel dimensions. (e) Close up view on one isolation compartment. (f) Design of the isolation traps to enhance isolation efficiency. All dimensions in µm.

Furthermore, the isolation traps are divided into 6 compartments as shown in figure 4.3c, spanning over two sections that facilitated the maximal retrieval of isolated cells. During cell retrieval, the rounded inverted crescent-shaped structures provide a favorable path in the opposite flow direction to enable the cells to be extracted out to the cell collection point (a thorough computational study is presented in section 4.2). It also minimized physical interactions as the laminar streamlines curves around the structures to reduce possible mechanical damage during retrieval. For each microdevice, there are a total of 900 isolation structures.

A detailed schematic of the microdevice design is presented in figure 4.3. The overall size of the microdevice spans 5.1 by 3.7 mm as shown in figure 4.3a. Reservoirs (figure 4.3b) are tapered and rounded in shape to minimize air bubbles and dead volume during the injection of fluids into the microdevice. The system is divided into various compartments and separated into 2 sections as depicted in figure 4.3c. These effectively help to maintain similar flow conditions throughout the microdevice, ensuring a smooth cell retrieval path and also aid in enumeration of isolated cells. The uniform array of isolation traps in the design as shown in figures 4.3e and 4.3f further enhance the cell counting process and will facilitate digital image analysis for process automation. To increase hydrodynamic efficiency to ensure better cell isolation, rows of isolation traps are offset from each other to make certain that cells that escape the initial traps will more likely enter traps in subsequent rows. Lastly, the design has a set of pre filters before the cell isolation region (figure 4.3d) that aims to hold debris or larger particulates and prevents them from entering the isolation traps. These large foreign matters are potential

problems if they enter the cell isolation region and will likely clog up the system. The design of the microdevice allows a direct and instantaneous means of removing large particles trapped in the pre-filters by manipulating the flow conditions and sending them out through the adjacent waste port which is connected to the left side of the inlet (figure 4.1c). Miniaturized systems are particularly susceptible to issues such as clogging and trapped bubbles which will limit its reliability (Pan 2004), and these are taken into consideration during the designing phase of the microdevice.

4.2 Design Considerations and Computational Fluid Dynamics (CFD) Simulations of Flow Parameters

The purpose of the computational study is to ascertain flow parameters as well as optimize the isolation trap design for better efficiency. A crescent shape with two 5 μm gaps was chosen as the final design for the isolation trap due to various considerations. Pillared structures which are ill designed have the tendencies for lateral collapse (figure 4.4b) (Schmid and Michel 2000). The failure modes are closely linked to the material properties of the polymer and the dimensions of the structures (Hui, Jagota et al. 2002; Sharp, Blackman et al. 2004). Equation 4.1 highlights the conditions that will result in the lateral collapse of pillared structures.

$$\frac{h}{2a}\left[\frac{4\gamma_s}{3E^*a}\right]^{1/4} < \sqrt{\frac{w}{a}} \qquad (4.1)$$

Here, $E^* \equiv E/(1 - \nu^2)$ is the plane strain modulus of the PDMS block, where E is the Young's modulus and ν is the Poisson's ratio of the material. Furthermore, γ_s is the surface energy of the material, and a, w, and h are the dimensions of the features' width, spacing, and height, respectively as shown in figure 4.4a. The reliability of the system will be highly dependent on the pillar size and the gap between them as depicted in equation 4.1. Failure can occur due to capillary forces from the retained solvents on the structures during the cleaning cycle of the PDMS before bonding, which are sufficiently large enough to cause them to contact during air or blow drying. Contact can also occur during improper peeling from the master mold. Once contact occurs, pillars may adhere to each other as a result of surface adhesive forces as shown in figure 4.4b. This renders the microdevice unusable and will have an effect on the process reliability for the

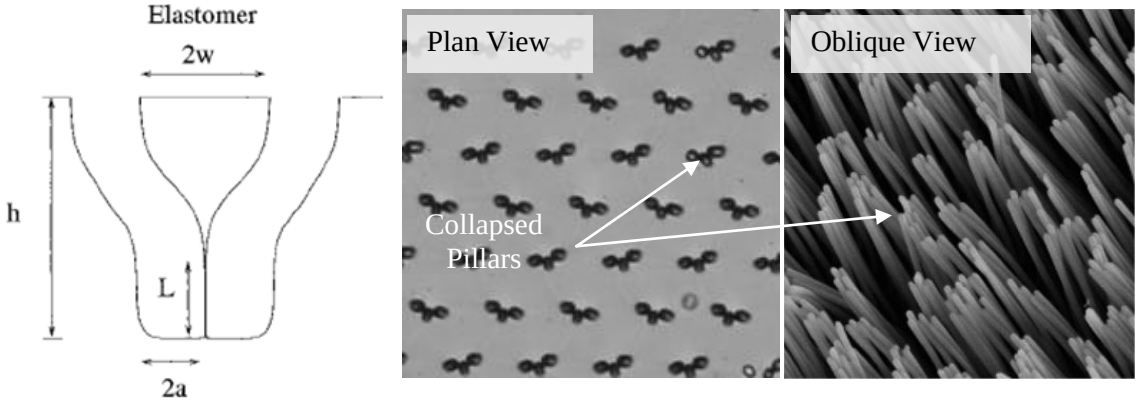

Figure 4.4 Failure modes of pillared structures. (a) Schematic of adjacent pillars sticking to each other (Hui, Jagota et al. 2002). (b) Left: Collapse of pillars in an earlier microdevice design after a washing cycle. Right: SEM image of epoxy nanopillars collapsing on its own weight (Zhang, Lo et al. 2006).

production of the biochips. The design of interest for the isolation trap has a *w/a* of 2.5 and an aspect ratio of approximately 4 for the height to width of the structures. γ_s is taken as 21.6 ergs/cm^2 for PDMS as reported by Chaudhury and Whitesides (Chaudhury and Whitesides 1991).

Another design consideration that will affect the reliability of the microdevice fabrication is the possibility for the collapse of the top surface of the PDMS which is termed roof collapse by Sharp et al. (Sharp, Blackman et al. 2004). Equation 4.2 puts forward the relationship for the event which is a direct result of unstable structures formed.

$$\frac{-4\sigma_\infty w}{\pi E^* h}\left(1+\frac{a}{w}\right)\cosh^{-1}\left[\sec\left(\frac{w\pi}{2(w+a)}\right)\right] < 1 \tag{4.2}$$

Here σ_∞ is the uniform stress applied to the top of the PDMS block, E^* is the plane strain modulus defined earlier and a, w, h are dimensional parameters depicted in figure 4.5. The instability is a direct result of the soft characteristics of the polymer and large unsupported region in the design. Emmanuel et al. (Delamarche, Bernard et al. 1997) demonstrated that if the aspect ratio is too large, the microchannels can collapse even under its own weight (Delamarche, Schmid et al. 1997). Henceforth, the considerations in the current design of the microfluidic chip minimize such large areas. This is also a key consideration for the compartmentalization of isolation traps as supporting structures can

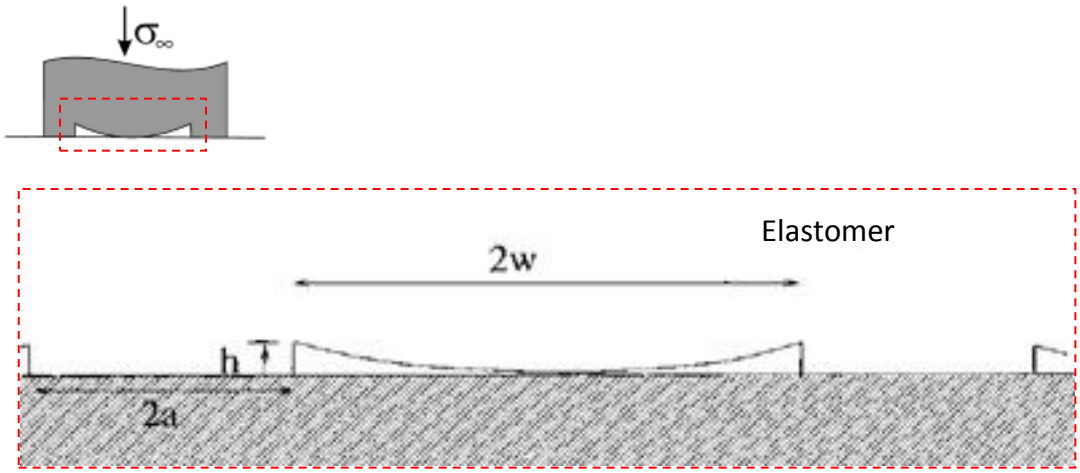

Figure 4.5 Collapse of the top surface between two supporting regions in a patterned polymer (Hui, Jagota et al. 2002; Sharp, Blackman et al. 2004).

be introduced. This facilitated a straight forward means for the scale up of the current design to allow more samples and cells to be trapped.

In order to understand the flow profile around the irregular shaped structures and ascertain minimal damage on the isolated cancer cells due to hydrodynamic forces, the fluid velocity and shear stress profiles were simulated for the operating pressure differentials applied. A 3D model was used in all the simulated conditions and the results from the mid plane of the model were extracted. Figure 4.6 depicts the velocity patterns and flow path surrounding the cell isolation structures at a maximum operating pressure of 15 kPa which is likely the critical case in this investigation. The simulated conditions during cell isolation (forward flow direction) and retrieval (backflow direction) were analyzed. This allowed a measure to estimate the effectiveness of the design before actual prototyping which is time consuming and laborious. Computational methods are also cost

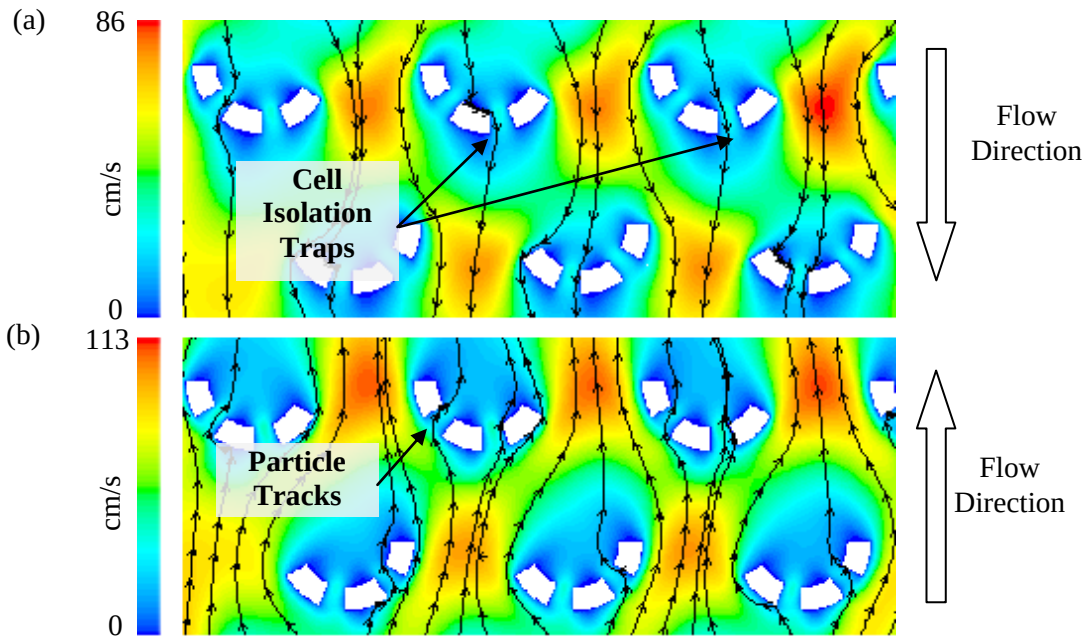

Figure 4.6 Computational analyses of the flow and shear stress around the isolation structures at the operating condition of 15 kPa. (a) Velocity profile when isolating cells taken at mid-plane (10 μm from the base) of the model. (b) Velocity profile during the retrieving of isolated cells.

effective as numerous designs can be tested by merely generating the model and running the analyses. By examining the streamlines and particle paths in the model, a gauge of the cell isolation efficiency of the setup can be predicted, assuming a perfectly rigid particle in the flow.

In isolating cancer cells (figure 4.6a), the gaps in the isolation traps facilitated the entry of the cells as shown by the path lines. These path lines were derived from simulated particles placed in the microdevice as they passed through the cell isolation regions. This was evident from the computational study showing successful interactions of free flowing cells in the flow with the isolation structures, which would ensure that cells that were

larger and less deformable to be impeded. Flow velocities were also much lower near the isolation structures which translate to lower shear stresses for an isolated cell. During the sample processing phase, the flow paths were actively changed as more of the traps were occupied. Cells began to favor adjacent sides of occupied traps (figure 4.7a) due to lower fluid resistance and the flow paths were diverted to prevent a local build up of cells. This averted the possibility of clogging in the microdevice and allowed a smooth processing of the blood specimens.

For the purpose of cell retrieval, the flow direction was reversed (figure 4.6b) by applying a positive pressure differential across the waste outlet and cell collection point. This was

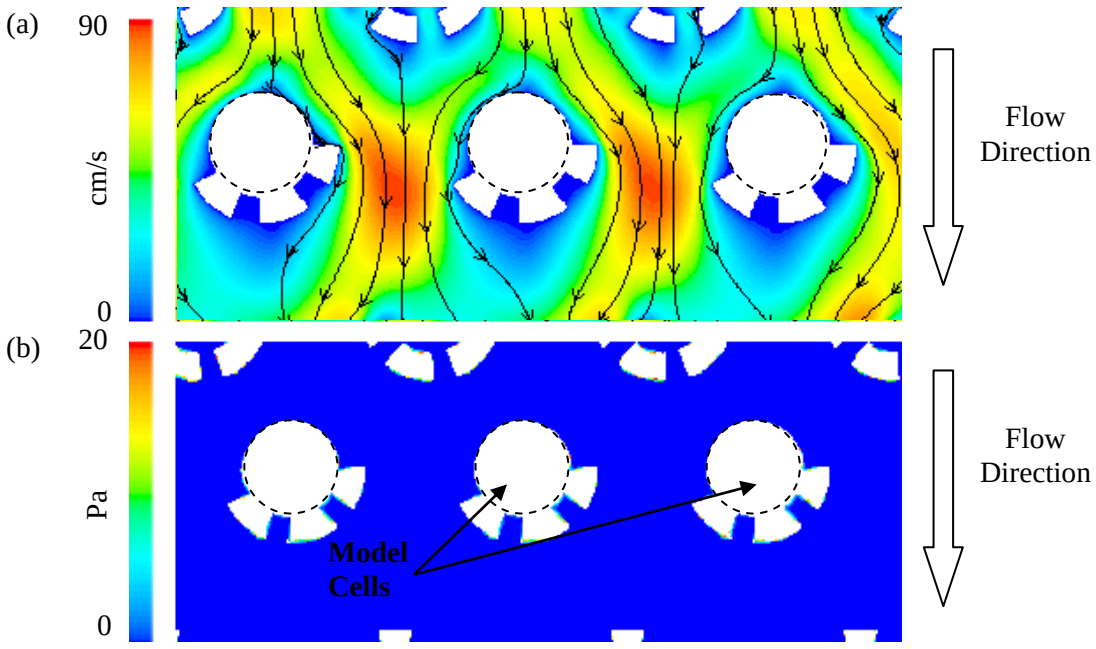

Figure 4.7 Computational analysis of the flow and shear stress around the isolation structures at the operating condition of 15 kPa when the traps are occupied. (a) Velocity profile and simulated particle tracks. (b) Shear stress acting on a spherical cell model when the cells were arrested in the isolation structures.

accomplished by switching the pressure settings on the computer controlling the pressure lines to achieve an instantaneous change in the flow conditions in the microdevice. During cell retrieval, the inverted isolation structures enabled a streamline profile around the crescent shape isolation traps as shown in figure 4.6b. Cells that were dislodged from the structures were immediately pushed towards the region in between the traps which had a lower fluid resistance. That minimized obstruction of the cells on the recovery route and was less likely to get wedged in between traps. These would ensure a high percentile of cell retrieval in the collection outlet.

In order to make certain that the system was gentle to cells in the microdevice, the average wall shear stresses on isolated cells subjected to a constant flow were characterized. This was to prevent excessive forces which could be damaging to the cells or altering many of its signal transduction responses (Papadaki and Eskin 1997; Haier, Nasralla et al. 1999; Hodgson, Kohn et al. 2000; Chang, Chang et al. 2008; Liang, Slattery et al. 2008). A simulated condition using 15 kPa is presented in figure 4.7b. It is noted that the regions of high shear stresses occur near the surface of the isolated cells and the structures. The average wall shear stresses on the cells due to the fluid flow are tabulated to establish that it did not exceed physiological conditions. Contrasting with the physiological wall shear stresses experienced in large arteries (10-70 dynes/cm^2) (Malek, Alper et al. 1999), the estimated average shear stress around the isolated cells due to the flow were much lower as shown in figure 4.8. The wall shear stress acting on an isolated cell was predicted to be between 1.8 Pa to 5.3 Pa, corresponding to 5 kPa and 15 kPa respectively for the pressure differential driving the fluid in the microdevice. This

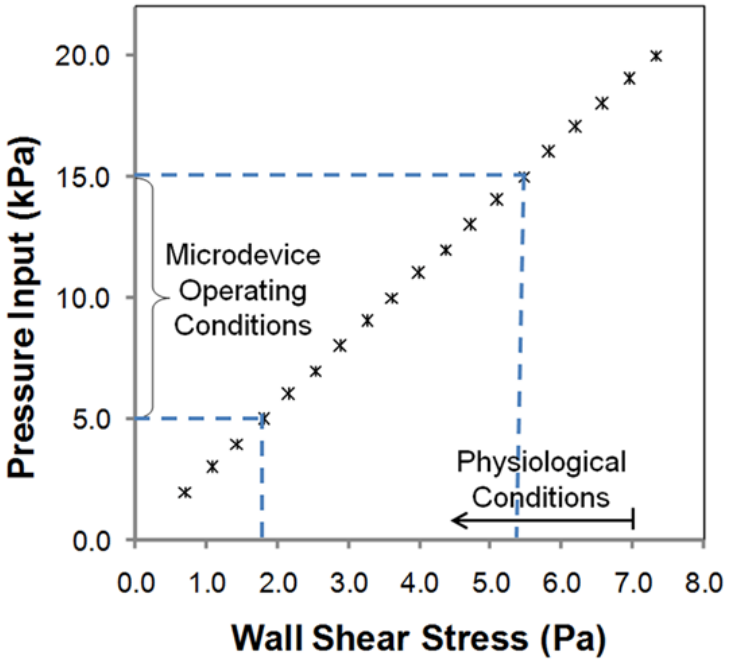

Figure 4.8 Effects of input pressure on the estimated wall shear stress of an isolation cell using simulation studies.

indicated a low possibility that cells would be affected as a result of the interactions of the flow and the small enclosed volume in the system. Cell integrity was likely to be maintained whilst in the microdevice, providing the opportunities to examine and analyze these rare cells in peripheral blood to understand the disease better.

4.3 Feasibility Studies

The concept of cell isolation using physical characteristics of cancer cells on a microfluidic device was tested with a macro setup by means of ideal rigid beads of 45 µm

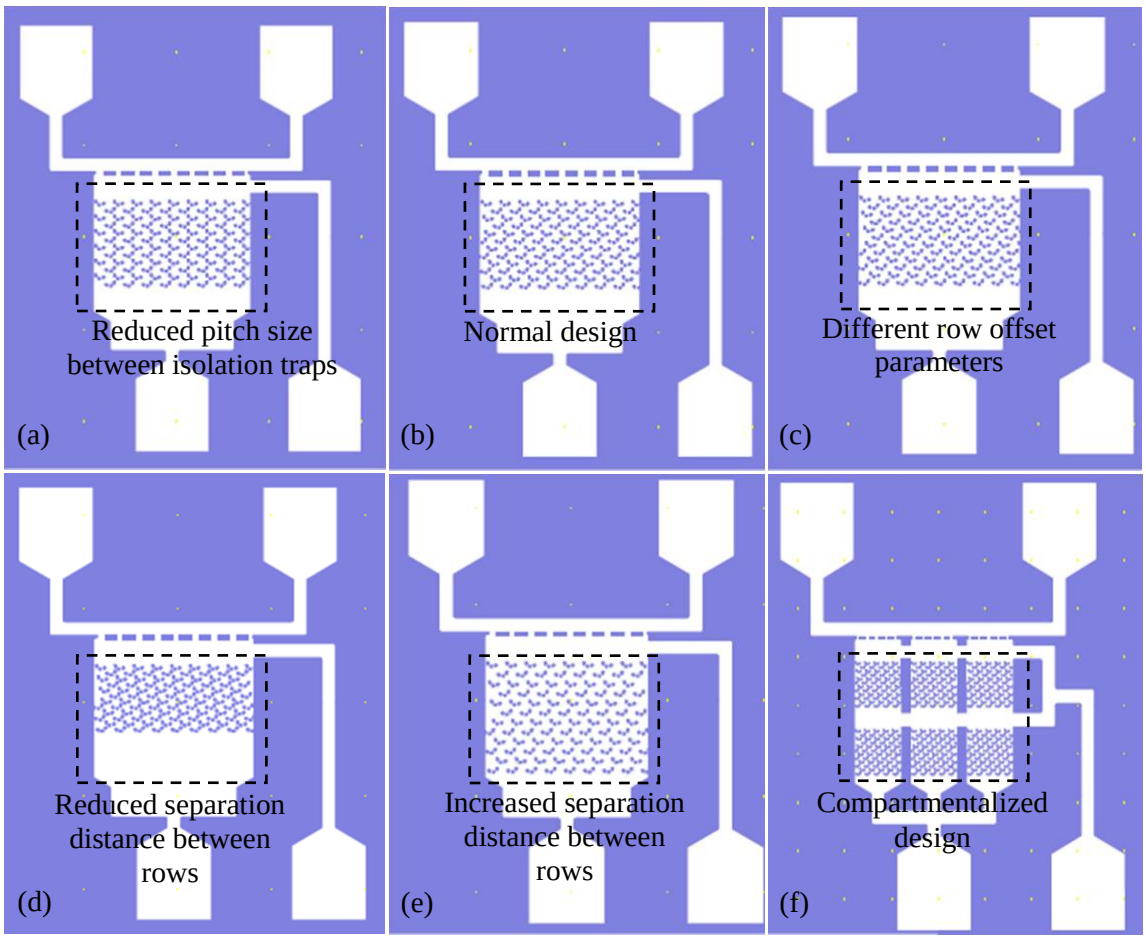

Figure 4.9 Feasibility studies designs. (a-e) Evaluation of the placement of isolation traps and traps density per unit area. (f) Evaluation of compartmentalized design.

(Polystyrene Polybead® Microspheres, Polysciences Inc., Warrington, PA, USA). This was to ascertain that the design parameters used in the simulations were effective. Furthermore, the trials were used to confirm several other design considerations such as reduced pitch size between isolation traps, reduced row separation distances and ensure failures modes like lateral collapse of pillars and roof collapse of top PDMS surface do not occur. The various experimental design layouts extracted from the photolithography mask drawing are shown in figure 4.9. Six different configurations were tested for its

isolation efficiency using rigid polystyrene beads that simulated the presence of cells in the samples. The size of the isolation traps were scaled up by a factor of 2 from the optimal layout simulated in the computational analyses and designed to be suitable to hold particles between 40-55 μm in diameter. This is analogous to the use of dimensionless analysis to predict the responses. A plastic mask (Infinite Graphics Inc., Singapore) was employed in the photolithographic process given that the features sizes of the trial designs were significantly larger with critical dimensions of 10 μm. Fabrication of the master mold and casting of PDMS microdevices were similar to the steps described in section 3.1. The sole difference was in the use of SU 8 2050 instead of SU 8 2025 which was recommended by the manufacturer for a more uniform photoresist layer of 50 μm.

A PDMS replica mold for testing the reduced separation distance between isolation rows (figure 4.9d) is shown in figure 4.10a. The design consisted of a single chamber with 102 isolation traps set out in a uniform array. Six different arrangements of the microdevice were put forward in the trial to confirm the simulation results experimentally. Standardized samples with concentration of approximately 1000 microbeads per milliliter of 1×PBS solution were used. Figure 4.10b shows the experimental results from one of the designs in a typical run. Within 20 minutes, almost all the isolation traps were occupied which indicated a fast loading capacity in the microdevice and likely an effective means to hold cells which were stiffer and significantly larger than the gap size in the crescent shape traps. It was also observed that single bead trappings were prevalent

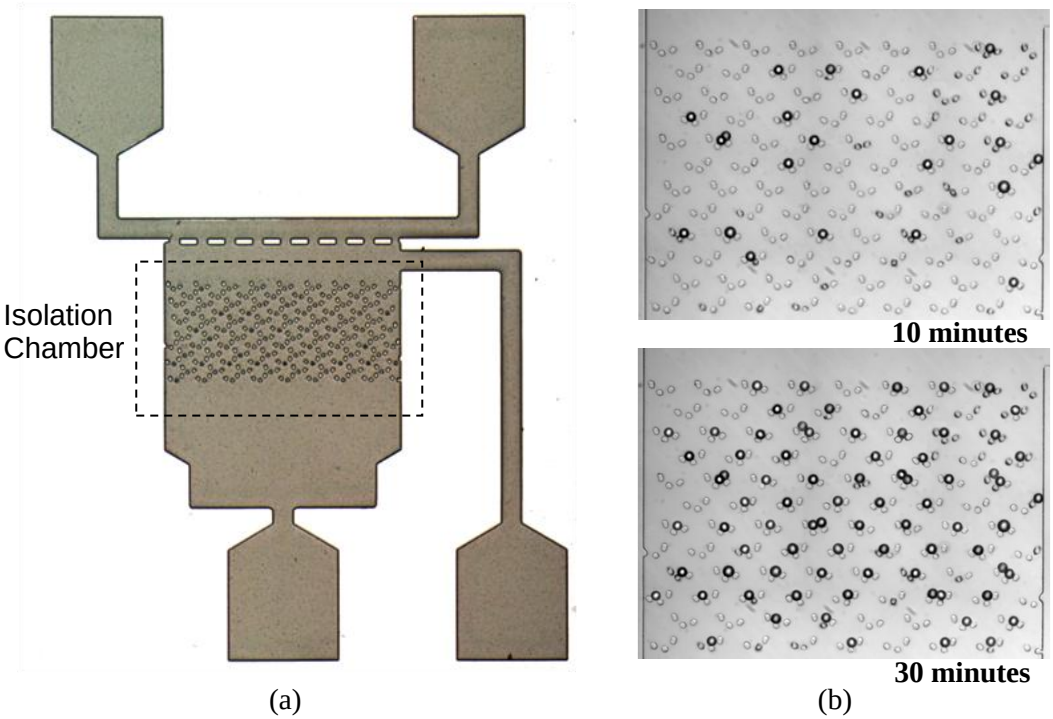

Figure 4.10 Feasibility study design using a scale-up version of the microdevice. (a) SU 8 master mold for PDMS replica molding. (b) Micro beads loading showing high isolation efficiency and mostly single bead trapping.

in all the tests conducted for this particular design as demonstrated in figure 4.10b. This is coherent with the design considerations set out in section 4.1 that the occupied isolation traps direct incoming particles to subsequent traps which would prevent a local build up of particles and clog up the system. It was also evident from the study that a large blood sample volume could be processed on this platform with minimal risk of failure due to obstruction of blood constituents in the microdevice. The single bead per trap is also useful to aid enumeration and analyses, as compared to alternative techniques which have isolated cells in clusters in physical traps or far apart on anti-body coated substrates (Mohamed, Turner et al. 2007; Nagrath, Sequist et al. 2007; Mohamed, Murray

et al. 2009; Kuo, Zhao et al. 2010). Having cells in clusters make distinction and exact counting difficult, while cells that are too far apart are laborious during counting and risk increased human random errors. Furthermore, a general observation from the study showed that initial capture rates were high when all or most of the isolation traps were unoccupied. There were significant bead losses when approximately 50% of the traps were engaged. This was a consequence of diverting incoming particles to the next isolation row when the earlier isolation traps were occupied. As more of the traps became taken, it increased the probability of a non engagement and allowed the bead to be washed away.

In terms of fabrication issues, no roof collapsed were encountered which indicated that the design was overall stable. There was however slight lateral collapses of the crescent shape isolation traps which occurred during bonding when a force was applied to form a complete seal of the PDMS block to a glass slide after the oxygen plasma treatment. The

Table 4.1 Microdevice isolation efficiency using 45μm rigid beads in the feasibility experiments

No	Design	Sample Size	Efficiency (%)	Standard Error (%)
1	Design 1	10	65.24	0.34
2	Design 2	9	75.24	0.54
3	Design 3	10	68.28	0.27
4	Design 4	10	77.67	0.67
5	Design 5	10	78.70	0.55
6	Design 6	10	70.75	0.53

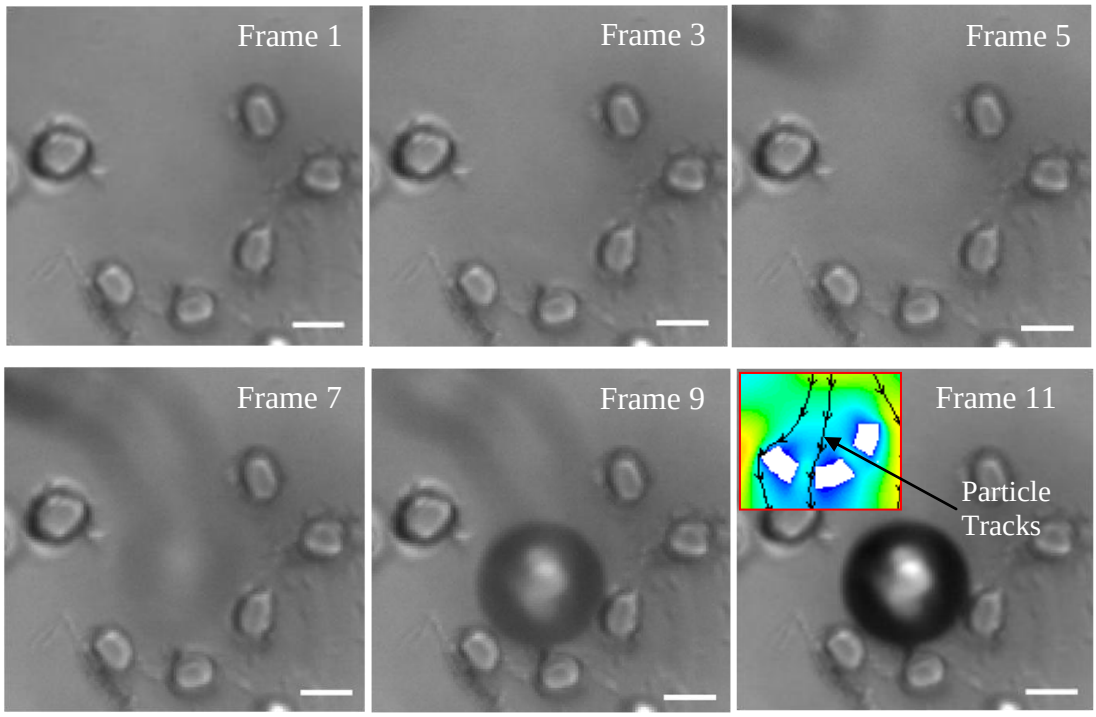

Figure 4.11 Feasibility study using 45 µm beads. Image captured at approximately 100fps. Scale bar represents 20 µm.

problem was overcome by controlling the applied force after numerous practices. Table 4.1 summarizes the results for the isolation efficiency of rigid beads of 45 µm in the microdevice for all the trial designs. The choice of using the 45 µm beads is due to the design of the traps that ensured an optimal fitting of the bead in the crescent well. The experimental spilt considered various placement issues of the isolation traps as well as to ascertain the stability in a compartmentalized design. A maximum isolation efficiency of 78.7% was attained from the designs with the lowest being 65.2%. Using a Student's t test, the isolation efficiency obtained from design 5 was significantly higher than designs 1 and 3, with $p < 0.05$ but no significant conclusions with designs 2 and 4. However, it was observed that there was a higher chance of a localized build-up of beads when the separation distances between the rows became compacted due to the difficulties of the

rigid beads to move in the much confined region, which ruled out the selection of design 4. With no statistical significance between designs 2 and 5, the selection criteria reviewed the space requirements and decided on design 2 as it conserved about 10% less space. Results from design 6 were also promising that will enable scaling up of the platform by simply stacking or arranging in uniform array for each of the isolation chambers into a single microdevice. This will speed up sample processing or cater for the isolation of more cells which may be present. An illustration of the isolation route is depicted in figure 4.11 which showed a smooth entry of the bead into the trapping structures and was consistent with the particle tracks derived from simulation studies.

It was estimated from computational analyses that the wall shear stresses acting on the particles were within the physiological range of forces experienced by blood cells in circulation. Confirmation tests were conducted by analyzing the behavior of cancer cells in the microdevice which provided an instantaneous means of verifying the cell integrity. It was observed that cancer cells were able to adhere and spread near the isolation structures. Trypan blue exclusion tests established that the isolated cells were viable and most of the cells remain unstained. Figure 4.12 shows a 2 day culture of the isolated cells directly in the microdevice. MCF-7 was used in the experiments and pressure driven into the microdevice. The flow was left stationary for approximately 1 hr for cells to attach to the surface before a gentle washing cycle using culturing media to remove any residue. A control with normal culture was used to compare the proliferation rate of the cells. The microdevice and the control culture were then left in a CO_2 rich (5%) incubator (Thermo

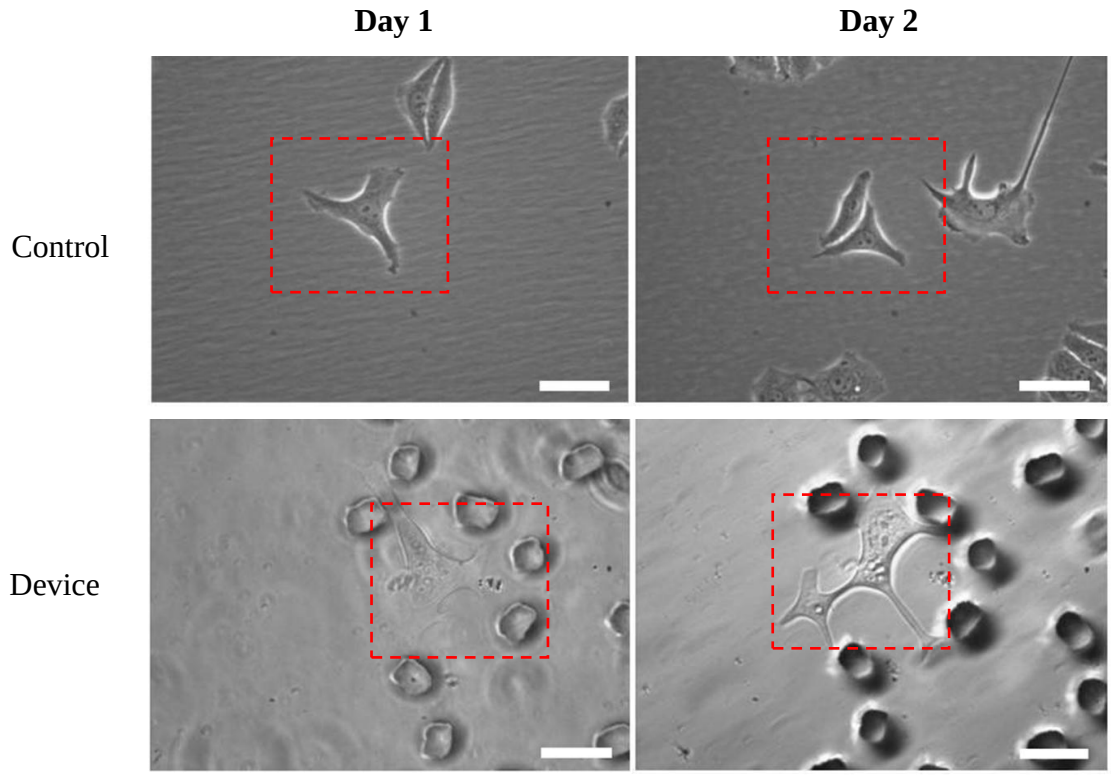

Figure 4.12 Cell integrity after the isolation process in the microdevice. Control experiments are obtained from normal cultures and proliferation of cancer cells are assessed in the microdevice. Scale bar represent 20 µm.

Electric Corp., Singapore) overnight. From figure 4.12, it is shown that proliferation of the cancer cells are not hindered after passing through the microdevice. The outcome indicated that the system was gentle during the process of cell isolation and less likely to damage the cells with the pillars in the microdevice. To sum up, the experiments depicted the bio compatibility of the biochip and that negligible external forces are exerted on these cells in the device.

In brief, the feasibility studies demonstrated the successful and efficient isolation of rigid polystyrene beads. The isolation trap arrangement presented in design 2 (figure 4.9b) was

selected as the finalized configuration for its advantages of lesser space requirements and being effective to isolate the beads. The investigation also verified certain design considerations such as achieving mostly single bead trapping without clogging the system. The platform was also determined to be gentle to cells during sample processing which is crucial in CTC analyses.

Chapter 5 Microdevice Characterization

The characterization of the microdevice is of paramount importance to achieve the optimal setting for CTC isolation. Earlier discussions presented the design and feasibility studies of using a microfluidic device for this function. To sum up what has been put forward thus far, the system utilizes the biorheological differences in the cell size and deformability of cancer cells to achieve an effective separation.

For blood processing operations, the sample is pressure driven through the system from the sample inlet past the cell traps and the effluence is collected in the waste outlet. The pressure control allows instantaneous manipulation of the fluid conditions in the microdevice. Each of the microdevices has 900 crescent shaped isolation structures formed into a uniform array where cancer cells being generally larger and stiffer than blood cells will be retained. The design of the traps also prevents build up of cells when the structures are occupied, unlike most direct filtration methods and allows processing of large sample volumes. Due to the rarity of CTCs in peripheral blood, processing of larger volumes of samples is desired and the laminar flow around the cell traps channel cells away to prevent clogging due to lower fluid resistance on the adjacent sides. In addition, each trap is likely to hold only a single cell and this simplifies enumeration either optically or through an image processing software.

The clinical benefits of enumerating CTCs in peripheral blood have been widely reported (Beitsch and Clifford 2000; Gogas, Kefala et al. 2002; Hoon 2004; Budd, Cristofanilli et

al. 2006; Hayes, Cristofanilli et al. 2006; Cristofanilli, Broglio et al. 2007). This method is also minimally invasive as compared to traditional biopsies. The number of CTCs in blood is directly associated with the disease progression and can help in evaluating cancer treatment efficacy (Nole, Munzone et al. 2007). Thus, it is important to have a high cancer cell isolation efficiency for the microdevice to count these rare cells in blood specimens accurately. Our approach draws mainly upon the highly deformable nature of erythrocytes (Shelby, White et al. 2003) and leukocytes (Liang, Liu et al. 2005) that enable these cells to traverse capillaries as small as 2-5 μm whose cell diameters can range from 8 to 25 μm. On the other hand, cancer cells are more likely to be arrested in capillaries of similar dimensions (Weiss and Dimitrov 1984). Henceforth, the gaps in the isolation traps will hold cancer cells while allowing blood constituents to pass through with ease.

5.1 Cell Size Measurement

From table 5.1 which included measurements taken from cancer cell lines of various origins, it was noted that there existed a diverse range in terms of the dimensions of these cells. Figure 5.1 shows the cells that were just resuspended after cell culture which clearly highlighted the differences. Furthermore, it was observed that the morphology and appearances of these cells differs. At the molecular level, the genetic makeup of these cells is largely dissimilar due to different mutations which can explain their different behaviors. Hence the heterogeneity of the disease is an important factor to consider in the

Table 5.1 Measurement of the cell size of cancer cell lines

Cancer Cell Line	Cancer Origin	Sample Size	Average Diameter (μm)	Standard Deviation (μm)
MCF-7	Breast adenocarcinoma	300	15.7	1.8
MDA-MB-231	Breast adenocarcinoma	300	16.6	2.8
HT-29	Colorectal adenocarcinoma	100	15.5	1.3
AGS	Gastric carcinoma	300	14.0	1.8
N87	Gastric carcinoma	300	14.2	1.8
HepG2	Hepatocellular carcinoma	100	16.9	1.7
HuH7	Hepatocellular carcinoma	100	19.3	2.9
CAL27	Tongue squamous carcinoma	100	15.0	1.7
FADU	Pharynx squamous carcinoma	100	16.9	2.1

* Measurements of cell size was done with NIS Elements software using 3 points to estimate the curvature of the cells

study. For the current work, we aim to demonstrate the use of a microfluidic device using purely physical differences of cancer cells to isolate them from blood specimens. It is hypothesized that the technique is versatile to handle tumor cells from diverse origins though the molecular aspects of these cells are heterogeneous. The isolation rate and capture purity are of interest as these parameters dictates the accuracy of the tests which is to be associated to the state of health of the patient. Sensitivity of the microdevice to small numbers of tumor cells in peripheral blood is of paramount importance as well in the tests and we hope also to show the detection limit of the proposed platform.

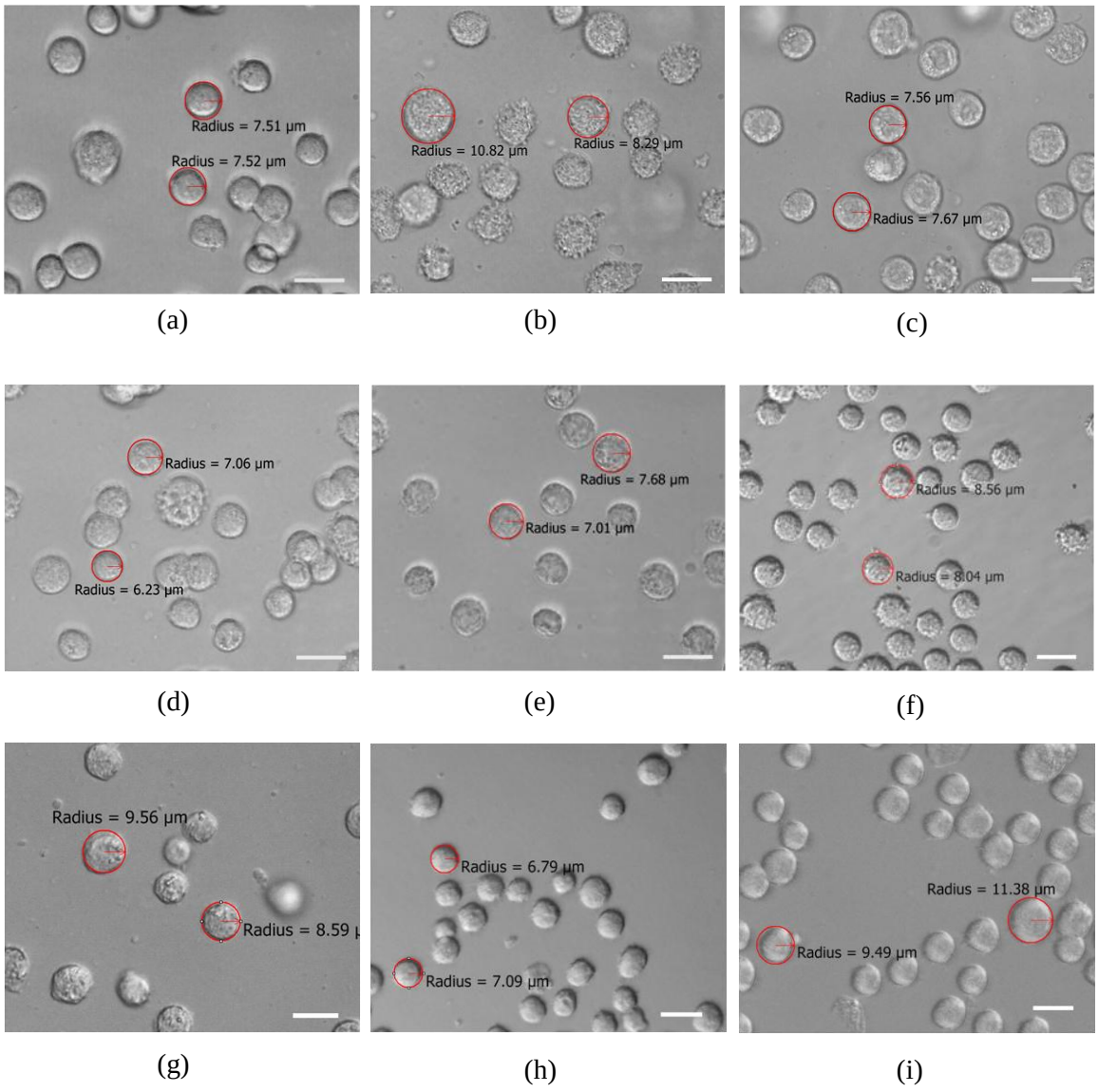

Figure 5.1 Cancer cells in suspension for measurements of cell diameters. (a) MCF-7. (b) MDA-MB-231. (c) HT-29. (d) AGS. (e) N87. (f) HepG2. (g) HuH7. (h) CAL27. (i) FADU. Scale bar represents 20 µm

5.2 Cancer Cell Isolation Efficiency

For characterizing the cell isolation efficiency, low concentration of cancer cells (100 cells per milliliter) spiked in 1×PBS is injected into the microdevice at various pressure differentials. Small numbers of cancer cells in the sample solution mimic the rarity of CTCs in peripheral blood. By visually counting the number of trapped and escaped cancer cells, the efficiency of tumor cell capture can be determined using equation 5.1 where a ratio of the trapped cells are taken, over the total number of cells that enters the microdevice. Visual inspection is preferred to minimize random errors that might occur during serial dilution leading to discrepancies in cell concentration in the solution. This is especially critical when dilution is performed to obtained very low cell counts and visual means will aid to circumvent the problem as all the cells that enter the microdevice is actively monitored.

$$\underset{\text{Efficiency}}{\text{Isolation}}(\%) = \frac{\text{Trapped Cells}}{\text{Trapped Cells} + \text{Escaped Cells}} \times 100\% \tag{5.1}$$

The main factor affecting cell isolation efficiency is the pressure applied as the input values directly alters the flow conditions in the microdevice. With a larger applied pressure differential to drive the sample solution, flow rates will increase leading to a proportionate increase of forces acting on the cells. This might induce a large

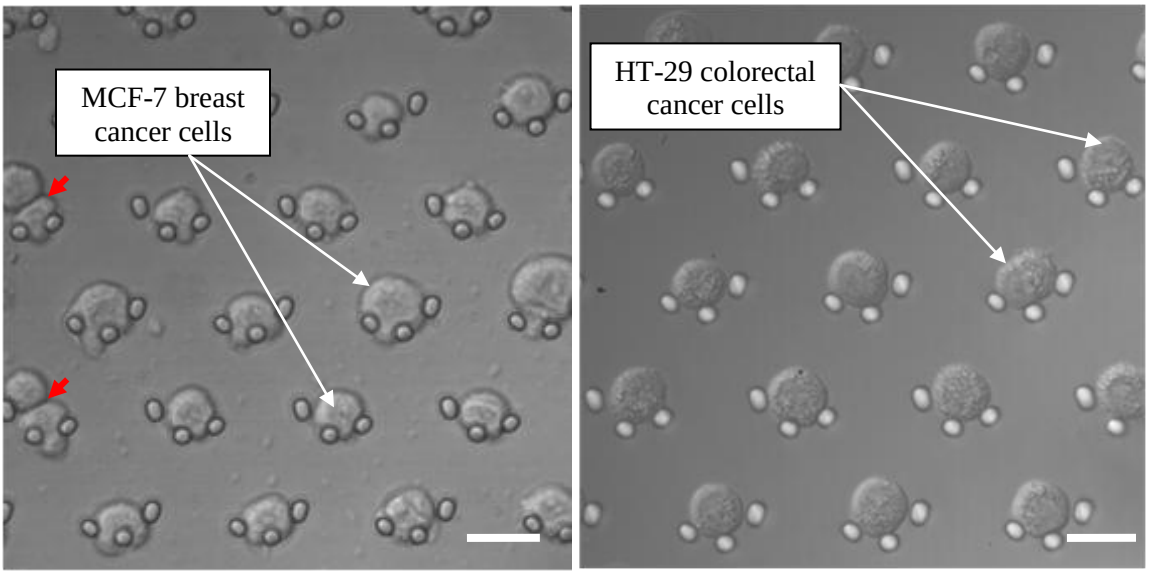

(a) (b)

Figure 5.2 Cancer cells isolation in the microdevice which presented mostly single cell per trap. (a) MCF-7 (breast adenocarcinoma). Red arrows indicated regions where more than 1 cell was trapped. (b) HT-29 (colorectal adenocarcinoma). Scale bar represents 20 μm.

deformation on cells to be able to pass through the gaps in the crescent shaped wells which will compromise on the efficiency for cell capture. Although, higher flow rates meant lesser sample processing time, the larger shear forces on the cells are undesirable as they can cause cell behaviour modifications due to mechanical activated signal pathways or cell death (Chang, Chang et al. 2008). In this investigation, the selected pressure differentials included 5 kPa, 10 kPa and 15 kPa which are comparable to physiological conditions and verified using computational analyses in section 4.2.

Figure 5.2 shows the successful arrest of MCF-7 breast cancer cells and HT-29 colorectal adenocarcinoma in the isolation structures. Consistent with the observations from the feasibility tests, mostly single cells were loaded in each of the traps. It was also noted that

despite the diverse range of dimensions existed between different cell lines or even within the same cell line, the platform was able to hold them in place. The single or doublet cells arrested in each isolation trap facilitated cell counting with ease. For traps holding more than 1 cell, they were generally observed to be of smaller diameters than others as depicted in figure 5.2a with the red arrows. The outcome is expected as excess space with small cells in the traps is able to accommodate another. It can be resolved by tuning the trap size to suit the dimensions of the tested sample. This aspect is advantageous for the system as controlling the size of the traps can potentially allow the microdevice to be used for a wide variety of cells and applications in single cell studies. In addition, the experiments demonstrated that these cancer cell lines differ significantly in their ability to deform as well. For instance, MCF-7 (figure 5.2a) cells in the traps showed certain amount of deformation into the gaps in each of the cell trap that were meant to allow blood constituents to pass through, while HT-29 cells (figure 5.2b) remained perfectly spherical in the isolation structures under the same flow conditions. This is indicative of dissimilar physical characteristics and that HT-29 is stiffer than MCF-7 cells.

Using the computer to control and maintain the pressure differential in the system, the quantitative analyses from comparing cell isolation efficiencies at various pressure settings is plotted in figure 5.3. In the current study, 9 dissimilar cell lines from 6 different cancer types were used to ascertain the microdevice characteristics. A total of 264 experimental runs were performed for the entire investigation, showing an approximate effective isolation rate of 80% for the tested samples, at an operating

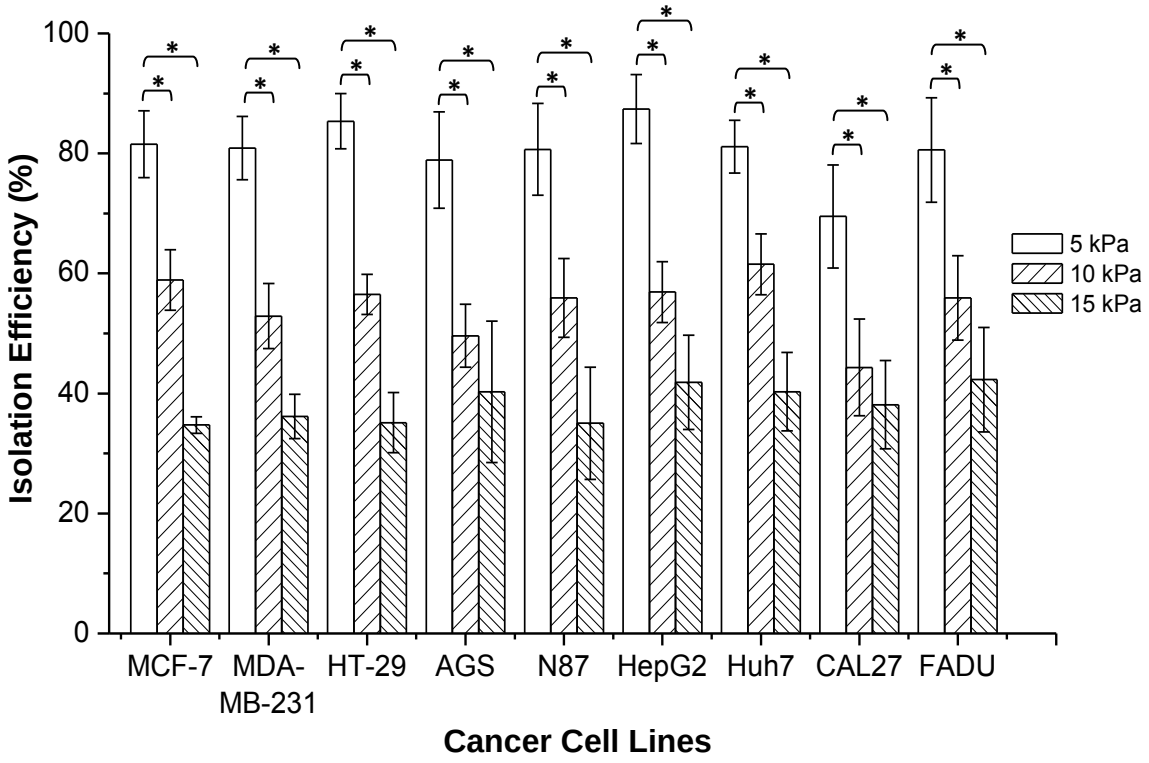

Figure 5.3 Cancer cell isolation efficiency for various cancer cell lines in the microdevice over a range of operating pressure applied. Hypothesis testing was performed comparing the mean isolation efficiency at 5 kPa to 10 kPa and 15 kPa. * refers to $p < 0.01$ with a Student's t-test

condition of 5 kPa. The Student's t-test verifies that isolation efficiencies at 5 kPa are significantly higher ($p<0.01$) for all 3 samples than at higher pressure inputs as illustrated in figure 5.3. It was also noticed that a downward trend was experienced as the pressure differential increased. The reduction in cell capture efficiency can be accounted for by the dislodgement of the arrested cells due to increased hydrodynamic forces acting on these cells at higher pressure differentials or the forcing of smaller cells through the gaps in the crescent traps. At the pressure setting of 5 kPa, the microdevice was capable of

processing samples at 0.71 ml/hr with a high isolation efficiency needed for an accurate diagnosis. A typical experiment with the isolation of CAL27 is shown in figure 5.4.

From the time sequence images extracted from the high speed camera (figure 5.4), it can be clearly observed for cells that try to enter an occupied trap will be pushed downwards to engage an empty one. This mechanism allowed single cell trapping to occur and prevented a local build-up of cells that might clog up the system.

Other leading techniques to enrich cancer cells from peripheral blood have efficiency ranging from 20% to 90% (Allard, Matera et al. 2004; Lara, Tong et al. 2004; Balic, Dandachi et al. 2005). However, there are also numerous restrictions and complex preparation procedures. For example, there is limited purity when detecting low concentrations of CTCs (Smirnov, Zweitzig et al. 2005) in peripheral blood and various preparatory steps such as centrifugation, incubation and functional modifications which can be tedious and time consuming. The proposed microdevice is comparable to other

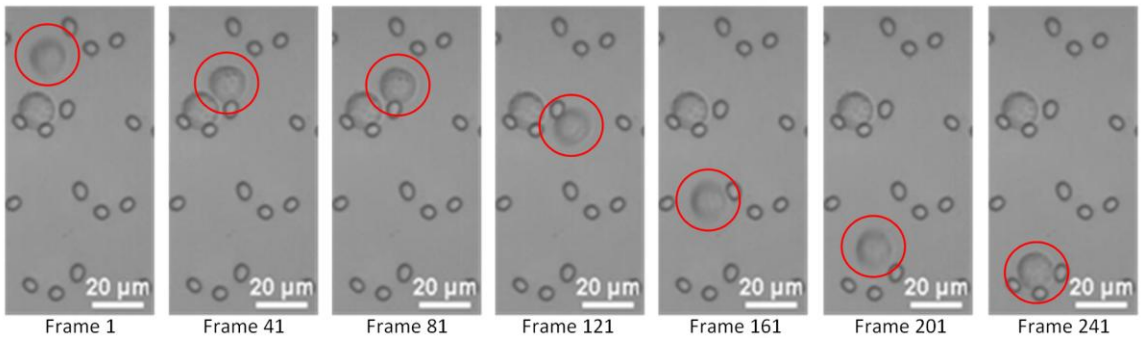

Figure 5.4 Time sequence images showing the capture of a cancer cell. The arrangement of the cell traps enables the capture of cells that circumvent occupied traps and prevents clogging in the microdevice. Images taken with a high speed camera at 1000fps.

leading biochemical techniques in terms cancer cell enumeration from blood and is done without any functional modifications. The results favor the lower input pressure of 5 kPa to effectively isolate cancer cells given the Student's t-test with a significance level of 0.01 confirmed that isolation efficiencies at 5 kPa were significantly higher than other operating pressures for all the samples. Single cell trapping is also affirmed in our studies and that the system proves to be suitable to process large sample volume without clogging.

5.3 Cancer Cell Isolation Purity

The cell isolation efficiencies of the microdevice were performed with pure spiked samples of cancer cells in 1×PBS to minimize random errors that would occur in the presence of blood. With blood samples, it was difficult to count the number of escaped cancer cells due to the presence of large amounts of blood constituents. Henceforth, the cell isolation efficiency and the capture purity were characterized in separate experiments.

With cancer cells spiked into blood samples from healthy volunteers, the quantitative analyses for the isolation purity could be determined. Spiking concentrations of 100 cancer cells per millilitre of blood which was further diluted in 5mM EDTA buffer (1:2) were used in all the tests. EDTA buffer was used in place of PBS to prevent blood coagulation. Standard staining protocols were then followed in the identification of cancer cells from the isolated cell population in the microdevice.

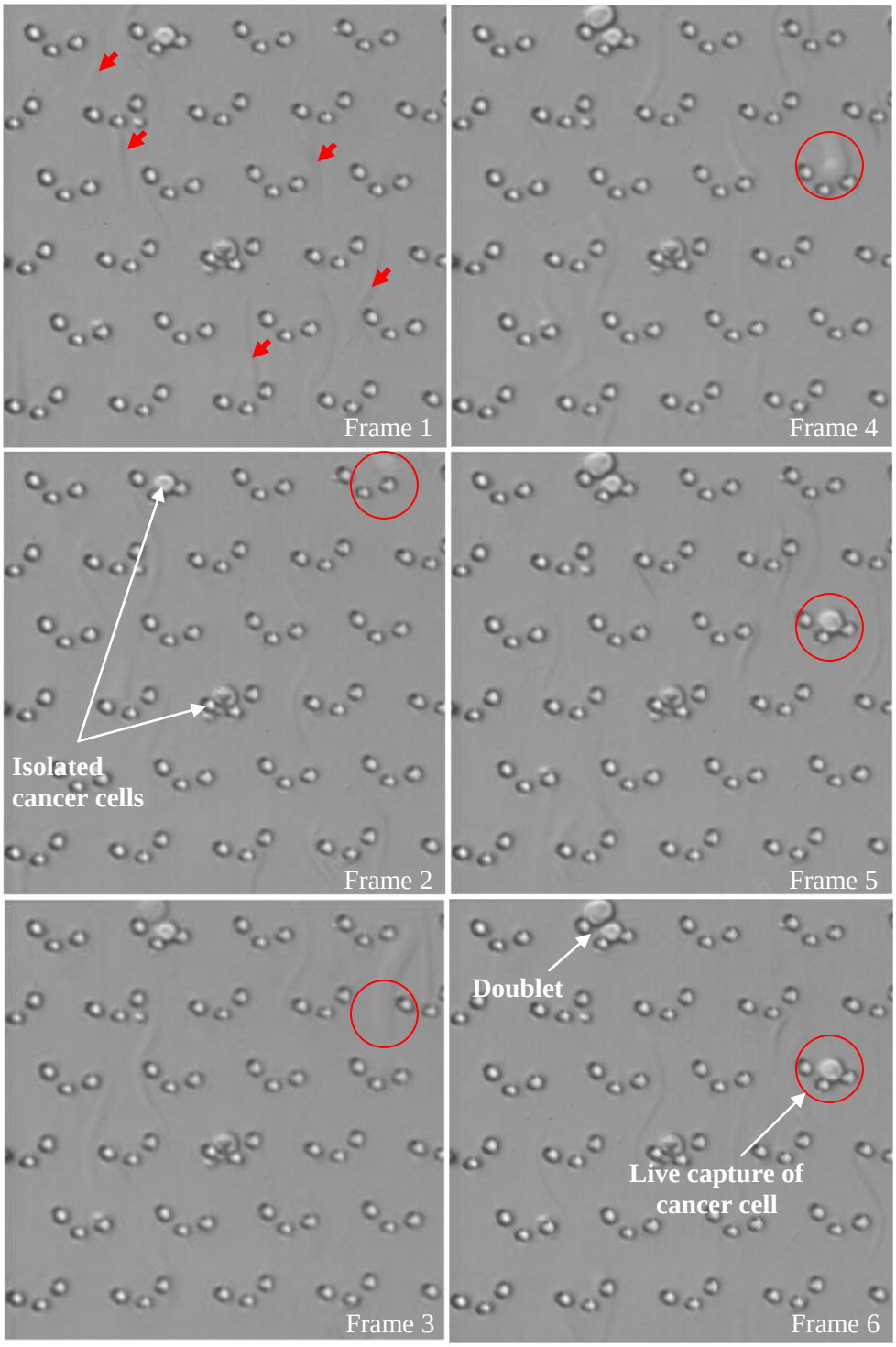

Figure 5.5 Live visualization of the isolation of MCF-7 breast cancer cells in a spiked blood sample of approximately 1% hematocrit. Red arrows indicate the passage of blood cells in the microdevice. Image taken at 60 fps.

Figure 5.5 shows the live capturing process of MCF-7 breast cancer cells spiked in a 1% hematocrit blood sample taken at the input condition of 5 kPa. The blood sample was deliberately diluted from 50% hematocrit to 1% to permit clear visualization for demonstration purposes and spiked samples used in the characterization of the capture purity of cancer cells in the system was performed with approximately 15% hematocrit as stated in the preparation process in section 3.7. From the images extracted off the live video capture, it was observed that blood constituents passed through the structures with ease given their highly deformable nature. It was also evident that a build-up of blood cells due to the presence of the structures in the flow path was negligible and processing of 3 ml of sample solution was smooth. As denoted earlier and observed from the experiments, the cell traps held mostly single cells and was occasionally having a doublet, were coherent with the earlier tests for the isolation efficiency of the microdevice. This is also shown in figure 5.5 where the trap with an initial occupied small cell allowed the entry of another cell.

For the isolation purity characterization, in order to differentiate between hematologic and cancer cells, immuno-fluorescence staining of the isolated cells was carried out. It is reported that the EpCAM is over-expressed in human carcinoma (Osta, Chen et al. 2004; Baeuerle and Gires 2007) which makes this an ideal marker to identify the cancer cells. All the selected cell lines in this study (MCF-7, MDA-MB-231, HT-29, FADU, CAL27, AGS, N87, HepG2 and HuH7) had been reported to be positive for EpCAM (Flieger, Hoff et al. 2001; Di Paolo, Willuda et al. 2003; Pauli, Münz et al. 2003; Osta, Chen et al. 2004; Yamashita, Budhu et al. 2007; Joka, Pietsch et al. 2009; Wenqi, Li et al. 2009) and

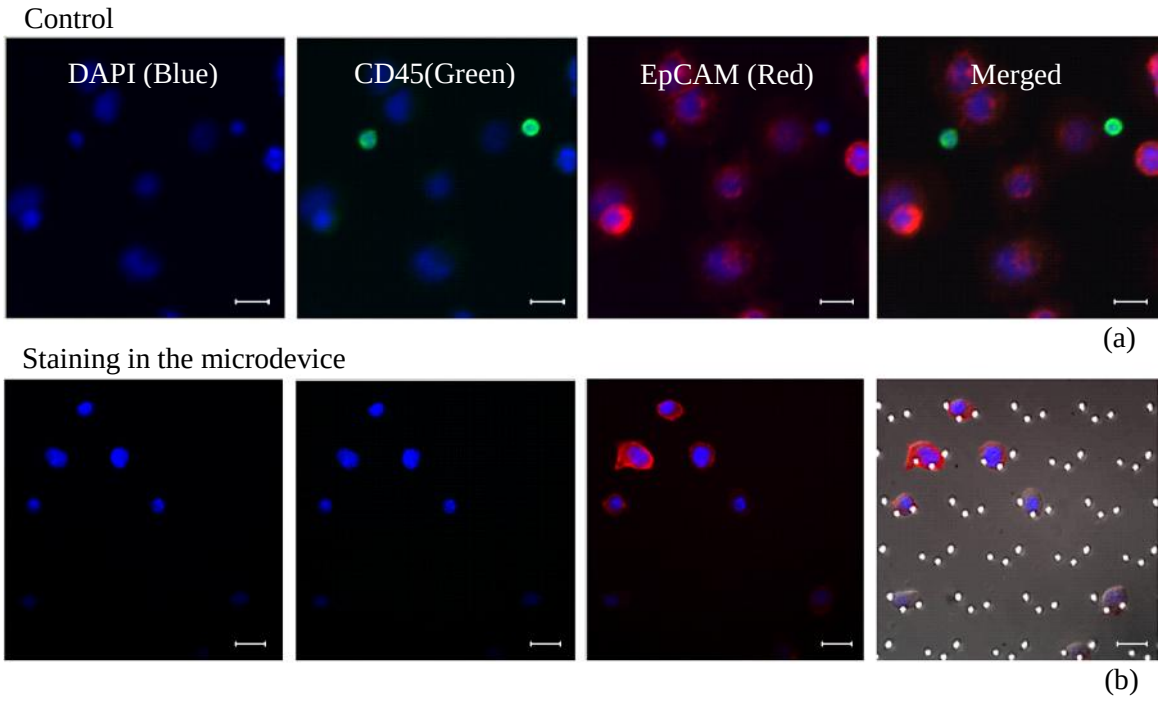

Figure 5.6 Isolation purity of tumor cells in a spiked sample using the microdevice. Immuno-fluorescence staining to detect cancer cells using DAPI(blue) to counterstain the cell nucleus, CD45(green) for hematopoietic cells and EpCAM(red) to detect tumor cells. (a) Control was done with a mixture of blood and resuspended cancer cells. (b) Staining in the microdevice is to distinguish between the different cell types. Scale bar represents 20 µm.

were confirmed in control experiments. In addition, DAPI was used to counterstain the cell nucleus to identify all peripheral blood mono-nucleated cells (PBMC). CD45, a trans-membrane glycoprotein is expressed among hematologic cells and will be used to distinguish white blood cells (WBCs).

Figure 5.6 shows the immuno-fluorescence staining results of a typical experiment for the isolated cells in the microdevice. The individual reagents were added into the system via pressure differential that drive fluid into the microdevice. A stationary holding time allowed the antibodies to bind to the isolated cells so that a distinction could be made. A positive cancer cell count for this investigation were identified using red (EpCAM

positive) and blue fluorescence (DAPI positive) while hematologic cells are identified using green (CD45 positive) and blue fluorescence (DAPI positive). This is clearly depicted in the control experiment in figure 5.6a. The first picture (left) shows the blue channel which highlights all PBMCs. The second pictures shows the presence of WBCs using CD45 (green) and the third picture shows cancer cells using EpCAM (red) in the population of PBMCs. The last picture depicts a merged view of all the coloured channels that highlights the positions of the cancer cells and the WBCs in the same image.

For the isolated cells in the microdevice, the staining protocols was repeated and figure 5.6b shows that high purity can be achieved, with the absence of WBCs (no visible green fluorescence) in the isolated cells. In the same view, it was observed also that the expression levels of EpCAM in the cells vary quite significantly, even within cells from the same cancer cell lines. The deduction was also confirmed in the control experiments with cells showing different level of fluorescence (different degree of brightness) which underwent the same processes for staining. This is likely to have an impact in the identification of CTCs from cancer patients as it might be difficult to recognize cells with low expression levels, leading to false negatives. Sieuwerts et al. (Sieuwerts, Kraan et al. 2009) also presented evidence that EpCAM is unsuitable on breast cancer cell given the large diverse expression patterns and called for new anti bodies to be adopted. Nonetheless, the cell lines used in the investigation had been confirmed with the presence of the antibody and would have minimal impact on the characterization experiments.

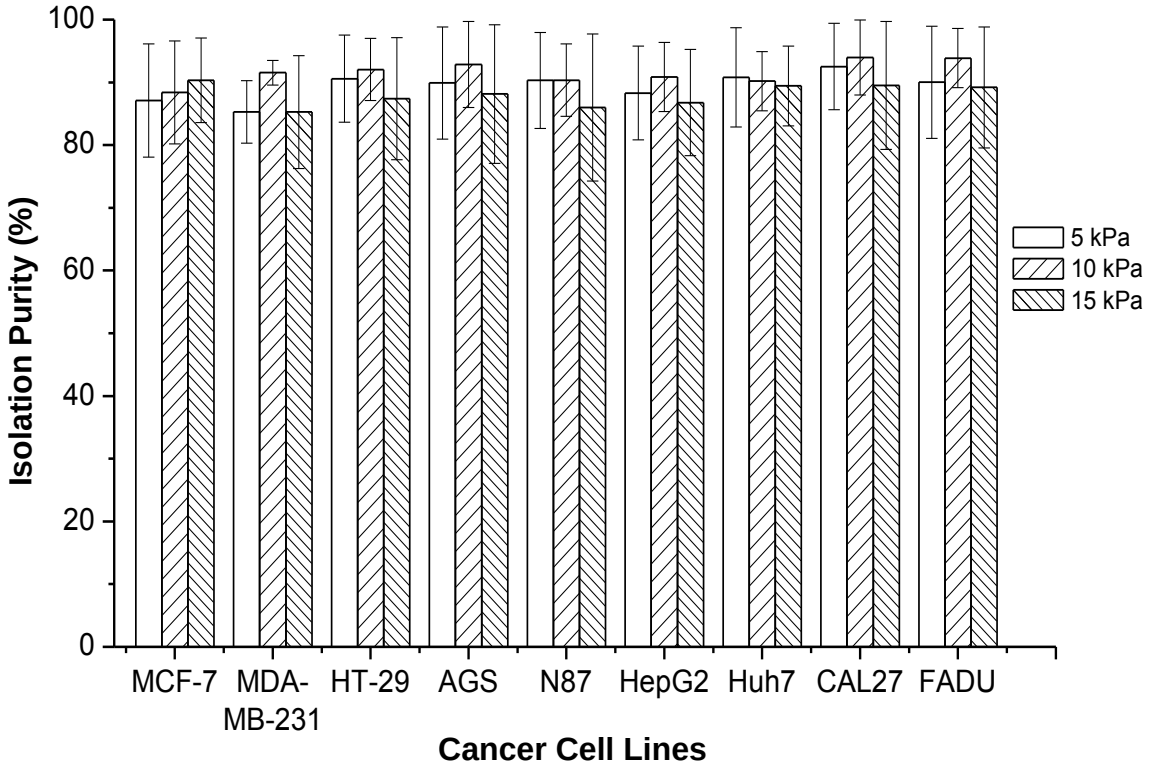

Figure 5.7 Cancer cell isolation purity for various cancer cell lines in the microdevice over a range of operating pressure applied.

Figure 5.7 shows the cancer cell capture purity in the experiments over the range of operating pressures applied. A mean isolation purity of 89% was obtained at the operating pressure of 5 kPa and showed insignificant variations at larger operating conditions. A Student's t-test performed on each individual cell line showed no significant differences in the mean isolation purity over the range of operating pressures at $p<0.01$. The tumor cell purity in each of the tests was maintained over the entire pressure range. Cell isolation purity was calculated as the ratio of cancer cells to the total number of cells isolated from the blood mixture as illustrated in equation 5.2.

$$\underset{\text{Purity}}{\text{Isolation}}\ (\%) = \frac{\text{Trapped Cancer Cells (EpCAM+)}}{\text{Total Number of Isolated Cells}} \times 100\% \quad (5.2)$$

The results were also significantly higher than leading techniques which claimed a separation purity of approximately 50% using biochemical means (Nagrath, Sequist et al. 2007). The insignificant change of capture purity over a wide range of applied pressure differentials and a mean capture purity of above 85% is indicative that the physical properties of cancer cells are distinctively different from blood constituents. The results also highlighted that the microdevice was effective to remove blood constituents. The gap size of 5 μm in each of the crescent traps was sufficiently large enough to allow blood cells to deform through while holding the cancer cells effectively.

5.4 Microfluidic Chip Versatility with Cancer of Different Origins

For the characterization of the microdevice, a diverse range of cancer cell lines were used to determine the versatility of the technique to handle different cancers as the disease is genetically heterogeneous (Braun, Hepp et al. 1999; Reya, Morrison et al. 2001; Shah, Mehra et al. 2004; Sergeant, Penninckx et al. 2008). A total of 9 different cancer cell lines from 6 different origins were utilized as denoted earlier to ascertain the microdevice characteristics. Table 5.2 summarizes the maximum cell isolation efficiencies obtained in processing the samples and the corresponding cell capture purity. A 95% confidence

Table 5.2 Maximum isolation efficiency and corresponding cell capture purity in the microdevice using various cancer cell lines.

Cancer Cell Line	Isolation Efficiency (%)	95% Confidence Interval	Capture Purity (%)
MCF-7	81.5 ± 5.6	[78.7% 84.3%]	87.1 ± 9.0
MDA-MB-231	80.9 ± 5.3	[77.6% 84.2%]	85.3 ± 5.0
HT-29	85.4 ± 4.6	[82.7% 88.1%]	90.6 ± 7.0
AGS	78.9 ± 8.0	[73.9% 83.9%]	89.9 ± 9.0
N87	80.7 ± 7.6	[76.0% 85.4%]	90.3 ± 7.7
HepG2	87.4 ± 5.8	[83.8% 91.0%]	88.3 ± 7.5
HuH7	81.1 ± 4.4	[78.4% 83.8%]	90.8 ±7.9
CAL27*	81.6 ± 8.6	[76.3% 86.9%]	86.8 ± 10.3
FADU	80.6 ± 8.7	[75.2% 86.0%]	90.0 ± 8.9

* Measurements taken at the operating pressure of 3 kPa

interval is also calculated for each of the individual cell isolation efficiencies to gauge the degree of uncertainty around the mean estimates. For the current tests, the isolation of HepG2 proved to be the most effective with an isolation efficiency of 87.4%.

Comparing across the different sets of experimental trials with different cell lines, the spread of the data was small as denoted by the standard deviation of each sample. This is likely to indicate that the results are consistent and the technique is reliable in isolating cancer cells from peripheral blood at the particular pressure setting which is applied. With a 95% confidence interval, the deviation from the mean showed little variations and

constantly above 73%, which can be inferred that a high cell isolation efficiency is probable when the operating pressures are optimized. Furthermore, it showed that the technique is suitable to achieve a precise measure for each of the cancer cell lines in peripheral blood which is required for an accurate assessment of the state of health of metastatic cancer patients. Collectively, an average cell isolation efficiency of 82.0% was obtained with the results acquired from all the cancer cell lines. A 95% confidence interval of the mean cell isolation efficiency of the system was between [82.3% 83.7%]. This is indicative of an accurate platform for the processing and detection of tumor cells in peripheral blood of cancer patients as cell yield is high. Comparing across different cell lines, the sample standard deviation for the cell isolation efficiencies was approximately 2.6% which is suggestive of a rather small spread of data. The results showed that the system fluctuates very little across different cancer types and can be versatile to handle cancer cells from different origins. Furthermore, it can be inferred that physical properties of cancer cells remained distinctly different from blood cells across different cancer types, though they may differ considerable at the genetic level. These made separation via size and deformability of cancer cells an attractive method which will also resolve numerous issues surrounding affinity based separation.

5.5 Conditions of Isolated Cells and Cell Retrieval

The main aims of the system are to provide a direct means of detecting tumor cells from peripheral blood which will also keep cells viable so that downstream analyzes can be

supported. This is because the conditions of cancer cells after isolation are of interest, as these tumor cells in circulation are likely to be responsible for the progression of the disease cancer. For this aspect, preserving the native state of the cells after isolation will help to determine their exact nature and allow a detailed study of CTC sub-populations such as in the investigation of cancer stem cells which are reported to be critical to progressive disease (Reya, Morrison et al. 2001; Wicha 2006). This will hopefully elucidate clearer the metastatic process to aid in diagnostics, prognosis, monitoring and in the search for new therapeutic targets.

Figure 5.8 shows the isolation paths of MCF-7, MDA-MB-231 and HT-29 cells into each of the single traps. Results from other cell lines were similar as well and hence the data were not shown. Cell isolation followed rather similar tracks as denoted in the CFD simulations and met with little resistance from the physical structures created from PDMS. The simulated data also presented that the wall shear stress acting on isolated cells were within the physiological range which meant fluid shear forces acting on these cells were minimized. To ascertain the deductions experimentally, the isolated cells were retrieved from the cell traps in the microdevice and cultured under normal conditions.

Retrieval of the isolated cells in the microdevice can be achieved by altering the flow conditions inside the microdevice, using the valve connections and the computer which controls the pressure lines. Firstly, the waste reservoir was cleared to prevent backflow of waste materials, followed by closing of the sample inlet fluidic port. The valve leading to the cell collection point was then opened and the pressure differential between the waste

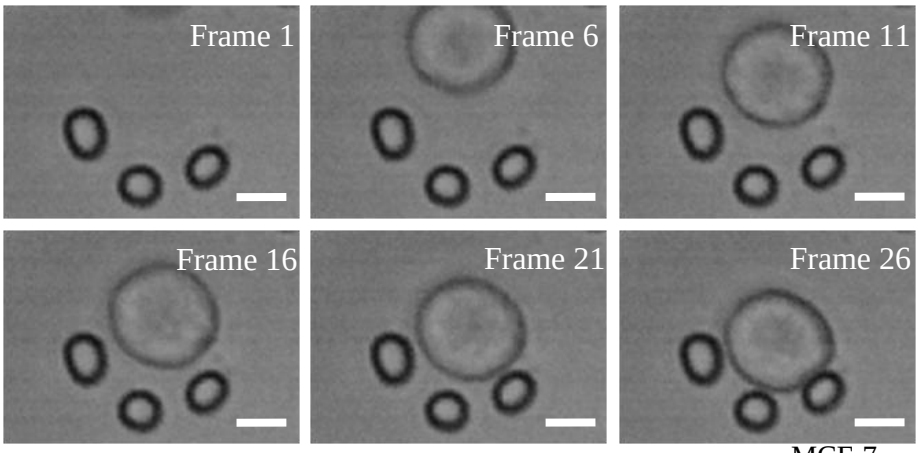

(a) MCF-7
2000fps – 5 kPa

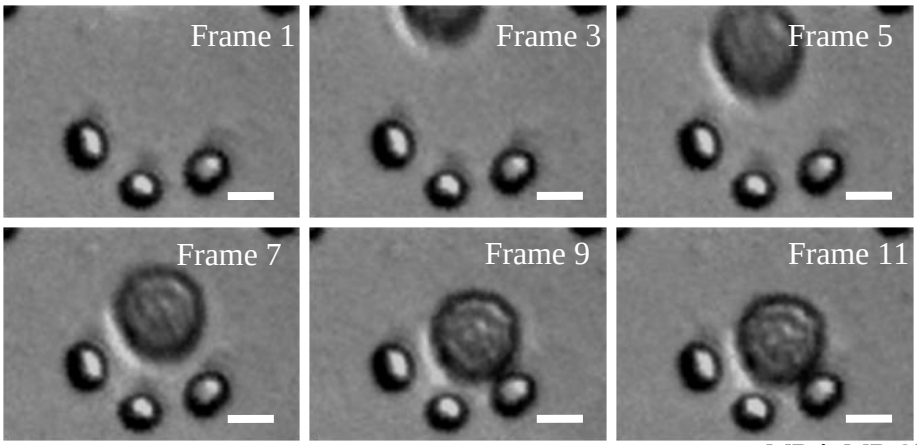

(b) MDA-MB-231
110 fps – 2 kPa

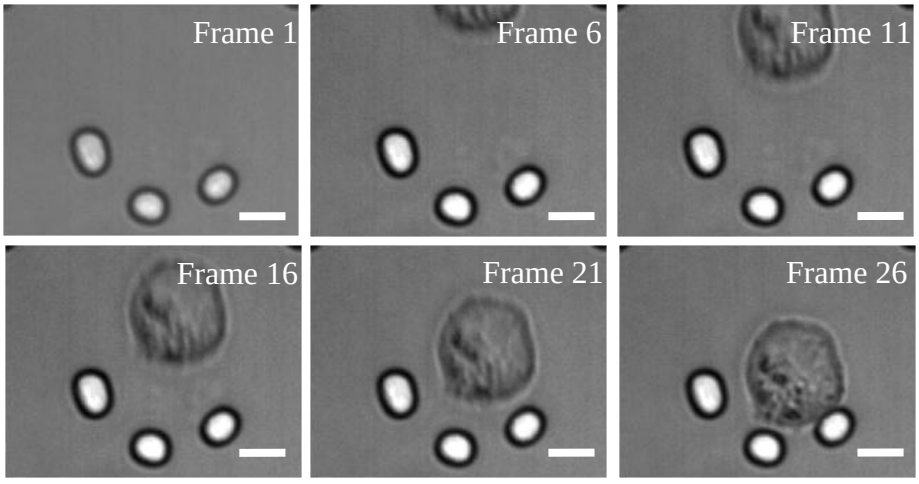

(c) HT-29
2000fps – 5 kPa

Figure 5.8 Time sequence images to isolate a cancer cell from a spiked sample. (a) MCF-7 cells taken at 2000 fps at the operating pressure of 5 kPa. (b) MDA-MB-231 cells taken at 110 fps at the operating pressure of 2 kPa. (c) HT-29 cells taken at 2000 fps at the operating pressure of 5 kPa. Scale bar represent 10 µm.

outlet and cell collection point quickly increased to 20 kPa. Isolated cells would then be dislodged as shown in figure 5.9 for the 3 cancer cell lines mentioned earlier. The returned path did not hinder the disengagement of cells from the cell traps and most of the events were instantaneous. Recovery of cells following the release from the traps were smooth as the inverted isolation structures directed the free floating cells to the adjacent sides and not restricting their movement. An exception in the experimentations lies in HuH 7 (hepatocellular carcinoma cells) where it was observed that cells' dislodgement from the traps posed an issue. This is highlighted also in table 5.3 which showed that HuH 7 had the lowest recovery rate comparing with all the cell lines tested. The recovery rate is calculated based on the number of cells that are dislodged to the initial number of trapped isolated cells as denoted in equation 5.3.

$$\underset{\text{Recovery}}{\text{Cell}}(\%) = \frac{\text{Number of dislodge cancer cells}}{\text{Initial number of isolated cells}} \times 100\% \tag{5.3}$$

The probable reason for the lower successful recovery rate is due to the strong adherence of the cancer cells to the glass substrate and the PDMS structures. This is an inherent property of the cell and differs in strength between different cell types. In order to remove them from the structures, it will require a force larger than 20 kPa for the recovery settings. Otherwise, chemical agents like trypsin-EDTA (0.25%) can be used to release them from the adherent state, before the activation of the cell recovery protocol. A larger backflow is not desired as it may breached the critical shear stresses that will in turn

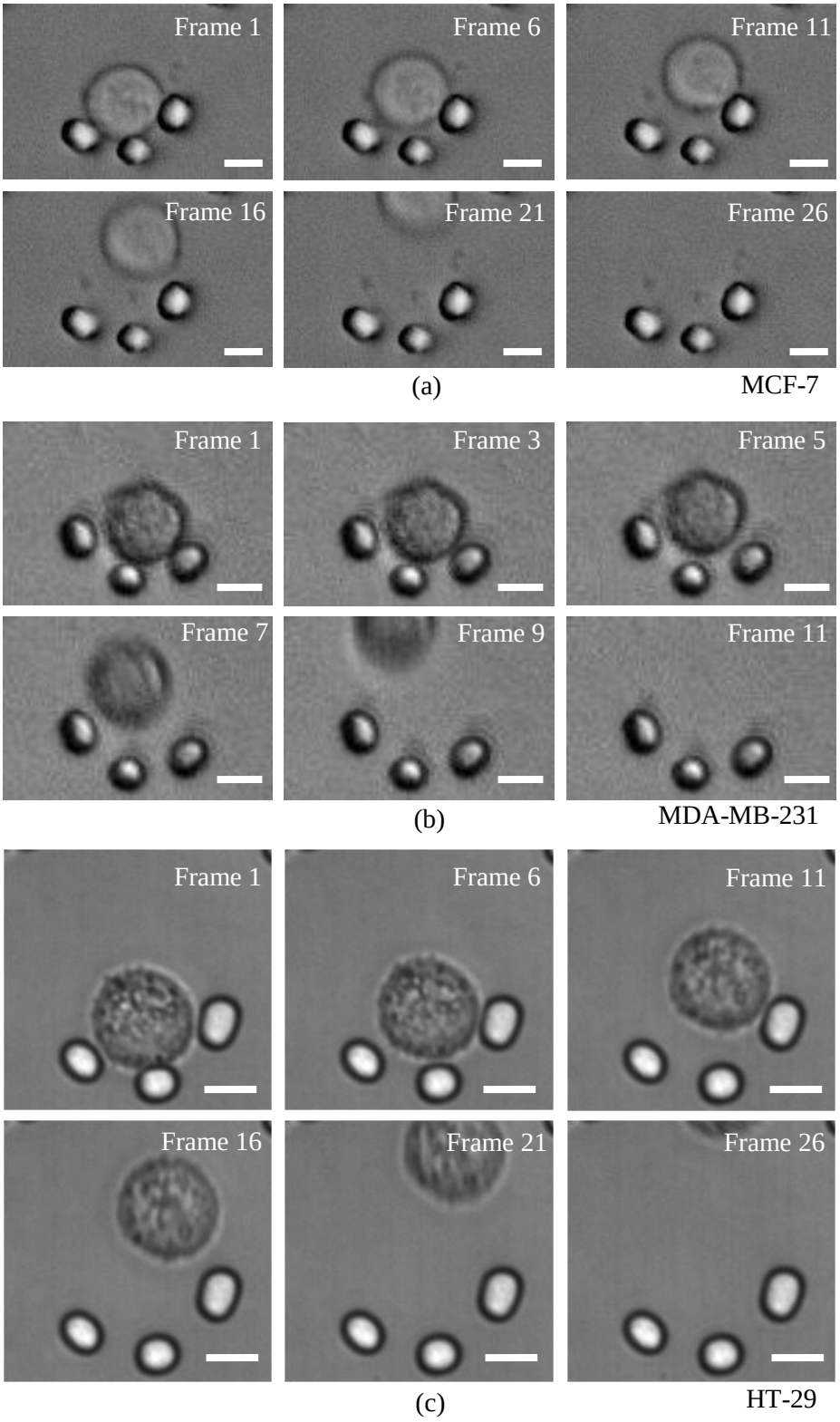

Figure 5.9 Time sequence images to retrieve a cancer cell from the isolation traps. (a) MCF-7 cells. (b) MDA-MB-231 cells. (c) HT-29 cells. Scale bar represent 10 μm.

Table 5.3 Recovery rate of isolated cells from the microdevice by exerting a back flow to collect the cells in the collection point

Cancer Cell Line	Recovery Rate (%)	95% Confidence Interval	Deviation from the mean (*p* value)*
MCF-7	94.9 ± 8.0	[92.1% 97.7%]	0.03499
MDA-MB-231	97.3 ± 2.6	[96.4% 98.2%]	≈ 0.00000
HT-29	96.0 ± 4.4	[94.5% 97.5%]	0.00002
AGS	94.4 ± 5.1	[92.6% 96.2%]	0.01253
N87	94.1 ± 7.4	[91.5% 96.7%]	0.08513
HepG2	92.4 ± 9.7	[88.9% 95.9%]	0.45543
HuH7	72.0 ± 13.2	[67.3% 76.7%]	≈ 1.00000
CAL27	96.0 ± 6.4	[94.0% 98.0%]	0.00028
FADU	92.5 ± 7.9	[89.7% 95.3%]	0.41834

*Hypothesis testing performed with null hypothesis H_0: μ=92.2 and H_1: μ>92.2. 92.2% is the mean recovery rate for all the cell lines.

permanently affect the cells' biochemistry (Patton, Menter et al. 1993; Chang, Chang et al. 2008) or even kill the cells (Brooks 1984). Another alternative is to block the interior of the microdevice with a surfactant such as polyethylene glycol (PEG) or pluronic acid F-127. These were reported to be effective to prevent cell adhesion on coated surfaces (Miqin, Desai et al. 1998; Boxshall, Wu et al. 2006) and yet had minimal effects on the viability of the cells when used at low concentrations (negligible toxicity effects). However, this incurs additional preparatory steps which will increase the total processing time per sample.

All the other cell lines were successfully recovered with high yields as shown in table 5.3. An average recovery rate of 92.2% was attained from all the cell lines, indicating a significant cell quantity that can be collected from the microdevice after the isolation process. A 95% confidence interval for the average cell recovery for this sampling was 92.2 ± 5.1%. The spread of the data measured by the standard deviation was approximately 7.7% which was largely attributed to the heterogeneity between the different cells lines in terms of the adhesion strength to the microdevice. MDA-MB-231 breast adenocarcinoma cells showed the best recovery rates from the microdevice and coincidently had also the lowest value for standard deviation. The results were indicative that the adherent properties of MDA-MB-231 cells were relatively weaker than the other cell lines tested which made it easy to be removed under the same extraction conditions. A Student t-test was performed on each individual cell line comparing the recovery rate with the mean value from the entire group. This clearly differentiated the groups which showed some of the cell lines faced less difficulties in recovery. For instance, with a significance level, α of 0.05, we reject the null hypothesis (refer to table 5.3) for MCF-7, MDA-MB-231, HT-29, AGS and CAL27. It is statistically significant to claim that this group of cancer cell lines showed a higher recovery rate comparing with the mean retrieval quantity.

The integrity of the isolated cells was measured by the behavior of the retrieved cells under normal culturing conditions. It is hypothesized that the cells initiating tumors have stem cell like properties (Marx 2007) and CTCs being circulating in bloodstream are the potential targets. Isolating sufficient living CTCs have been a challenge with limited

success (Pantel, Brakenhoff et al. 2008) mainly due to the harsh conditions that were subjected to the cells in the body before it was retrieved. Current leading techniques do not suffice to maintain the quality of these cells and an optimal culturing condition needs to be further examined (Kaiser 2010). Removing isolated cells in the proposed microdevice for further analysis could be achieved with ease by altering the flow conditions to induce the cells to flow towards the cell collection point. The process of cell recovery was repeated for 5-8 cycles to obtain enough cell number and the retrieved cells were then reseeded to a culture flask. A normal culture from the same batch was concurrently maintained that served as a control for comparison.

Figures 5.10, 5.11 and 5.12 illustrate an overview of a 5-day culture for MCF-7, MDA-MB-231 and HT-29. Similar conclusions were also obtained for the rest of the cancer cell lines that were tested. The proliferative rates of reseeded cells were compared to normal cultured cells to ascertain that isolated cancer cells were not affected by the microdevice. Initial seeding of cells was approximately similar in all experiments and can be verified by observing the cultures at day 1. Comparable initial cell numbers were observed on the control and experimental culture flasks at day 1. Cells were then allowed to grow for 5 days with a medium change every 2 days. Over the same duration, there were no observable differences in proliferation rate for all cell-lines as shown in figures 5.10, 5.11 and 5.12 when compared to their respective normal cultures. The morphology of the retrieved cells and its control experiment were also rather similar. For instance, reseeded MDA-MB-231 (figure 5.11) showed a spindle shape trait which was coherent with the control experiment and reseeded HT29 (figure 5.12) proliferated in clusters

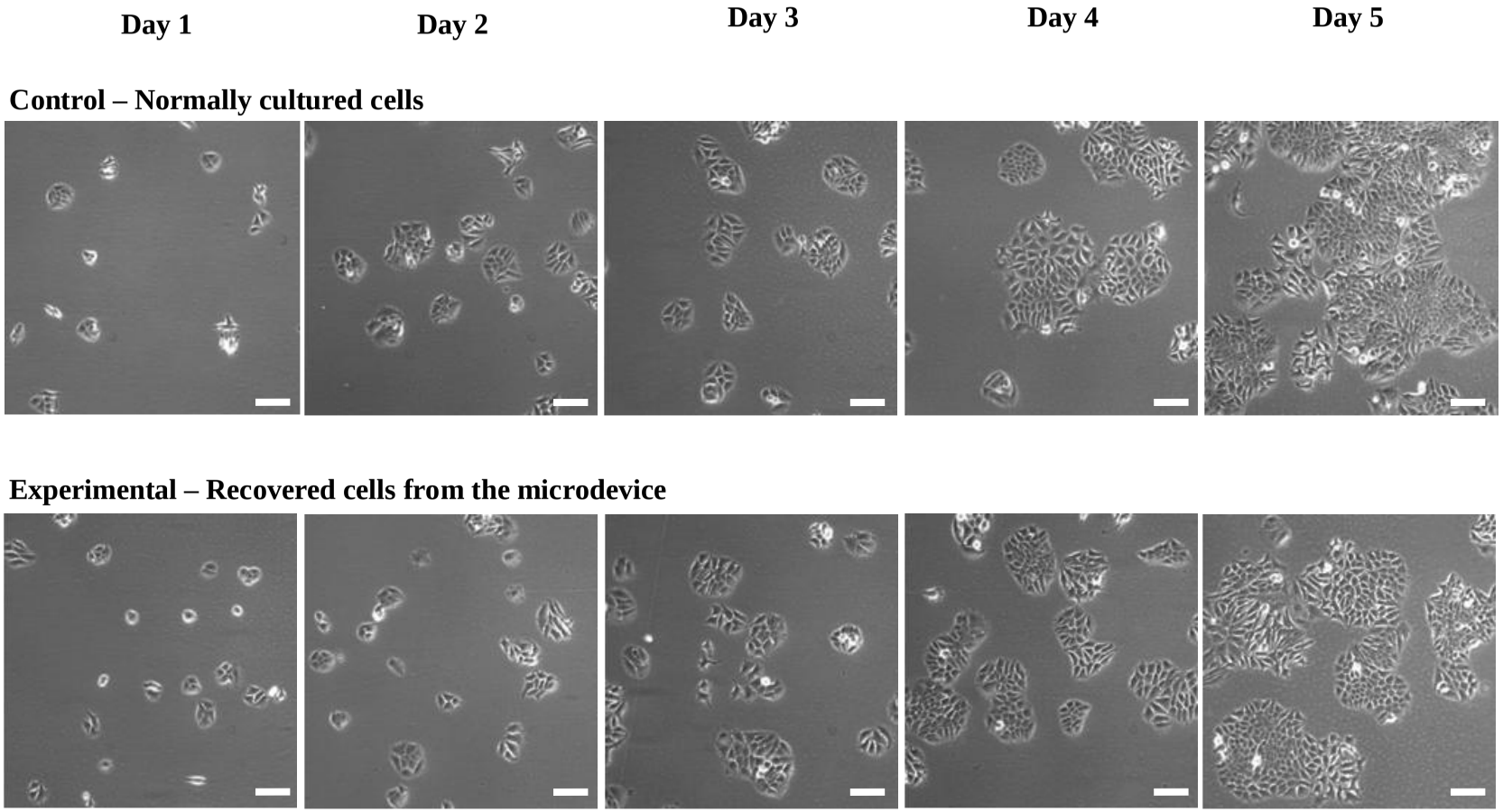

Figure 5.10 Cell proliferations for recovered MCF-7 cells from the microdevice in comparison with normal cultures (control) over a period of 5 days. Scale bar represents 100 µm.

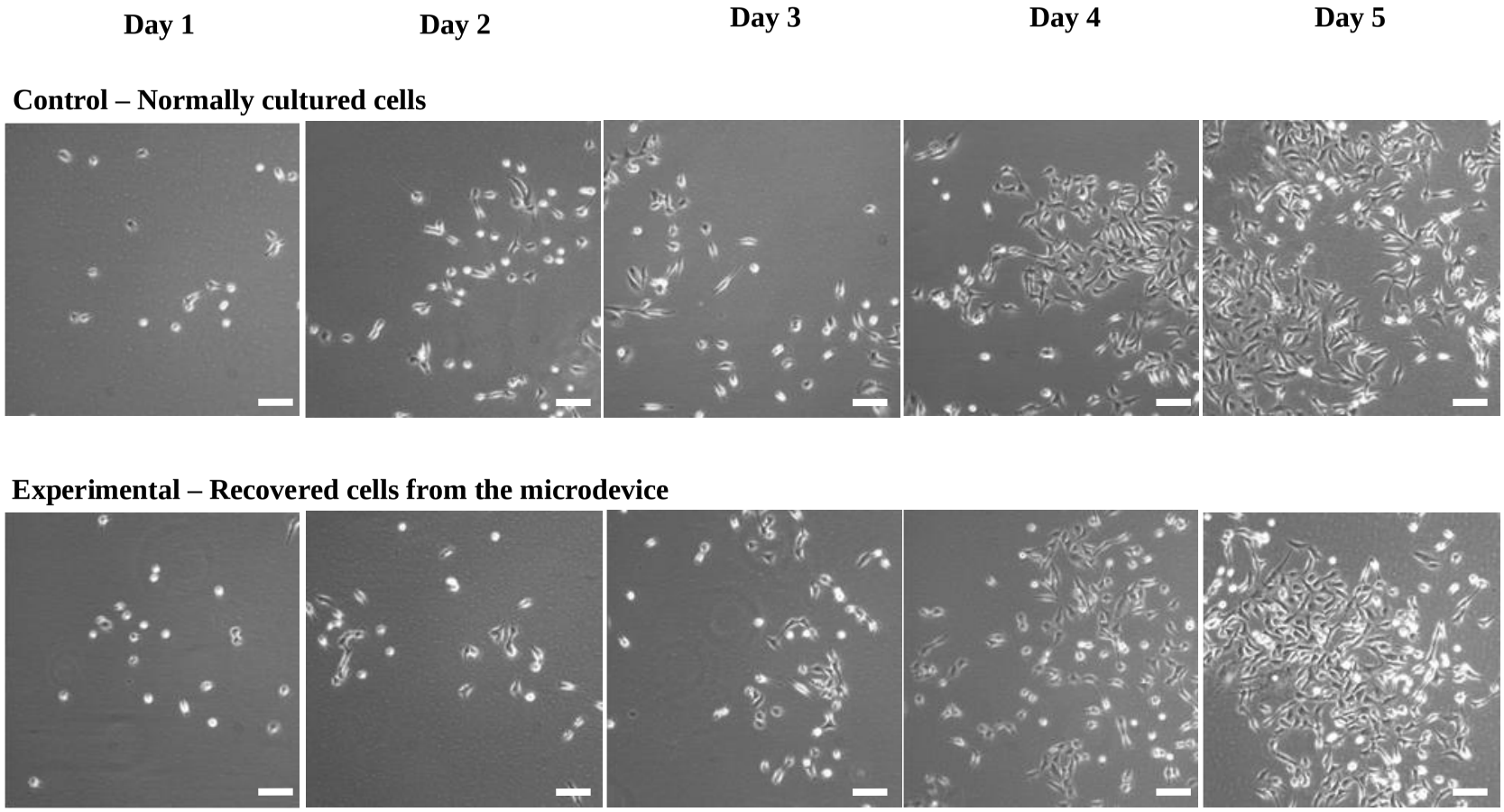

Figure 5.11 Cell proliferations for recovered MDA-MB-231cells from the microdevice in comparison with normal cultures (control) over a period of 5 days. Scale bar represents 100 µm.

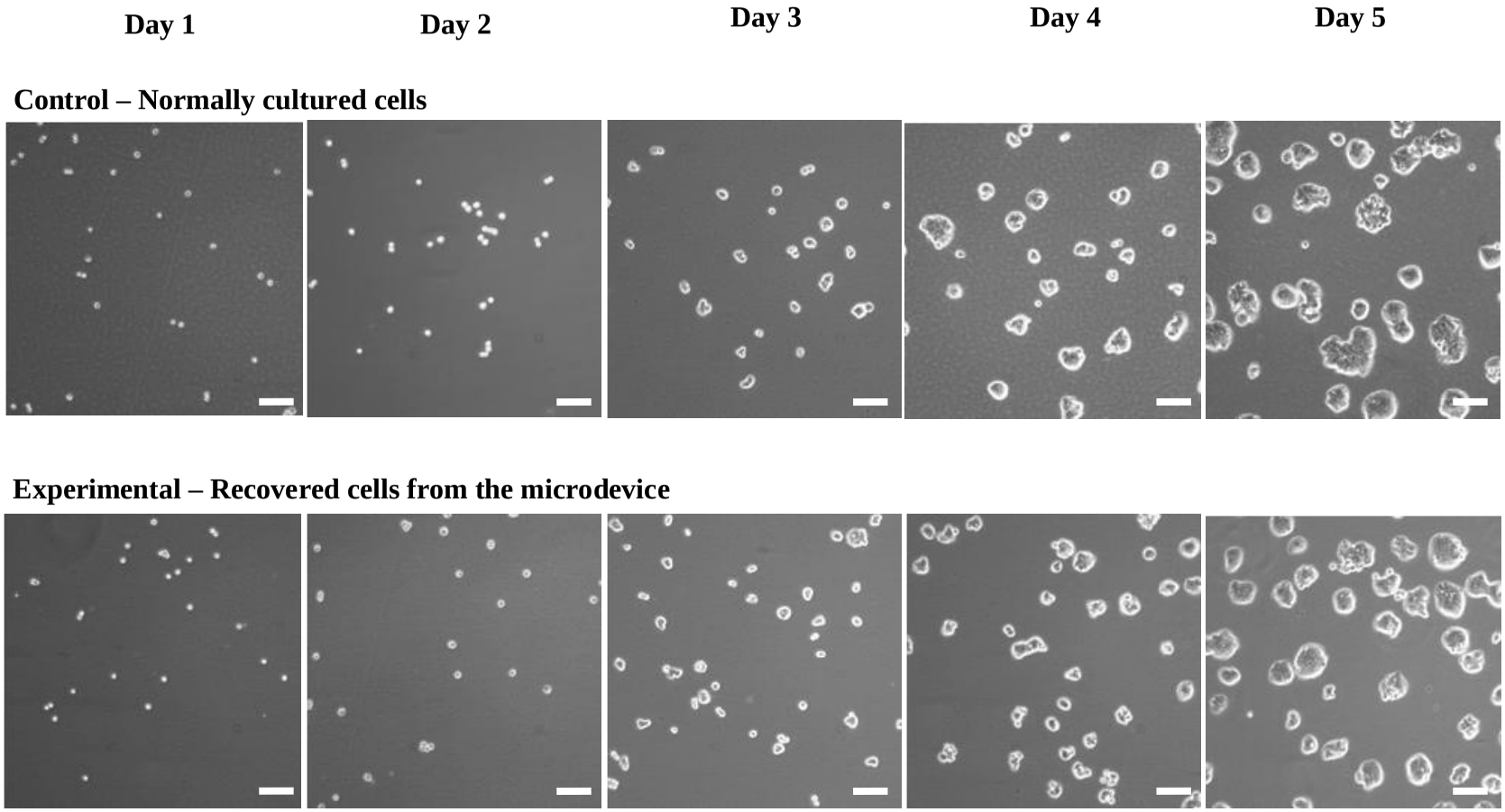

Figure 5.12 Cell proliferations for recovered HT-29 cells from the microdevice in comparison with normal cultures (control) over a period of 5 days. Scale bar represents 100 µm.

which were also exhibited in the control experiments. This uniformity in cell behaviour confirmed that the retrieved cells were unaffected after isolation in the microdevice and that the system was gentle during the processing.

5.6 Microdevice Detection Limit

The rarity of CTCs in the presence of a multitude of blood cells is the main technical challenge to identify them. The ratio of CTCs to blood cells can be of a billion orders of magnitude difference which implies a high noise to signal ratio in the pre-processed specimen. An enrichment step is thus crucial and a sensitive setup is desired to detect small numbers of cells in the mixture. Therefore, the detection limit of the system is of interest as it represents the sensitivity of the microfluidic chip in CTC detection. For these experiments, very low counts of cancer cells were added to 1×PBS, either with manual pipetting or FACS, and made to pass through the microdevice. It is noted that manual pipetting is a laborious and unreliable procedure which will not always yield the collection of one single cell. The cell number can vary between 1 to 5 cells but this can be clearly observed under the microscope. Using the FACS on the other hand is a straightforward process but errors associated in the separation can be quite high when trying to obtain a live single cell in each sample from our observations. As the separation process cannot be visualized directly, the errors associated cannot be determined empirically.

Table 5.4 Isolation efficiency and positive ratio for low cancer cell count using spiked (1-3 cells) samples.

Cell Line	Cancer Type	Sample Size, n	Positive Case Ratio
MCF-7	Breast adenocarcinoma	10	1.00
MDA-MB-231	Breast adenocarcinoma	10	0.78
HT-29	Colorectal adenocarcinoma	10	0.80
AGS	Gastric adenocarcinoma	10	0.80
N87	Gastric carcinoma	10	0.60
HepG2	Hepatocellular adenocarcinoma	10	0.75
HuH7	Hepatocellular adenocarcinoma	10	1.00
CAL27	Tongue squamous carcinoma	10	0.68
FADU	Pharynx squamous carcinoma	10	0.90

We used 1-3 cells in each of our experiments to mimic the rarity in the specimen and determine the detection limits of the platform. All other experimental procedures are similar to that used in establishing the microdevice cell isolation efficiency as illustrated in section 5.1. We define a positive ratio for the number of trials for which at least one of the total number of cells spiked into PBS is retrieved, over the total number of cases. A value closer to 1 denotes most of the trials were successful to recover the cells while a lower value illustrates the converse situation. This provided a gauge of the detection limit for the microdevice with respect to each of the cell lines. A total of 90 experimental runs were performed for all the cell lines listed in table 5.4.

To sum up, the mean positive rate achieved from the investigation was approximately 0.81 from all the nine different cancer cell lines. The results were promising to indicate an average success rate for 8 out of every 10 tries in detecting low cell counts from the specimens using the proposed microdevice. This was also coherent with the microdevice efficiency characterizations in section 5.1 which predicted an average isolation efficiency of 80%. However, within cancer cells of the same origin, it was observed that there existed distinct isolation rate variations. For instance, MCF-7 was found to have a higher positive detection rate at low cell numbers in the sample solution than MDA-MB-231 which was of the same cancer type. This could be attributed to a number of factors such as the heterogeneity of different cancer cell lines, random errors in FACS separation when preparing the spiked sample or a result of the setup with cancer cells adhering to tubes before entering the microdevice. From the diverse range of cell lines tested, MCF-7 and HuH7 showed a perfect detection process with all positive responses from each tests. On the other spectrum, N87 and CAL27 fared poorly in the study with a detection rate of 0.6 and 0.68 respectively. Nonetheless, an overall effective rate of 81% is hopeful and significant enough to accurately detect CTCs with high sensitivities from the peripheral blood of cancer patients.

Chapter 6 Clinical Blood Processing to Detect and Analyze Circulating Cells

The enrichment of CTCs in peripheral blood using the microdevice is based on cell size and deformability differences, with the assumption that CTCs are generally larger and much stiffer than blood constituents. In this way, as the mixture of cells passes through the isolation regions in the microdevice as shown in figure 6.1, cancer cells will be impeded by the physical cell traps while blood cells passes through with ease. With a uniform array of 900 crescent shaped cell isolation structures optimally positioned, the isolation efficiency was maximized for the detection of CTCs and fully characterized with techniques illustrated in chapter 5. For the microdevice, it processes whole blood directly to isolate CTCs, which simplifies operations and experimental preparation. No prior work is required to modify the blood specimen which makes it attractive and straightforward. Various features are also built into the device to ensure the smooth processing of blood, such as pre-filters, compartmentalized isolation regions and the ability to retrieve isolated cells.

6.1 CTCs in Patients with Renal Cell Carcinoma (Kidney Cancer)

In this study, we seek to demonstrate the isolation of CTCs in peripheral blood of renal cell carcinoma (RCC) patients using purely CTCs' cell size and deformability differences

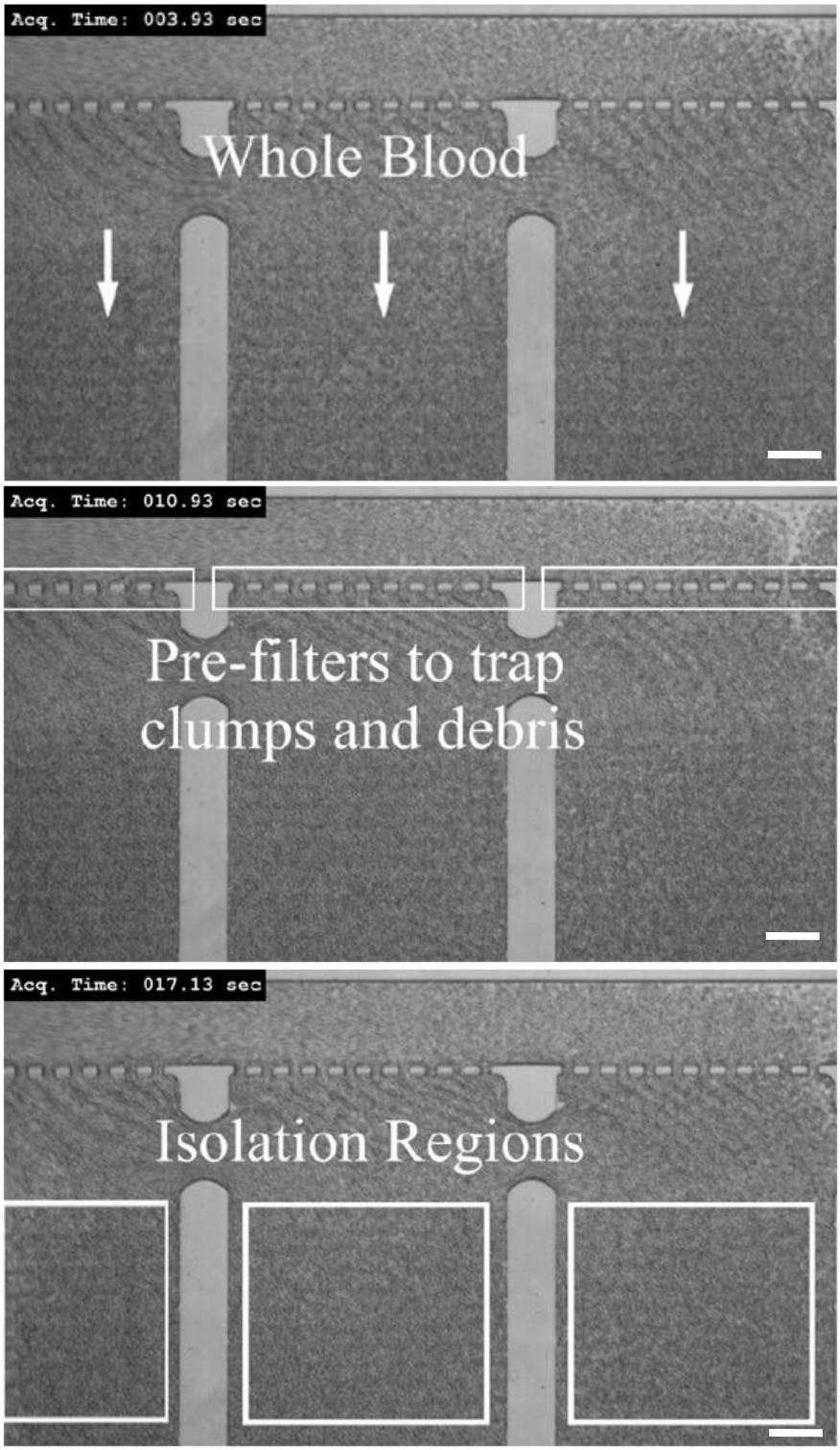

Figure 6.1 Overview of the microdevice during the processing of whole blood directly for the isolation and detection of CTCs. The images were extracted from a real time video taken at 60 fps of the procedure using a 5× magnification lens on an inverted microscope. Scale bar represents 100 μm.

from that of blood cells. Patients with RCC have a high probability of haematogenous metastasis (Weiss, Harlos et al. 1988; Pagano, Franzoso et al. 1996) and disseminated tumor cells from the bone marrow of RCC patients have demonstrated a strong prognostic value (Buchner, Riesenberg et al. 2006). By applying biorheological differences in cell separation such as that of the cell dimensions and ability to deform, it bypasses the need for a selection antibody during the CTCs enrichment process. Furthermore, the lack of a suitable universal tumor marker for diagnosis or monitoring for RCC (Loberg, Fridman et al. 2004) limits the efficacy of the affinity based separation technique. In addition, Allard et al. (Allard, Matera et al. 2004) reported low sensitivities in CTC detection using the Cell Search system with EpCAM as the selection marker on patients with renal cancer They hypothesized that the heterogeneity in the expression levels of EpCAM on CTCs' surfaces causes variations in the ability of the system to recover and detect these cells. Our approach is thus attractive as it is a label free method to effectively isolate CTCs from blood, and cells that are generally larger and stiffer will be retained. The system being gentle to the isolated cancer cells is likely to maintain the integrity of these cells.

Here, the device processes whole blood directly without the need for intermediate preparation, thus minimizing potential cell losses as shown in figure 6.1. Biochemical functional modifications are also not required for the microdevice which simplifies device preparation. Also in the design for a smooth operation, the pre filters in the microdevice are necessary to block out large clumps or debris which can come from the blood specimen or the fluidic connections of the microdevice from entering the cell

isolation region (figure 6.1). This is required to ensure that the tests are not hindered due to blocked isolation traps from the large clumps.

Furthermore, the compartmentalized isolation regions aids in the overall support of the microdevice as noted in section 4.2 and make certain that the flow characteristics are uniformly distributed across the microfluidic channel. The uniform array of the isolation traps facilitated cell enumeration in situ and allows processing of large blood sample volume (in the range of millilitres) in a microscale device. Contrary to direct filtration methods where clogging is an issue, this microdevice directs incoming cells from occupied isolation traps to the next row of unoccupied traps, thus preventing potential build up of cells in a particular region, which has been demonstrated in chapter 5 using spiked samples.

In addition, the optical transparency of the microdevice enables the use of immunofluorescence to detect CTCs in situ. The detection of CTCs using immunofluorescence staining is performed directly on the microdevice which ensures maximum cell yield and minimizes the usage of expensive reagents.

For this investigation, blood samples of RCC patients are examined using this microdevice and the system is characterized for its stability, sensitivity and isolation capability.

6.1.1 Blood Sampling of Metastatic Renal Cancer Patients and Control Experiments from Blood Extracted from Healthy Volunteers

Ten healthy volunteers and 32 RCC patients participated in the study after informed consent were taken as approved by the institutional review board. Blood samples from healthy volunteers serve as control experiments to ascertain the microdevice accuracy. In all, 99 peripheral blood samples were extracted from 32 RCC patients from the National Cancer Center, Singapore between June 2009 to February 2010. 9 – 10 ml of blood are extracted from every patient each time with the first 0.5 – 1 ml of blood discarded to prevent false positive responses. Samples were stored in EDTA tubes (BD, Franklin Lakes, NJ, USA) prior to use and most blood samples were processed within 24 hours after extraction.

6.1.2 Linearity of Circulating Tumor Cell Detection

In order to determine a suitable amount of blood volume and measure the variability for the tests, we analyzed the first 10 blood specimens taken from RCC patients and varied the volume of blood processed. This is important from the considerations on both the patient's comfort level for the amount of blood drawn and the operation time to process the sample. Minimizing the amount of blood required per test is advantageous as the emotional burden is reduced for the patient and may further aid to convince future test subjects to participate in the trials to use CTCs as a monitoring tool for their disease. This

is also likely to minimize dropout rate as the level of discomfort from the tests are minimal. On the operations, optimizing the quantity of blood in each test will help to decrease the blood specimen processing time. This will be beneficial in maintaining the conditions of CTCs by reducing the exposure time of these cells to fluid shear forces in the microdevice. It this way, this will hopefully help in the culturing of CTCs which are important in the study of cancer stem cells and therapeutic treatments (Kaiser 2010).

Figure 6.2 illustrates the enumeration of CTCs from all 10 patients. From each of the EDTA tubes, experimental splits of 1 ml, 2 ml and 3 ml of whole blood were set aside. It

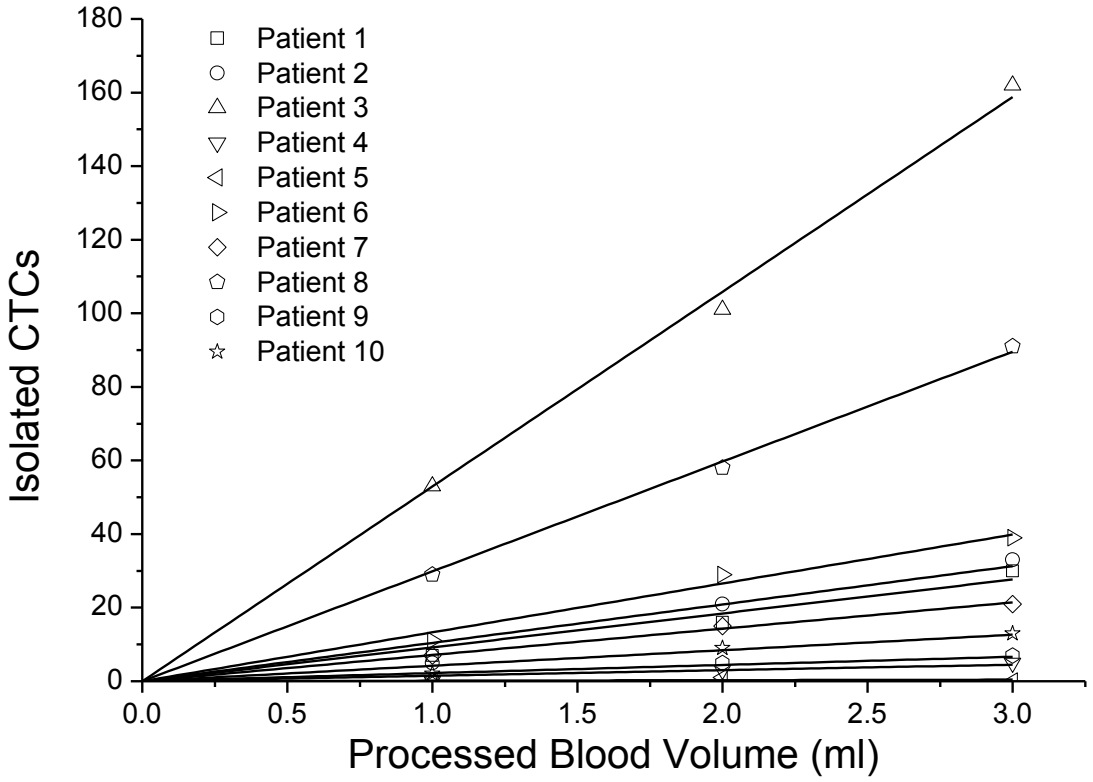

Figure 6.2 Isolated CTCs from different volumes of blood from the each of the 10 specimens to investigate the linearity of the capture. A linear curve fit was performed on each sample with an intercept at 0.

Table 6.1 Linear correlation coefficient, R^2 for the tested samples to measure the linearity of CTC detection

Patient Number	1	2	3	4	5	6	7	8	9	10
R^2	0.94	0.92	0.99	0.80	0.00	0.97	0.99	1.00	0.79	0.91
CTCs/ml >5*	Yes	Yes	Yes	No	No	Yes	Yes	Yes	No	No

* The value is calculated based on an average CTCs count of all the samples tested ie. For Patient 1 who had 7, 16 and 30 CTCs detected in 1ml, 2ml and 3ml of blood specimens respectively had an average of (7+16+30)/(1+2+3) = 9 CTCs/ml (rounded up)

was observed that a range between 0 and 53 CTCs per ml of blood was obtained for this study. The results of each trial were curve fitted using a straight line that passed through the origin to determine the linearity of the data. Theoretically, the values should follow a linear relationship as it is assumed that CTCs are distributed homogeneously throughout the blood specimen and thus it will not matter how much blood is being processed. We derived the goodness of fit with a linear model for each of the patient sample and listed them in table 6.1. For 7 out of 10 cases, it was noted that a R^2 value of 0.9 or greater were attained that indicated a clear linear correlation.

To further examine the discrepancies associated with certain patient samples, we divided the 10 samples into 2 groups based on the average quantity of CTCs detected in each of the samples as denoted in table 6.1. It was observed that for samples having a good linear relationship, it was achieved when the concentration of CTCs were larger than 5 CTCs per ml of blood. The R^2 values in this group cover over than range of 0.92 to 1.00. As the concentration of CTCs in blood increases, the linear correlation is better defined. This

could be clearly seen with specimens taken from patients 3 and 8 (figure 6.2) where the correlation coefficients were 0.99 and 1.00 respectively.

Henceforth, it can be inferred that with a CTC concentration of larger than 5 in the sample, sampling volume of 1 ml is sufficient. As an added safety factor, we proposed to increase the sampling volume to 2 ml instead to boost the CTC count so that the results were more sensitive, given a larger quantity of isolated cells. This investigation also demonstrated the suitability of the technique on clinical blood samples.

6.1.3 Technical Stability for Blood Processing in the Microfluidic Device

We investigated the effects of blood storage time prior to sample processing and defined that as the stability of the system. Although blood specimens are kept in EDTA tubes before being processed in the microdevice, the deterioration of the sample is inevitable due to the environment we reside in. As the quality of the sample worsens, it can be expected that there will be more coagulated clumps of blood cells present in the samples. For instance, repeated freeze thaw cycles can result in the formation of large precipitates (Cheng, Hochlowski et al. 2003). Such situations commonly arise during the transportation route, in between blood extraction and the delivery of the specimens from the hospital to the laboratory, where the blood processing is performed. This is detrimental to the processing of the specimen in minuscule platforms (Pan 2004) as these materials pose the issue of clogging in the microdevice.

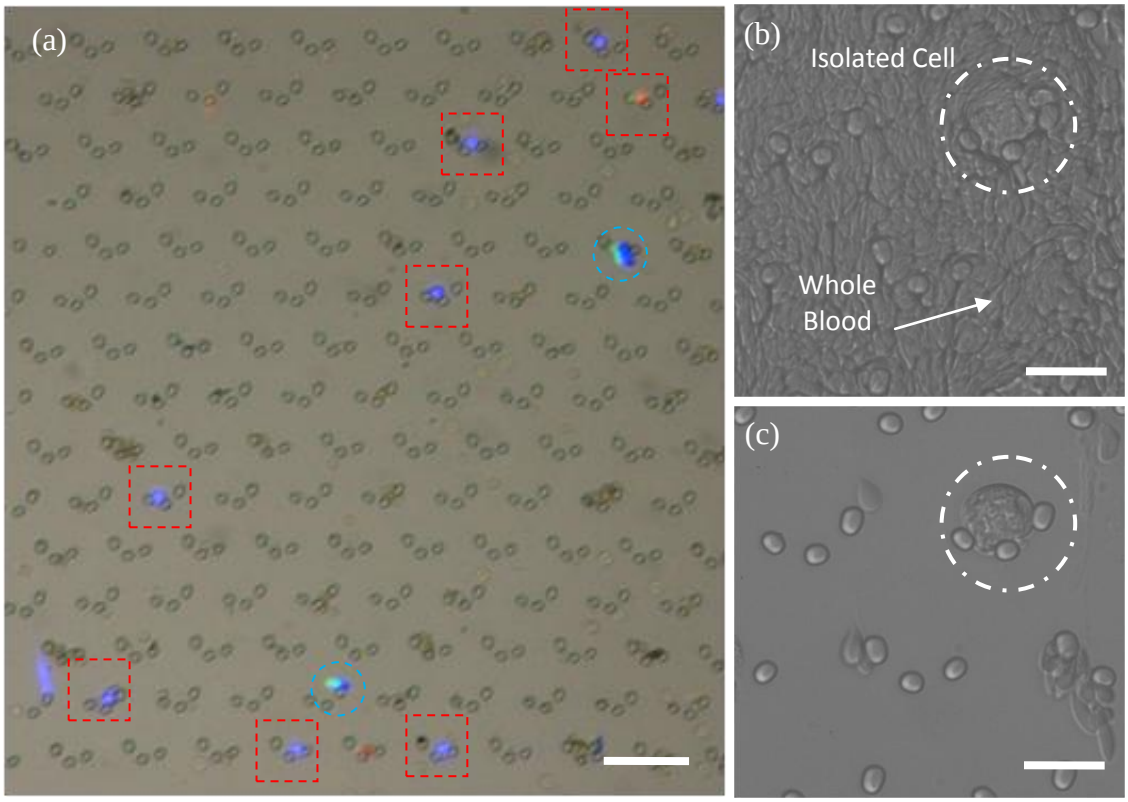

Figure 6.3 CTCs detection from the peripheral blood of cancer patients. (a) Overview of one compartment in the microdevice. The red squares highlights the confirmed CTCs isolated from blood specimens and the circle encompasses the WBCs. Scale bar represents 50 µm (b) Real time visualization of the blood processing process. Scale bar represents 20 µm (c) Same view of the isolated cell after a washing cycle which removes blood residues. Scale bar represents 20 µm.

The stability of the microdevice to process blood samples is important as it determines the overall effectiveness of the system. This prevents wastage of valuable samples and allows for the logistic planning of blood extraction to maximize output. Figure 6.3 illustrates the overview of the interior of the microdevice after the processing of blood. The isolated cells underwent a secondary detection procedure using immunofluorescence to further confirm their status and to allow a comparable platform with other techniques.

Figure 6.3a depicts the overview of a compartment of isolation traps in the microdevice after the staining process which clearly distinguishes apart the CTCs from residual hematopoietic cells that remains in the system. Figure 6.3b and 6.3c show the intermediary steps during the blood processing and washing cycle that removes blood residual off the microdevice. The isolated cells can then proceed further for immunofluorescence detection for CTCs. A clear imagery of isolated cells was seen in real time during blood processing as whole blood passes through the microdevice. Being optical transparent and compatible with existing microscopes, the microfluidic device and the setup permitted visualization during the process, allowing corrections to the system if errors or clumps enter the platform. In addition, cells that are of larger dimensions and higher stiffness will be actively impeded and can be observed instantaneously.

A total of 119 blood specimens from both healthy volunteers and RCC patients are analyzed and summarized in table 6.2. We extracted 20 control samples from 10 healthy volunteers and 99 specimens from 32 renal cancer patients. Hence, an average of 2 samples was taken from each healthy volunteer and 3 from each cancer patient. Samples are categorized by the duration of storage before blood processing and gauged by the microdevice's ability to successfully analyze these samples. As noted earlier, the quality of the samples are of paramount importance to the successful blood processing. For healthy volunteers, blood processing through the microdevice either before or after 24 hrs possed no significant problems. However, for RCC patients, the stability of the system was 85.5% for samples that were being processed within 24 hrs after blood extraction. A significant decline was also seen with older samples that were kept for more than 24 hrs

Table 6.2 Stability of the microfluidic device on the detection of circulating tumor cells in peripheral blood of healthy volunteers and metastatic RCC patients

	No of subjects	Sample Size	<24hrs (+ve)	<24hrs (-ve)	≥24hrs (+ve)	≥24hrs (-ve)	Stability <24hrs	Stability ≥24hrs
Healthy subjects	10	20	10	0	10	0	100%	100%
RCC patients	32	99	71	12	2	14	85.5%	12.5%

as shown in table 6.2. The discrepancies are attributed to the fast deterioration of clinical samples where large clumps start to form over time in the stationary EDTA tubes. These are likely incurred during the idle and transportation times. As the microdevice operates within a small enclosed volume, such coagulated materials are detrimental to the blood processing and likely to obstruct the microfluidic device.

It is thus recommended that the storage to processing time be kept within 24 hrs after blood extraction. Furthermore, to prevent the formation of precipitates in the specimen, it is proposed to keep specimens cool and under a slight agitation using a slow rocking mechanism on a shaker until blood processing is available.

6.1.4 Sensitivity for CTCs Detection using Physical Separation

The detection of CTCs in RCC is attractive as it is reported that the dissemination of tumor cells into the circulation is an early event (Blumke, Bilkenroth et al. 2005). Studies

have also shown that CTCs are present in RCC patients with different tumor grades (McKiernan, Buttyan et al. 1999), indicating a high probability of detecting these circulating cells. There are reported significant prognostic values of CTCs enumeration for RCC patients (Buchner, Riesenberg et al. 2006; Bluemke, Bilkenroth et al. 2009) and current methods focuses on immunomagnetic separation to enrich CTCs (Bilkenroth, Taubert et al. 2001; Allard, Matera et al. 2004). The sensitivities of such systems can be affected by the selection of antibodies during enrichment, as specific renal tumor markers are lacking (Loberg, Fridman et al. 2004). Physical methods are attractive as it does not rely upon specific biomarkers on the tumor cells and are efficient in cell separation (Pamme 2007). The lung, being a prominent site for secondary tumor formation (Assouad, Petkova et al. 2007) is an excellent in vivo example to illustrate that size based arrest of tumor cells are possible. As shown in various reports, the lung has been effective at arresting CTCs by impeding them in small capillaries and exerting lethal mechanical trauma to these cells, which contributes to the inefficiency of the metastatic process (Weiss and Dimitrov 1986).

Analogous to the principle of CTCs trapping in the lungs, the microdevice provides an efficient enrichment process using the physical differences of CTCs to blood constituents. By controlling the flow conditions inside the microdevice, the highly deformable erythrocytes (Shelby, White et al. 2003) and leukocytes (Yap and Kamm 2005) are removed as these cells traverse through without much difficulty, and arresting CTCs which are generally larger and less deformable. Figure 6.3a shows the successful isolation of cells with positive responses for pan-cytokeratin and DAPI. A summary of

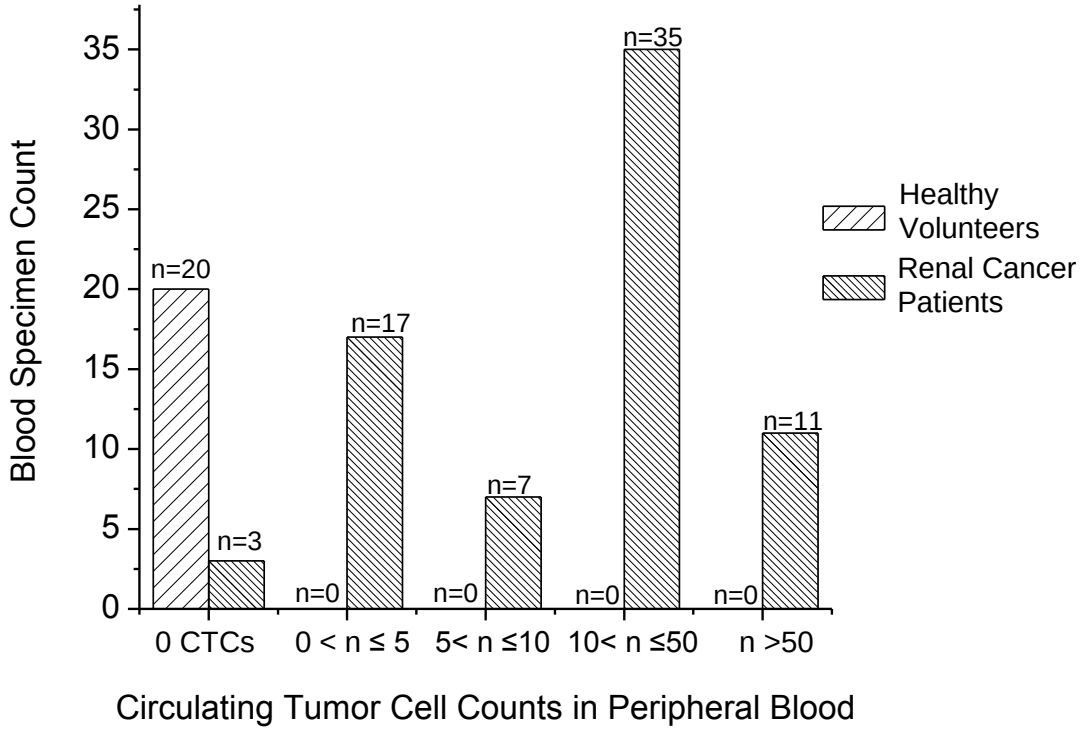

Figure 6.4 Isolated CTC count in renal cancer patients blood in comparison with healthy volunteers. The variable n denotes the number of specimens within the range.

the results are presented in figure 6.4 and table 6.3. A total of 73 blood samples from renal cancer patients which have been successfully processed by the system are tested using immunofluorescence staining for pan-Cytokeratin, CD45 and DAPI. A positive count of CTC is determined to be pan-Cytokeratin positive, CD45 negative and DAPI positive. A close up view of isolated CTCs and WBCs are illustrated in figure 6.5. The secondary anti-bodies which are tagged to the fluorophores determine the colour of the stains and can be interchange based on the complementary pair on the primary anti-body. The selection of anti-bodies using this technique is thus versatile and can be tailored to suit the needs of the analysis. Figure 6.5 shows CTCs which are tagged with

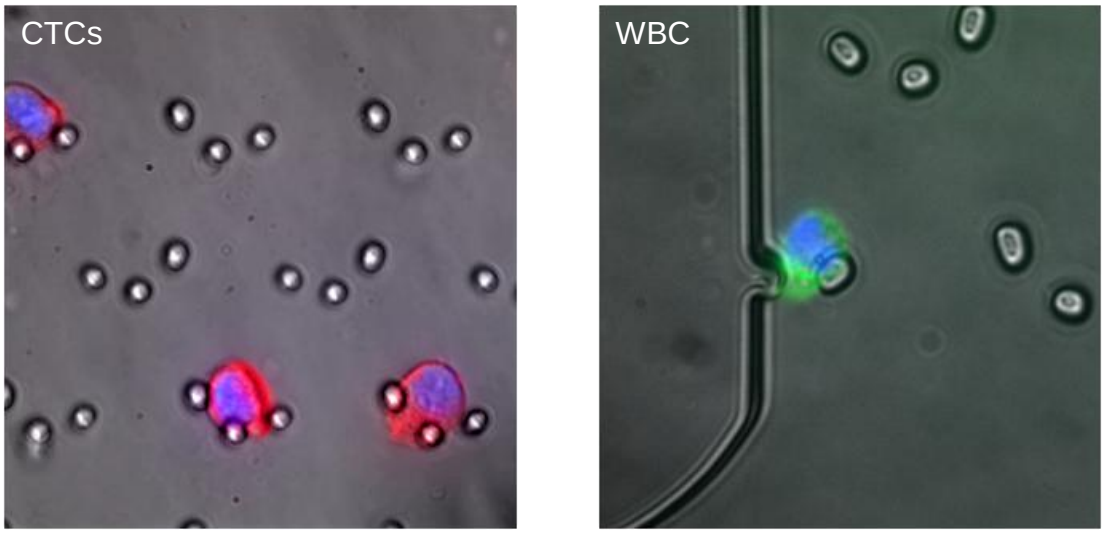

Figure 6.5 General view of the microdevice showing isolated CTCs (pan-cytokeratin positive, CD45 negative, DAPI positive) and a hematopoietic cell (pan-cytokeratin negative, CD45 positive, DAPI positive).

Table 6.3 Summary of CTCs enumeration with metastatic renal cell carcinoma patients showing the sensitivity and purity of the system

	Sample Size	Mean ± SD	Positive Rate	Average Purity ± SD
Healthy volunteers	20	0	0%	NA
RCC patients	73	27 ± 35	95.9%	71.5 ± 28.6%

Alexafluor 568 showing a red fluorescence and can be readily changed with other secondary antibodies to display CTCs in other colours. CTCs are detected in 70 out of 73 samples, achieving a 95.9% detection rate in RCC patients.

This is a significant increase in sensitivity comparing with previous studies (Allendorf, Ippagunta et al. 2004) and is likely a result of the direct processing of whole blood and

the redundancy of a selection antibody used in immunomagnetic separation. By processing whole blood directly, it minimizes any potential loss from any intermediary preparation steps and the isolation methodology retains every cell that are physically different. For the samples tested, an average count of 27 CTCs was detected in the peripheral blood from all patient samples. Furthermore, the spread of the data comparing across different specimens was contrasting which can be useful to better differentiate and gauge the severity of the disease. Previous studies by Allard et al. (Allard, Matera et al. 2004) presented a 25% detection rate using CellSearch's affinity based separation and having positive samples with 2 cells or less with renal cancer patients. Such detection numbers are likely to pose issues in the linearity of the results as mentioned in section 6.1.2 which may be erroneous when used to determine the average concentration of CTCs in peripheral blood. Using the same data range, it was observed that there was a better spread of samples in each of the data bins as illustrated in figure 6.4. However, it was noted that the nature of the samples and patients conditions presented were different in both cases which could be the reason for the dissimilarities as well. This also made a direct comparison difficult.

For the capture purity in the microdevice, the average rate was approximately 71.5% and a 95% confidence interval of 64.9% to 78.1%. The large spread of purity values was likely a direct consequence of the different conditions of blood being processed. It was observed that the quality of samples was an important parameter in obtaining good capture purity. Samples that were significantly deteriorated tend to have more WBCs trapped after blood processing.

Nonetheless, achieving a 95.9% positive detection rate from a random selection of renal cancer patients proved the technology promising in the detection of CTCs. We had also achieved a significant sensitivity for the investigated set of blood specimens using the microdevice with an average detection rate of 27 tumor cells. The platform will provide a sensitive and accurate measure of the quantity of CTCs in peripheral blood for various clinical applications. For control experiments, there were no positive responses from healthy volunteers, signifying the specificity of the technique with RCC patients' blood samples.

6.1.5 Heterogeneous Behaviour in RCC CTCs

The molecular characteristics are different for various cancer types and thus it is expected that such variations manifest in the circulating cells as well. Comparing against cancer of different origins, it is reported that these distinct divergent features are important to achieve a good understanding of the disease and for prognostic purposes (Riethdorf, Wikman et al. 2008; Steen, Nemunaitis et al. 2008). Within circulating cells of the same type, such disparities are also present. Sieuwerts et al. (Sieuwerts, Kraan et al. 2009) observed that for breast cancer cell lines, a diverse expression pattern of EpCAM existed which may limit its usefulness in it use for cell separation as potential cancer cells with low EpCAM levels are not detected. Hautkappe et al. (Hautkappe, Lu et al. 2000) also reported the detection of specific mutations in the von Hindel-Lindau tumor-suppressor gene in CTCs of renal cancer patients, showing diversities in cancer cell populations.

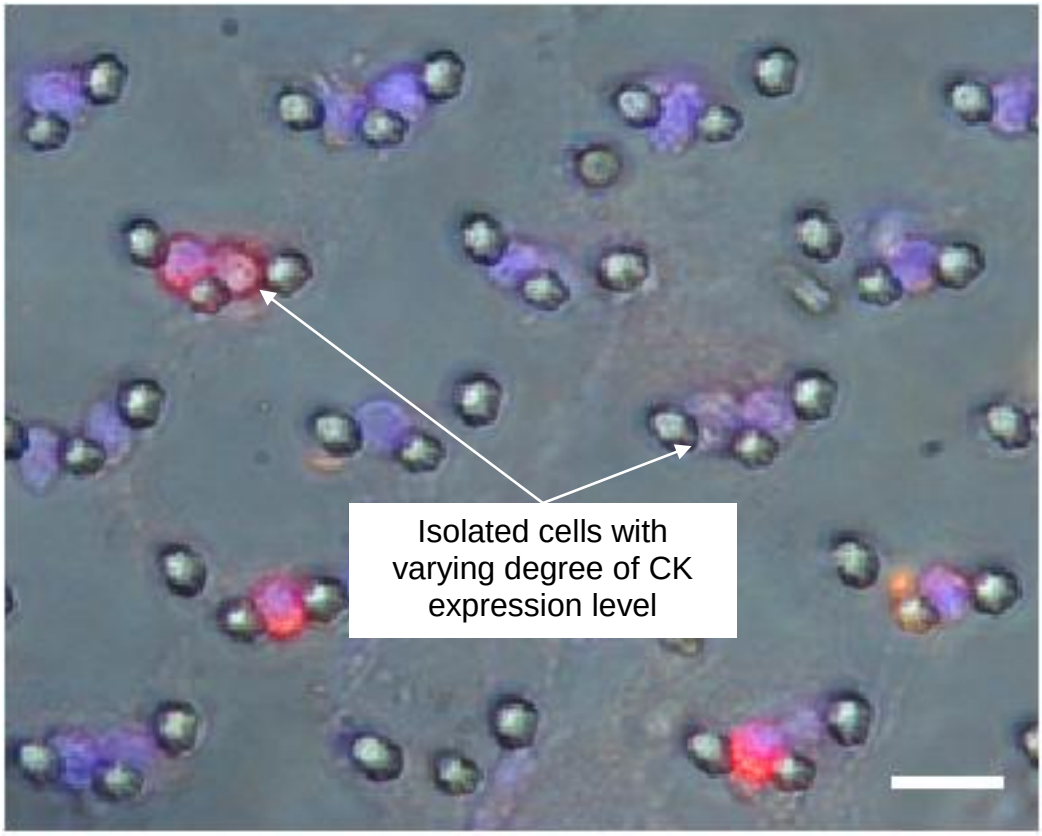

Figure 6.6 Isolated cells from peripheral blood of patients. Identification using pan-cytokeratin (red) on the isolated cells. Scale bar represents 20 μm.

These studies demonstrated that the pursuit to decipher the differences that existed in CTCs will be clinical beneficial.

We had also observed various heterogeneous behaviours in the isolated CTCs from renal cancer patients in the microdevice. A clear distinction was in the pan-cytokeratin expression levels detected across different blood specimens, which was used to confirm the presence of CTCs. Within isolated cells in the sample blood sample, the expression patterns were also varied and could be clearly observed under the microscope. Figure 6.6

depicts a fluorescent image of isolated cells from a patient's peripheral blood which clearly demonstrated CTC variants having different pan-cytokeratin expression levels. Most of the isolated CTCs tend to show weak pan-cytokeratin staining while small proportions display distinct expression levels. These results are in coherence with previous studies conducted by Blumke et al (Blumke, Bilkenroth et al. 2005), having shown using immunocytochemistry that cytokeratin expression levels in RCC CTCs differs. The observation is intriguing and likely to suggest the presence of diverse populations of cells within the same cancer type in our specimens.

In addition, another interesting result from our tests shows a diverse variation in cell sizes of CTCs. The different dimensions of cells were rather uniformly distributed for all the CTCs isolated from the 73 blood samples. The difference between the smallest and largest cell was however rather distinct with isolated CTCs as small as 8 μm to cells as large as 30 μm which were pan-cytokeratin positive, CD45 negative and DAPI positive. Figure 6.7 is a clear illustration of the differences, with the isolated cells in the traps and showing positive responses fluorescently for CTC markers. The voluminous ratios of the cell nucleus to its cytoplasm were large which typically are characteristics observed in cancer cells. These are features that can be observed in figures 6.6 and 6.7 and also in all other isolated cells from the tests.

The design of the microdevice initially targeted to hold cells in the size range of 15 μm to 25 μm, and the presence of smaller cells resulted in traps holding more than 1 cell at times. The ability to hold CTCs below the desired range indicated that the stiffness of the

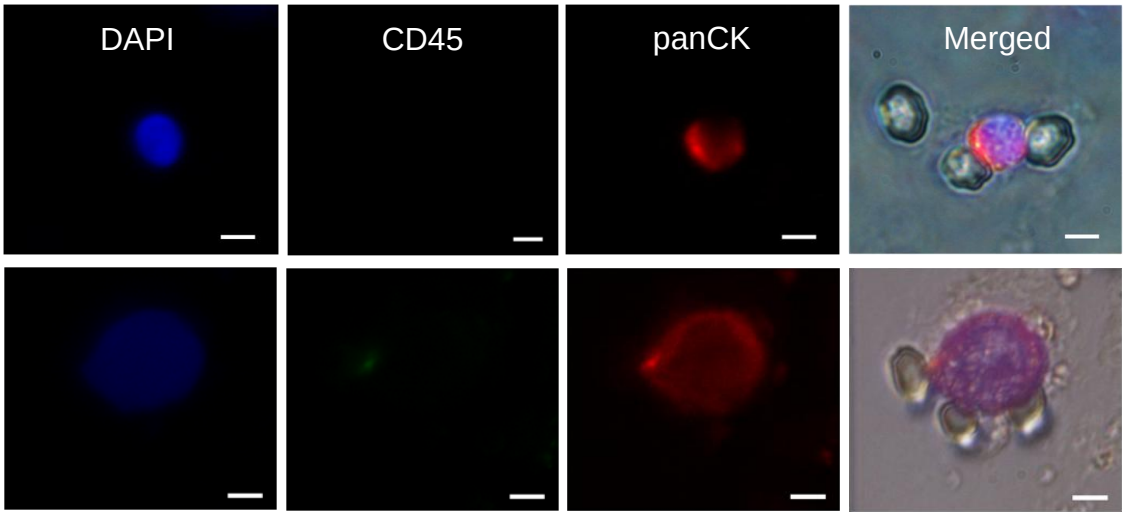

Figure 6.7 Isolated cells from peripheral blood of RCC patients and immunofluorescence staining in situ on chip. (b) Isolated CTCs of various sizes showing pan-cytokeratin positive, CD45 negative and DAPI positive. Scale bar represents 5 µm.

cells is significantly dissimilar enough to be impeded by the isolation structures. An example of trapping a small CTC is visibly demonstrated in figure 6.7. The results are also likely to indicate the diverse and complex nature of CTCs in haematogenous metastasis. It concurs with various hypotheses from numerous studies that a diverse group of circulating cells are present in peripheral blood (Racila, Euhus et al. 1998; Sledge 2006; Pantel and Alix-Panabieres 2007; Pantel, Brakenhoff et al. 2008; Sastre, Maestro et al. 2008; Sergeant, Penninckx et al. 2008). The capability to isolate the different subtypes of CTCs is useful for further characterizations which might be valuable to disease prognostication and treatment monitoring.

6.1.6 CD44 Staining of CTCs in RCC patients

The system is shown to be suitable to handle the challenges involved in the finding of CTCs, with a high detection rate in the peripheral blood of cancer patients. Heterogeneity of the circulating cells are also important study parameters and physical techniques for enrichment and detection of CTCs will further the endeavour. By using cell and deformability of cells for tumor cell isolation, it relies solely upon the differences in biorheological properties and will retain all cells that are significantly different than blood constituents. This is in contrast to the use of biomarkers for CTCs enrichment which select a specific cell population as the markers are not entirely universal. Thus, the outcomes of using physical separation are likely to encompass a more diverse and unbiased range.

From the trials, 94.5% of the 73 blood samples presented additional mono-nucleated cells that were negative for both pan-cytokeratin and the hematopoietic marker (CD45). Though they were negative for standard CTCs selection markers, their physical characteristics such as the voluminous ratio of their nucleus to cytoplasmic content were large which was suggestive that they might be cancer cells. Furthermore their lack of positive response to hematopoietic markers indicated that these cells were not of blood origin. Blumke et al (Bluemke, Bilkenroth et al. 2009) also reported the presence of cytokeratin negative large cells in RCC patients using a CD45 depletion technique that removes leukocytes in an enriched sample after density gradient centrifugation, which showed that there were probably significant numbers of cancer cell subpopulations in

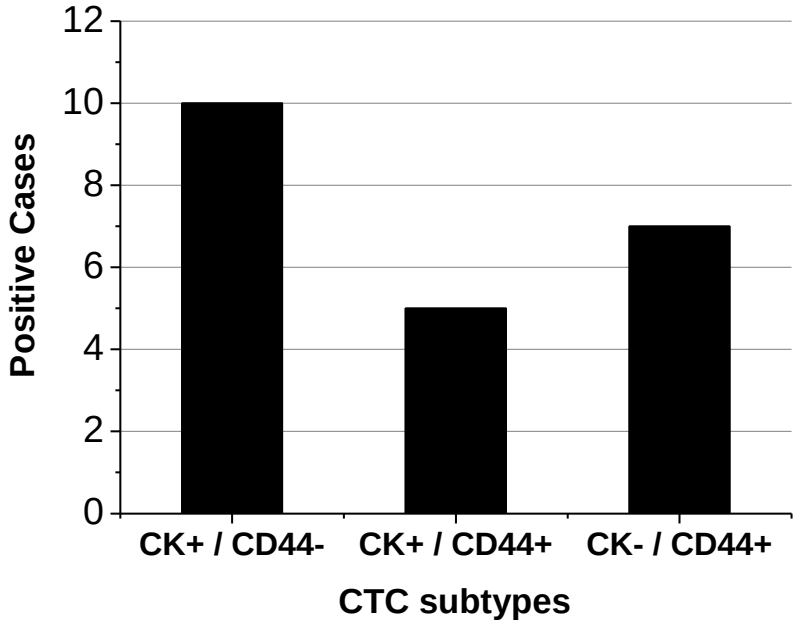

Figure 6.8 Investigation of the CD44 expression patterns on the isolated cells in RCC patients.

peripheral blood. It should be noted that these samples used in our tests were derived from patients with metastatic renal cell carcinoma, and may not represent the entire spectrum of patients with RCC.

CD44 that belongs to a family of transmembrane glycoprotein is shown to be associated with p53 expression (Zolota, Tsamandas et al. 2002) and has prognostic potential in RCC (Paradis, Ferlicot et al. 1999). Studies have also revealed strong correlations of CD44 expressions to tumor differentiation and cancer progression (Heider, Ratschek et al. 1996; Terpe, Storkel et al. 1996; Masuda, Takano et al. 1999). We investigated the expression patterns of CD44 standard form in CTCs by direct immunofluorescence techniques and staining the isolated cells in situ. 10 samples were randomly selected from the entire tests

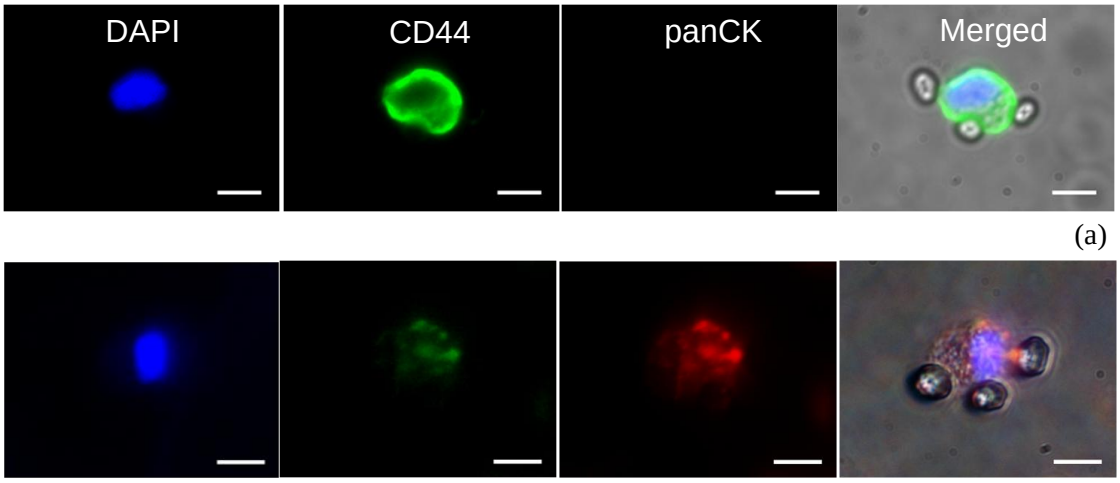

Figure 6.9 Immunofluorescence staining of pan-Cytokeratin and CD44 in RCC CTCs which show a heterogeneous cell population in the isolated cells by the microdevice. (a) Isolated cell with CD44 positive, pan-cytokeratin negative and DAPI positive. (b) Isolated cell with CD44 positive, pan-cytokeratin positive and DAPI positive. Scale bars represent 10 μm.

and repeated for the detection of pan-cytokeratin, CD44 and DAPI. We allowed the samples to be processed in parallel with two different microdevices at the same time, using blood samples from the same EDTA tubes. Different sets of primary antibodies are then added during the immunofluorescence staining process. The results are summarized in figure 6.8 with all the samples having a proportion of isolated cells positive for the standard CTC markers (pan-cytokeratin positive, CD45 negative and DAPI positive). In the parallel setup, 3 subtypes could be seen, namely isolated cells that were pan-cytokeratin positive/CD44 negative; both positives and pan-Cytokeratin negative/CD44 positive. A proportion of the isolated cells from all 10 samples were pan-Cytokeratin positive/CD44 negative. 5 out of 10 samples had isolated cells that were positive for both and 7 out of 10 had isolated cells only for CD44. Figure 6.9 shows a typical analysis from the samples illustrating the distinct expression patterns that are present. The results are indicative of the occurrence of CTC subtypes and the complex nature of tumor cells

dissemination into the blood circulation. The lack of CD44 in normal renal cells (Paradis, Ferlicot et al. 1999) suggest that CD44 can be a strong prognostic factor to detect CTCs in peripheral blood.

6.2 Non Small Cell Lung Cancer (NSCLC) and Nasopharyngeal Cancer (NPC)

Having optimized the system with controlled parameters described in chapter 5, the microdevice was tested initially on blood specimens from renal cancer patients. The benefits of CTC enumeration are being less invasive than surgical biopsies and can potentially be more responsive to the state of health of cancer patients (Mocellin, Hoon et al. 2006; Riethdorf, Wikman et al. 2008). In addition, it can provide an alternative source of tumor tissue for the detection, characterisation and monitoring of non-blood-related cancers (Maheswaran, Sequist et al. 2008; Panteleakou, Lembessis et al. 2009). The technique proposed in this report uses a microfluidic device which isolates CTCs directly from whole blood using purely rheological differences. Tumor cells which lack certain blood characteristics made them physically distinct from blood cells. This feature is probably not restricted to renal cancer alone and has been clearly demonstrated with a diverse range of cancer cell lines tested. The technique is potentially universal to handle most cancer types of non hematologic origin.

In a subsequent study, the platform was tested on clinical blood specimens from patients suffering from lung and nasopharyngeal cancer. Blood extraction followed protocols set out in sections 3.4 and 3.9 after obtaining consent from patients for the tests, as stipulated

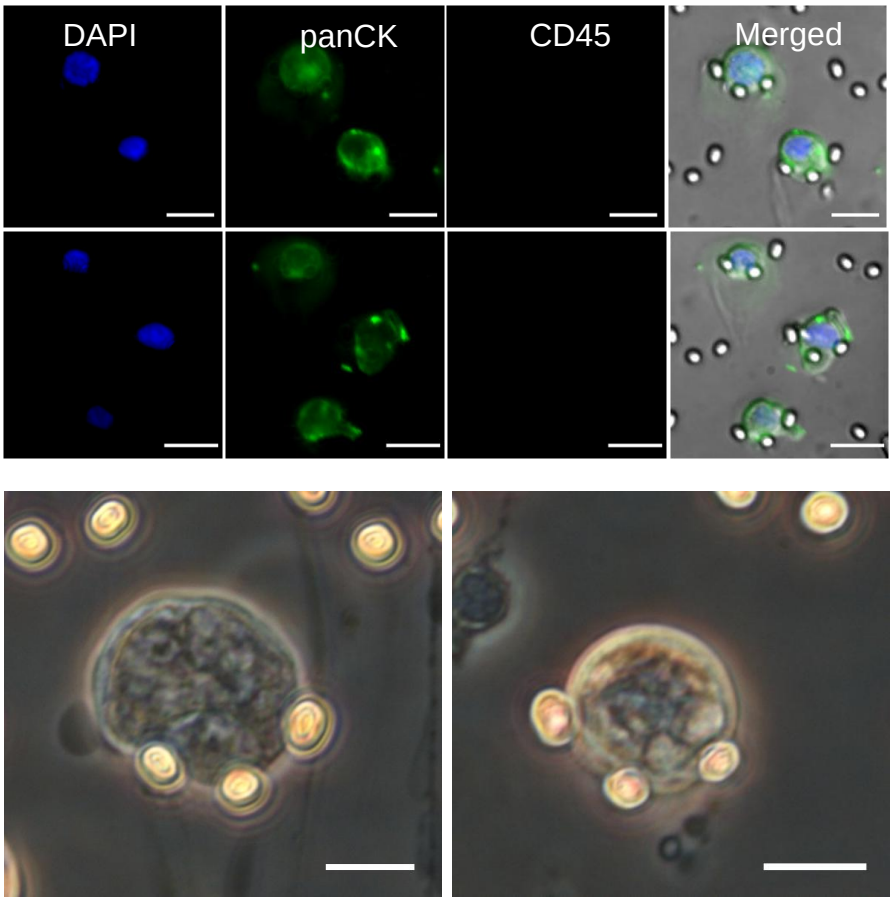

Figure 6.10 CTC isolation from clinical blood samples of metastatic lung cancer patients. (a) Immunofluorescence staining of isolated cells to identify cancer and hematopoietic cells. Scale bar represents 20 µm. (b) Phase contrast images of isolated CTCs after blood processing. Scale bar represents 10µm.

by the Institutional Review Board. The study is currently ongoing in parallel with other trials. For the tests on NSCLC and NPC, a total of 7 patients are currently involved in the trials. Figure 6.10 shows some of the isolated cells from the blood specimens. The isolated cells underwent an immunofluorescent labeling for cytokeratin, CD45 and DAPI which was similar to the procedures performed on RCC samples. Figure 6.10a shows the positively identified tumor cells from lung cancer patients. The isolated cells also showed typical large cell nucleuses which are clearly visible in figure 6.10b. Other physical

Table 6.4 CTCs isolation and detection from peripheral blood of metastatic lung cancer patients using the proposed microdevice.

Specimen Number	Cancer Origin	Volume Processed	Positive CTC count	WBC	Isolation Purity (%)
1	NSCLC	2 ml	30	4	88.2
2	NSCLC	2 ml	84	10	89.4
3	NSCLC	2 ml	82	10	89.1
4	NSCLC	2 ml	20	8	71.4
5	NSCLC	2 ml	36	11	76.6
6	NSCLC	2 ml	166	4	97.6
7	NSCLC	2 ml	79	3	96.3
8	NSCLC	2 ml	3	1	75.0
9	NPC	2 ml	70	2	97.2

characteristics concur with earlier deductions such as isolated cells display a wide range of sizes and were heterogeneous in behavior.

Table 6.4 summarizes the CTCs isolation and detection of NSCLC and NPC specimens. A 100% detection rate was achieved for both cancer types. This was indicative of the suitability of the technique and the microdevice to perform the tasks. Comparing with leading technologies on CTC enumeration for lung cancer (Allard, Matera et al. 2004; Maheswaran, Sequist et al. 2008), the sensitivity of the system showed comparable isolation efficiencies to work on patients' blood samples. An average cell count of 63 cells was obtained with specimens from lung cancer patients and a positive count of 70 cells for the NPC specimen. An average capture purity of 85.5% was achieved for lung cancer samples and a 95% confidence interval gave the range from 78.6% to 92.3%.

Table 6.5 Summary of CTC counts in 2ml of whole blood from patients with various types of carcinomas

	No of study subjects	No of Specimens	Mean	n = 0	n ≤ 5	≤ 10	≤ 50	> 50
Healthy Volunteers	10	20	0	20	0	0	0	0
RCC	32	73	27	3	17	7	35	11
NSCLC	6	8	63	0	1	0	3	4
NPC	1	1	70	0	0	0	0	1

The results from the tests showed a high signal to noise ratio that is beneficial for downstream processing, especially for the molecular detection methods to avoid false positives. It is also evident that physical dissimilarities between CTCs and blood constituents are significant in peripheral blood of cancer patients for an efficient tumor cell enrichment and separation. The methodology for the separation and isolation of CTCs from blood offers a new perspective to current performed techniques and will aid clinical applications to target the disease.

A sum up of all the results from clinical samples is shown in table 6.5. With clinical blood specimens from cancer patients, it is demonstrated that the system is sensitive to rare CTCs from various cancer types. This is potentially useful to gauge the disease severity, drug monitoring and prognostic purposes in clinical practices, which will hopefully aid and raise the patients' quality of life. The microdevice is specific in its blood processing which showed negative responses from all 10 healthy volunteers who participated in the study. The CTCs yield from the isolation process was large and

covered a wide range as shown in table 6.5. This is valuable to the further analyses of CTCs in cancer patients to better understand the disease.

Chapter 7 Conclusions and Future Work

7.1 Conclusions

Cancer metastasis is the key attribute to cancer-related deaths and much remains to be explored about this phenomena. Evolving techniques for isolating CTCs represents an unprecedented opportunity for clinical and biological insight into the nature of metastasis and cancer. In the present study, it is demonstrated that a microfluidic setup can yield an accurate and sensitive measure of CTCs in peripheral blood. CTCs which represent tumor cells in the blood circulation of cancer patients are likely to be useful and associated to the disease. The basis for an effective isolation of CTCs is to utilize their inherent physical differences of size and deformability from blood cells in a microfluidic system. With the platform, the objectives are to study these cells in circulation, with hopes to understand their characteristics in relation to the metastatic process.

Using computational analysis, various design layouts were put forward and tested in a systematic and controlled manner to show that the proposed system was plausible to handle the tasks. The proposed system was then tested with spiked samples using numerous cancer cell lines. Results from the tests showed that the microfluidic platform is successful in the isolation of various cancer cell types. The microdevice also achieved significant cancer cell isolation purity while preserving the integrity and state of these cells. Furthermore, the microfluidic platform is versatile, being capable of handling diverse cancer cell lines with minimal noise and yet maintaining cell viability and

phenotype through a gentle and straightforward processing. More importantly, the system is label-free, isolating cells in an unbiased fashion, and sensitive to detect small cancer cell count in the specimens. Through the use of distinctive biomechanical characteristics of the cells, neither functional modification nor complex enrichment procedures were required. Being label free also helped to address numerous concerns linked to affinity based isolation methods. Operational procedures were straightforward as minimal preparations were needed for the microdevice and samples. Cancer cells were captured in a single processing step thereby minimizing potential cell losses during intermediary procedures. Furthermore, immunofluorescence staining could be done in situ inside the microdevice as the system is optical transparent and designed to be integrated onto existing microscopes. Given the simplicity of the processing procedures, multiplexing of the system to concurrently run numerous samples is straightforward, which allowed processing and testing more parameters at the same time.

With clinical blood specimens from patients suffering from various cancer types, there was positive CTC detection in the preliminary studies, which was also promising for the isolation of viable cells. The microdevice which separates CTCs in a single step, without requiring biochemical modifications is attractive to maximize the yield for downstream analyses to enhance the understanding of the disease, and complement current cancer detection and prognosis techniques. Results obtained from RCC peripheral blood samples highlighted the heterogeneous nature of CTCs in haematogenous metastasis which presented variations in cell dimensions and pan-cytokeratin expression levels. The isolated cells also revealed the presence of CD44 in CTCs arising from the peripheral

blood of RCC patients which had shown in previous immunohistochemistry studies to have strong correlations to tumor progression. The microfluidic platform was capable of isolating the different subtypes of CTCs which is useful for further characterizations. The microsystem also allowed for real time visualization of the isolation process. With blood specimens from lung and nasopharyngeal cancer, the investigation presented a strong affinity to enrich and isolate these cells. The microdevice which separates CTCs in a single step without requiring biochemical modifications, is attractive for applications in oncology research particularly prognostication and prediction of drug response.

7.2 Recommendations

Moving forward, the system is currently in the process of testing various clinical specimens from cancer patients to determine the disease correlation, as well as to engage in the study of the epigenetics of the disease. Most clinical trials are currently still in progress and as the tests are done single blinded, such data are not available at this time. These trials are likely to continue over an extended period to track the progress of the patients. The work is also expected to expand into the molecular aspects of the problem which will help to identify genes and proteins that are involved in the disease. The current system can be optimized to fulfill the objectives by providing access to the recovered cells for DNA extraction and fluorescence in situ hybridization (FISH) analyses. With multiplexing of the setup to be straightforward as demonstrated, these parameters can be examined concurrently.

Furthermore, there are interests in the culture of CTCs in vitro and the system might be well poised to address these issues. Current limitations in this aspect of the study is in getting enough living cells for culture and may be addressed with larger volumes of extracted blood from the patients. The system will then have to be scaled up to meet the volume requirements. In addition, to improve upon current work, the designs of the isolation traps can be modified. For instance, a diverse range of cell diameters were observed in isolated CTCs which led to multiple cells within each isolation trap in some instances. A slight modification of design to have different sizes of traps in the same microdevice will address the discrepancies.

Minor improvements to the blood processing procedure may be implemented in the future such as the incorporation of an automated CTC counter from the isolation traps. This is crucial with the scaled up system meant for processing larger blood volumes, as it will likely incur a higher probability of human error during cell enumeration. Automated CTC counting will also ensure consistencies in the tests. Further efforts to improve upon the design of the microchip to allow greater flexibility in processing blood samples are also currently being pursued. Finally, it is of interest to explore other microdevice designs in the future work that utilizes similar separation mechanisms of CTCs from whole blood with the objectives of achieving better isolation efficiencies and shorter blood processing time.

In summary, our platform provides a unique opportunity to study the systemic circulation and activity of cancer in a simple, accessible and unbiased fashion over time. We anticipate its use in disease prognosis and therapeutic monitoring, thereby permitting personalization of therapy.

References

Allard, W. J., J. Matera, et al. (2004). "Tumor cells circulate in the peripheral blood of all major carcinomas but not in healthy subjects or patients with nonmalignant diseases." Clin Cancer Res **10** (20): 6897-6904.

Allendorf, J., N. Ippagunta, et al. (2004). "Management of liver metastases: new horizons for biologically based therapy." J Surg Res **117** (1): 144-153.

Ashida, S., H. Okuda, et al. (2000). "Detection of circulating cancer cells with von hippel-lindau gene mutation in peripheral blood of patients with renal cell carcinoma." Clin Cancer Res **6** (10): 3817-3822.

Ashworth, T. R. (1869). "A case of Cancer in which cells similar to those in the Tumours were seen in the blood after death." Aust Med J **4**: 146-147.

Assouad, J., B. Petkova, et al. (2007). "Renal Cell Carcinoma Lung Metastases Surgery: Pathologic Findings and Prognostic Factors." Ann Thorac Surg **84** (4): 1114-1120.

Baeuerle, P. A. and O. Gires (2007). "EpCAM (CD326) finding its role in cancer." Br J Cancer **96** (3): 417-423.

Balic, M., N. Dandachi, et al. (2005). "Comparison of two methods for enumerating circulating tumor cells in carcinoma patients." Cytometry B Clin Cytom **68** (1): 25-30.

Bashir, R. (2004). "BioMEMS: state-of-the-art in detection, opportunities and prospects." Advanced Drug Delivery Reviews **56** (11): 1565-1586.

Basso, U., E. Rossi, et al. (2009). "7117 Do circulating tumor cells (CTCs) correlate with response to first-line sunitinib in metastatic renal carcinoma?" European Journal of Cancer Supplements **7** (2): 428-428.

Becker, S., G. Becker-Pergola, et al. (2006). "Detection of cytokeratin-positive cells in the bone marrow of breast cancer patients undergoing adjuvant therapy." Breast Cancer Res Treat **97** (1): 91-96.

Beitsch, P. D. and E. Clifford (2000). "Detection of carcinoma cells in the blood of breast cancer patients." Am J Surg **180** (6): 446-448; discussion 448-449.

Berois, N., M. Varangot, et al. (2003). "Detection of bone marrow-disseminated breast cancer cells using an RT-PCR assay of MUC5B mRNA." Int J Cancer **103** (4): 550-555.

Bilkenroth, U., H. Taubert, et al. (2001). "Detection and enrichment of disseminated renal carcinoma cells from peripheral blood by immunomagnetic cell separation." Int J Cancer **92** (4): 577-582.

Bluemke, K., U. Bilkenroth, et al. (2009). "Detection of Circulating Tumor Cells in Peripheral Blood of Patients with Renal Cell Carcinoma Correlates with Prognosis." Cancer Epidemiology Biomarkers & Prevention **18** (8): 2190-2194.

Blumke, K., U. Bilkenroth, et al. (2005). "Detection of circulating tumor cells from renal carcinoma patients: experiences of a two-center study." Oncol Rep **14** (4): 895-899.

Boxshall, K., M.-H. Wu, et al. (2006). "Simple surface treatments to modify protein adsorption and cell attachment properties within a poly(dimethylsiloxane) micro-bioreactor." SURFACE AND INTERFACE ANALYSIS **38** (4): 198-201.

Braun, S., F. Hepp, et al. (1999). "Tumor-antigen heterogeneity of disseminated breast cancer cells: Implications for immunotherapy of minimal residual disease." Int J Cancer **84** (1): 1-5.

Brodland, D. G. and J. A. Zitelli (1992). "Mechanisms of metastasis." J Am Acad Dermatol **27** (1): 1-8.

Broll, R., K. Lembcke, et al. (1996). "[Tumor cell dissemination in bone marrow and peritoneal cavity. An immunocytochemical study of patients with stomach or colorectal carcinoma]." Langenbecks Arch Chir **381** (1): 51-58.

Brooks, D. E. (1984). "The biorheology of tumor cells." Biorheology **21** (1-2): 85-91.

Brunsvig, P. F., K. Flatmark, et al. (2008). "Bone marrow micrometastases in advanced stage non-small cell lung carcinoma patients." Lung Cancer **61** (2): 170-176.

Buchner, A., R. Riesenberg, et al. (2006). "Frequency and prognostic relevance of disseminated tumor cells in bone marrow of patients with metastatic renal cell carcinoma." Cancer **106** (7): 1514-1520.

Budd, G. T., M. Cristofanilli, et al. (2006). "Circulating tumor cells versus imaging--predicting overall survival in metastatic breast cancer." Clin Cancer Res **12** (21): 6403-6409.

Chambers, A. F., A. C. Groom, et al. (2002). "Dissemination and growth of cancer cells in metastatic sites." Nat Rev Cancer **2** (8): 563-572.

Chang, S. F., C. A. Chang, et al. (2008). "Tumor cell cycle arrest induced by shear stress: Roles of integrins and Smad." Proc Natl Acad Sci U S A **105** (10): 3927-3932.

Chang, Y. S., E. di Tomaso, et al. (2000). "Mosaic blood vessels in tumors: frequency of cancer cells in contact with flowing blood." Proc Natl Acad Sci U S A **97** (26): 14608-14613.

Chaudhury, M. K. and G. M. Whitesides (1991). "Direct measurement of interfacial interactions between semispherical lenses and flat sheets of poly(dimethylsiloxane) and their chemical derivatives." Langmuir **7** (5): 1013-1025.

Chen, X., D. F. Cui, et al. (2008). "Microfluidic chip for blood cell separation and collection based on crossflow filtration." Sensors and Actuators B: Chemical **130** (1): 216-221.

Cheng, X., J. Hochlowski, et al. (2003). "Studies on repository compound stability in DMSO under various conditions." J Biomol Screen **8** (3): 292-304.

Cohen, A. M., P. Garin-Chesa, et al. (1998). "In vitro detection of occult bone marrow metastases in patients with colorectal cancer hepatic metastases." Dis Colon Rectum **41** (9): 1112-1115.

Cohen, A. M., D. Kelsen, et al. (1997). "Adjuvant therapy for colorectal cancer." Curr Probl Surg **34** (8): 601-676.

Cohen, S. J., C. J. Punt, et al. (2009). "Prognostic significance of circulating tumor cells in patients with metastatic colorectal cancer." Ann Oncol.

Cote, R. J., P. P. Rosen, et al. (1991). "Prediction of early relapse in patients with operable breast cancer by detection of occult bone marrow micrometastases." J Clin Oncol **9** (10): 1749-1756.

Cristofanilli, M., K. R. Broglio, et al. (2007). "Circulating tumor cells in metastatic breast cancer: biologic staging beyond tumor burden." Clin Breast Cancer **7** (6): 471-479.

Cristofanilli, M., G. T. Budd, et al. (2004). "Circulating tumor cells, disease progression, and survival in metastatic breast cancer." N Engl J Med **351** (8): 781-791.

Cristofanilli, M., D. F. Hayes, et al. (2005). "Circulating tumor cells: a novel prognostic factor for newly diagnosed metastatic breast cancer." J Clin Oncol **23** (7): 1420-1430.

Davis, J. A., D. W. Inglis, et al. (2006). "Deterministic hydrodynamics: taking blood apart." Proc Natl Acad Sci U S A **103** (40): 14779-14784.

de Bono, J. S., H. I. Scher, et al. (2008). "Circulating tumor cells predict survival benefit from treatment in metastatic castration-resistant prostate cancer." Clin Cancer Res **14** (19): 6302-6309.

Delamarche, E., A. Bernard, et al. (1997). "Patterned delivery of immunoglobulins to surfaces using microfluidic networks." Science **276** (5313): 779-781.

Delamarche, E., H. Schmid, et al. (1997). "Stability of molded polydimethylsiloxane microstructures." Advanced Materials **9** (9): 741-746.

Di Carlo, D., J. F. Edd, et al. (2009). "Particle segregation and dynamics in confined flows." Phys Rev Lett **102** (9): 094503.

Di Carlo, D., J. F. Edd, et al. (2008). "Equilibrium Separation and Filtration of Particles Using Differential Inertial Focusing." Anal Chem **80** (6): 2204-2211.

Di Carlo, D., D. Irimia, et al. (2007). "Continuous inertial focusing, ordering, and separation of particles in microchannels." Proc Natl Acad Sci U S A **104** (48): 18892-18897.

Di Carlo, D., L. Y. Wu, et al. (2006). "Dynamic single cell culture array." Lab Chip **6** (11): 1445-1449.

Di Paolo, C., J. Willuda, et al. (2003). "A Recombinant Immunotoxin Derived from a Humanized Epithelial Cell Adhesion Molecule-specific Single-Chain Antibody Fragment Has Potent and Selective Antitumor Activity." Clinical Cancer Research **9** (7): 2837-2848.

Elshimali, Y. I. and W. W. Grody (2006). "The clinical significance of circulating tumor cells in the peripheral blood." Diagn Mol Pathol **15** (4): 187-194.

Ferlay J, S. H., Bray F, Forman D, Mathers C and Parkin DM. (2008). "Cancer Incidence and Mortality Worldwide: IARC CancerBase No. 10." International Agency for Research on Cancer, from http://globocan.iarc.fr

Fidler, I. J. (2003). "The pathogenesis of cancer metastasis: the 'seed and soil' hypothesis revisited." Nat Rev Cancer **3** (6): 453-458.

Flieger, D., A. S. Hoff, et al. (2001). "Influence of cytokines, monoclonal antibodies and chemotherapeutic drugs on epithelial cell adhesion molecule (EpCAM) and LewisY antigen expression." Clin Exp Immunol **123** (1): 9-14.

Fournier, R. L. (1998). Basic transport phenomena in biomedical engineering, Taylor & Francis.

Gilbey, A. M., D. Burnett, et al. (2004). "The detection of circulating breast cancer cells in blood." J Clin Pathol **57** (9): 903-911.

Gogas, H., G. Kefala, et al. (2002). "Prognostic significance of the sequential detection of circulating melanoma cells by RT-PCR in high-risk melanoma patients receiving adjuvant interferon." Br J Cancer **87** (2): 181-186.

Gomez, F. A. (2008). Biological Applications of Microfluidics. New Jersey, Wiley Interscience.

Gossett, D. R. and D. Di Carlo (2009). "Particle focusing mechanisms in curving confined flows." Anal Chem **81** (20): 8459-8465.

Gupta, G. P. and J. Massague (2006). "Cancer metastasis: building a framework." Cell **127** (4): 679-695.

Haier, J., M. Y. Nasralla, et al. (1999). "Beta1-integrin-mediated dynamic adhesion of colon carcinoma cells to extracellular matrix under laminar flow." Clin Exp Metastasis **17** (5): 377-387.

Harbeck, N., M. Untch, et al. (1994). "Tumour cell detection in the bone marrow of breast cancer patients at primary therapy: results of a 3-year median follow-up." Br J Cancer **69** (3): 566-571.

Hautkappe, A. L., M. Lu, et al. (2000). "Detection of germ-cell tumor cells in the peripheral blood by nested reverse transcription-polymerase chain reaction for alpha-fetoprotein-messenger RNA and beta human chorionic gonadotropin-messenger RNA." Cancer Res **60** (12): 3170-3174.

Hayes, D. F., M. Cristofanilli, et al. (2006). "Circulating tumor cells at each follow-up time point during therapy of metastatic breast cancer patients predict progression-free and overall survival." Clin Cancer Res **12** (14 Pt 1): 4218-4224.

Heider, K. H., M. Ratschek, et al. (1996). "Expression of CD44 isoforms in human renal cell carcinomas." Virchows Arch **428** (4-5): 267-273.

Helo, P., A. M. Cronin, et al. (2009). "Circulating prostate tumor cells detected by reverse transcription-PCR in men with localized or castration-refractory prostate cancer: concordance with CellSearch assay and association with bone metastases and with survival." Clin Chem **55** (4): 765-773.

Heyder, C., E. Gloria-Maercker, et al. (2006). "Visualization of tumor cell extravasation." Contrib Microbiol **13**: 200-208.

Hodgson, L., E. C. Kohn, et al. (2000). "Extracellular lipid-mediated signaling in tumor-cell activation and pseudopod protrusion." Int J Cancer **88** (4): 593-600.

Hong, J. W. and S. R. Quake (2003). "Integrated nanoliter systems." Nat Biotechnol **21** (10): 1179-1183.

Hoon, D. S. (2004). "Are circulating tumor cells an independent prognostic factor in patients with high-risk melanoma?" Nat Clin Pract Oncol **1** (2): 74-75.

Hou, H. W., A. A. S. Bhagat, et al. (2010). "Deformability based cell margination-A simple microfluidic design for malaria-infected erythrocyte separation." Lab Chip **10** (19): 2605-2613.

Huang, L. R., E. C. Cox, et al. (2004). "Continuous particle separation through deterministic lateral displacement." Science **304** (5673): 987-990.

Hui, C. Y., A. Jagota, et al. (2002). "Constraints on Microcontact Printing Imposed by Stamp Deformation." Langmuir **18** (4): 1394-1407.

Inglis, D. W., J. A. Davis, et al. (2006). "Critical particle size for fractionation by deterministic lateral displacement." Lab Chip **6** (5): 655-658.

Ito, S., H. Nakanishi, et al. (2002). "Quantitative detection of CEA expressing free tumor cells in the peripheral blood of colorectal cancer patients during surgery with real-time RT-PCR on a LightCycler." Cancer Lett **183** (2): 195-203.

Joka, M., K. Pietsch, et al. (2009). "Heterogeneous expression of prognostic and predictive antigens in primary and metastatic gastric cancer." ASCO Meeting Abstracts **27** (15S): e22030.

Kahn, H. J., A. Presta, et al. (2004). "Enumeration of circulating tumor cells in the blood of breast cancer patients after filtration enrichment: correlation with disease stage." Breast Cancer Res Treat **86** (3): 237-247.

Kaiser, J. (2010). "Medicine. Cancer's circulation problem." Science **327** (5969): 1072-1074.

Kasimir-Bauer, S., N. Schleucher, et al. (2003). "Evaluation of different markers in non-small cell lung cancer: prognostic value of clinical staging, tumour cell detection and tumour marker analysis for tumour progression and overall survival." Oncol Rep **10** (2): 475-482.

Koga, T., E. Tokunaga, et al. (2008). "Detection of circulating gastric cancer cells in peripheral blood using real time quantitative RT-PCR." Hepatogastroenterology **55** (84): 1131-1135.

Krivacic, R. T., A. Ladanyi, et al. (2004). "A rare-cell detector for cancer." Proc Natl Acad Sci U S A **101** (29): 10501-10504.

Kuo, J. S., Y. Zhao, et al. (2010). "Deformability considerations in filtration of biological cells." Lab Chip **10** (7): 837-842.

Lara, O., X. Tong, et al. (2004). "Enrichment of rare cancer cells through depletion of normal cells using density and flow-through, immunomagnetic cell separation." Exp Hematol **32** (10): 891-904.

Leinung, S., P. Wurl, et al. (2000). "Detection of cytokeratin-positive cells in bone marrow in breast cancer and colorectal carcinoma in comparison with other factors of prognosis." J Hematother Stem Cell Res **9** (6): 905-911.

Lekka, M., P. Laidler, et al. (1999). "Elasticity of normal and cancerous human bladder cells studied by scanning force microscopy." Eur Biophys J **28** (4): 312-316.

Leversha, M. A., J. Han, et al. (2009). "Fluorescence in situ hybridization analysis of circulating tumor cells in metastatic prostate cancer." Clin Cancer Res **15** (6): 2091-2097.

Li, X. and P. C. Li (2005). "Microfluidic selection and retention of a single cardiac myocyte, on-chip dye loading, cell contraction by chemical stimulation, and quantitative fluorescent analysis of intracellular calcium." Anal Chem **77** (14): 4315-4322.

Liang, S., M. J. Slattery, et al. (2008). "Hydrodynamic shear rate regulates melanoma-leukocyte aggregation, melanoma adhesion to the endothelium, and subsequent extravasation." Ann Biomed Eng **36** (4): 661-671.

Liang, X. J., A. Q. Liu, et al. (2005). Determination of refractive index for single living cell using integrated biochip.

Lindemann, F., G. Schlimok, et al. (1992). "Prognostic significance of micrometastatic tumour cells in bone marrow of colorectal cancer patients." Lancet **340** (8821): 685-689.

Loberg, R. D., Y. Fridman, et al. (2004). "Detection and isolation of circulating tumor cells in urologic cancers: a review." Neoplasia **6** (4): 302-309.

Losanoff, J. E., W. Zhu, et al. (2008). "Can mitochondrial DNA mutations in circulating white blood cells and serum be used to detect breast cancer?" Breast **17** (5): 540-542.

MacDiarmid, J. A., N. B. Mugridge, et al. (2007). "Bacterially derived 400 nm particles for encapsulation and cancer cell targeting of chemotherapeutics." Cancer Cell **11** (5): 431-445.

Mach, A. J. and D. Di Carlo (2010). "Continuous scalable blood filtration device using inertial microfluidics." Biotechnology and Bioengineering **107** (2): 302-311.

Maheswaran, S., L. V. Sequist, et al. (2008). "Detection of mutations in EGFR in circulating lung-cancer cells." N Engl J Med **359** (4): 366-377.

Malek, A. M., S. L. Alper, et al. (1999). "Hemodynamic shear stress and its role in atherosclerosis." JAMA **282** (21): 2035-2042.

Martini, J., W. Hellmich, et al. (2007). "Systems nanobiology: from quantitative single molecule biophysics to microfluidic-based single cell analysis." Subcell Biochem **43**: 301-321.

Marx, J. (2007). "Molecular biology. Cancer's perpetual source?" Science **317** (5841): 1029-1031.

Masuda, M., Y. Takano, et al. (1999). "Expression and prognostic value of CD44 isoforms in transitional cell carcinoma of renal pelvis and ureter." J Urol **161** (3): 805-808; discussion 808-809.

McKiernan, J. M., R. Buttyan, et al. (1999). "The detection of renal carcinoma cells in the peripheral blood with an enhanced reverse transcriptase-polymerase chain reaction assay for MN/CA9." Cancer **86** (3): 492-497.

Melchior, S. W., E. Corey, et al. (1997). "Early tumor cell dissemination in patients with clinically localized carcinoma of the prostate." Clin Cancer Res **3** (2): 249-256.

Melin, J. and S. R. Quake (2007). "Microfluidic large-scale integration: the evolution of design rules for biological automation." Annu Rev Biophys Biomol Struct **36**: 213-231.

Mimori, K., T. Fukagawa, et al. (2008). "A large-scale study of MT1-MMP as a marker for isolated tumor cells in peripheral blood and bone marrow in gastric cancer cases." Ann Surg Oncol **15** (10): 2934-2942.

Miqin, Z., T. Desai, et al. (1998). "Proteins and cells on PEG immobilized silicon surfaces." Biomaterials **19** (10): 953-960.

Mocellin, S., D. Hoon, et al. (2006). "The prognostic value of circulating tumor cells in patients with melanoma: a systematic review and meta-analysis." Clin Cancer Res **12** (15): 4605-4613.

Mohamed, H., L. D. McCurdy, et al. (2004). "Development of a rare cell fractionation device: application for cancer detection." IEEE Trans Nanobioscience **3** (4): 251-256.

Mohamed, H., M. Murray, et al. (2009). "Isolation of tumor cells using size and deformation." Journal of Chromatography A **1216** (47): 8289-8295.

Mohamed, H., J. N. Turner, et al. (2007). "Biochip for separating fetal cells from maternal circulation." J Chromatogr A **1162** (2): 187-192.

Moreno, J. G., S. M. O'Hara, et al. (2001). "Changes in circulating carcinoma cells in patients with metastatic prostate cancer correlate with disease status." Urology **58** (3): 386-392.

Nagrath, S., L. V. Sequist, et al. (2007). "Isolation of rare circulating tumour cells in cancer patients by microchip technology." Nature **450** (7173): 1235-1239.

Nole, F., E. Munzone, et al. (2007). "Variation of circulating tumor cell levels during treatment of metastatic breast cancer: prognostic and therapeutic implications." Ann Oncol **19** (5): 891-897

Nole, F., E. Munzone, et al. (2008). "Variation of circulating tumor cell levels during treatment of metastatic breast cancer: prognostic and therapeutic implications." Ann Oncol **19** (5): 891-897.

O'Sullivan, G. C., J. K. Collins, et al. (1997). "Micrometastases: marker of metastatic potential or evidence of residual disease?" Gut **40** (4): 512-515.

Oberneder, R., R. Riesenberg, et al. (1994). "Immunocytochemical detection and phenotypic characterization of micrometastatic tumour cells in bone marrow of patients with prostate cancer." Urol Res **22** (1): 3-8.

Ohlmann, C. H., E. Ozgur, et al. (2006). "Detection of circulating tumor cells in patients with renal cell carcinoma by reverse transcriptase polymerase chain reaction for G250/MNCA-9: results of a prospective trial." Urol Oncol **24** (4): 287-293.

Ohno, K., K. Tachikawa, et al. (2008). "Microfluidics: applications for analytical purposes in chemistry and biochemistry." Electrophoresis **29** (22): 4443-4453.

Osta, W. A., Y. Chen, et al. (2004). "EpCAM Is Overexpressed in Breast Cancer and Is a Potential Target for Breast Cancer Gene Therapy." Cancer Research **64** (16): 5818-5824.

Pagano, S., F. Franzoso, et al. (1996). "Renal cell carcinoma metastases. Review of unusual clinical metastases, metastatic modes and patterns and comparison between clinical and autopsy metastatic series." Scand J Urol Nephrol **30** (3): 165-172.

Paget, S. (1889). "THE DISTRIBUTION OF SECONDARY GROWTHS IN CANCER OF THE BREAST." The Lancet **133** (3421): 571-573.

Pamme, N. (2007). "Continuous flow separations in microfluidic devices." Lab Chip **7** (12): 1644-1659.

Pan, J. Y. (2004). "Reliability considerations for the BioMEMS designer." Proceedings of the IEEE **92** (1): 174-184.

Panaro, N. J., X. J. Lou, et al. (2005). "Micropillar array chip for integrated white blood cell isolation and PCR." Biomol Eng **21** (6): 157-162.

Pantel, K. and C. Alix-Panabieres (2007). "The clinical significance of circulating tumor cells." Nat Clin Pract Oncol **4** (2): 62-63.

Pantel, K. and R. H. Brakenhoff (2004). "Dissecting the metastatic cascade." Nat Rev Cancer **4** (6): 448-456.

Pantel, K., R. H. Brakenhoff, et al. (2008). "Detection, clinical relevance and specific biological properties of disseminating tumour cells." Nat Rev Cancer **8** (5): 329-340.

Pantel, K., R. J. Cote, et al. (1999). "Detection and clinical importance of micrometastatic disease." J Natl Cancer Inst **91** (13): 1113-1124.

Pantel, K., J. R. Izbicki, et al. (1993). "Immunocytological detection of bone marrow micrometastasis in operable non-small cell lung cancer." Cancer Res **53** (5): 1027-1031.

Pantel, K. and S. Riethdorf (2009). "Pathology: are circulating tumor cells predictive of overall survival?" Nat Rev Clin Oncol **6** (4): 190-191.

Panteleakou, Z., P. Lembessis, et al. (2009). "Detection of circulating tumor cells in prostate cancer patients: methodological pitfalls and clinical relevance." Mol Med **15** (3-4): 101-114.

Papadaki, M. and S. G. Eskin (1997). "Effects of fluid shear stress on gene regulation of vascular cells." Biotechnol Prog **13** (3): 209-221.

Paradis, V., S. Ferlicot, et al. (1999). "CD44 IS AN INDEPENDENT PROGNOSTIC FACTOR IN CONVENTIONAL RENAL CELL CARCINOMAS." J Urol **161** (6): 1984-1987.

Patton, J. T., D. G. Menter, et al. (1993). "Computerized analysis of tumor cells flowing in a parallel plate chamber to determine their adhesion stabilization lag time." Cell Motil Cytoskeleton **26** (1): 88-98.

Pauli, C., M. Münz, et al. (2003). "Tumor-specific glycosylation of the carcinoma-associated epithelial cell adhesion molecule EpCAM in head and neck carcinomas." Cancer Lett **193** (1): 25-32.

Pfitzenmaier, J., W. J. Ellis, et al. (2007). "The detection and isolation of viable prostate-specific antigen positive epithelial cells by enrichment: a comparison to standard prostate-specific antigen reverse transcriptase polymerase chain reaction and its clinical relevance in prostate cancer." Urol Oncol **25** (3): 214-220.

Pieterman, R. M., J. W. G. van Putten, et al. (2000). "Preoperative Staging of Non-Small-Cell Lung Cancer with Positron-Emission Tomography." N Engl J Med **343** (4): 254-261.

Pool E.H. and D. G.R. (1934). "Cancer cells in the bloodstream." Am. J. Cancer **21**: 99.

Racila, E., D. Euhus, et al. (1998). "Detection and characterization of carcinoma cells in the blood." Proc Natl Acad Sci U S A **95** (8): 4589-4594.

Ratto, C., L. Sofo, et al. (1998). "Prognostic factors in colorectal cancer. Literature review for clinical application." Dis Colon Rectum **41** (8): 1033-1049.

Reuben, J. M., S. Krishnamurthy, et al. (2008). "The role of circulating tumor cells in breast cancer diagnosis and prediction of therapy response." Expert Opinion on Medical Diagnostics **2** (4): 339-348.

Reya, T., S. J. Morrison, et al. (2001). "Stem cells, cancer, and cancer stem cells." Nature **414** (6859): 105-111.

Riethdorf, S., H. Fritsche, et al. (2007). "Detection of Circulating Tumor Cells in Peripheral Blood of Patients with Metastatic Breast Cancer: A Validation Study of the CellSearch System." Clin Cancer Res **13** (3): 920-928.

Riethdorf, S., H. Wikman, et al. (2008). "Review: Biological relevance of disseminated tumor cells in cancer patients." Int J Cancer **123** (9): 1991-2006.

Roberts, S., O. L. L. Jonasson, et al. (1961). "Clinical significance of cancer cells in the circulating blood: two- to five-year survival." Ann Surg **154**: 362-371.

Russom, A., A. K. Gupta, et al. (2009). "Differential inertial focusing of particles in curved low-aspect-ratio microchannels." New J Phys **11**: 75025.

Sastre, J., M. L. Maestro, et al. (2008). "Circulating tumor cells in colorectal cancer: correlation with clinical and pathological variables." Ann Oncol **19** (5): 935-938.

Schlimok, G., I. Funke, et al. (1987). "Micrometastatic cancer cells in bone marrow: in vitro detection with anti-cytokeratin and in vivo labeling with anti-17-1A monoclonal antibodies." Proc Natl Acad Sci U S A **84** (23): 8672-8676.

Schmid, H. and B. Michel (2000). "Siloxane Polymers for High-Resolution, High-Accuracy Soft Lithography." Macromolecules **33** (8): 3042-3049.

Sergeant, G., F. Penninckx, et al. (2008). "Quantitative RT-PCR Detection of Colorectal Tumor Cells in Peripheral Blood-A Systematic Review." J Surg Res.

Serrano, M. J., P. Sanchez-Rovira, et al. (2009). "Detection of circulating tumor cells in the context of treatment: prognostic value in breast cancer." Cancer Biol Ther **8** (8): 671-675.

Sethu, P., A. Sin, et al. (2006). "Microfluidic diffusive filter for apheresis (leukapheresis)." Lab Chip **6** (1): 83-89.

Shah, R. B., R. Mehra, et al. (2004). "Androgen-Independent Prostate Cancer Is a Heterogeneous Group of Diseases: Lessons from a Rapid Autopsy Program." Cancer Res **64** (24): 9209-9216.

Sharp, K. G., G. S. Blackman, et al. (2004). "Effect of Stamp Deformation on the Quality of Microcontact Printing: Theory and Experiment." Langmuir **20** (15): 6430-6438.

Shelby, J. P., J. White, et al. (2003). "A microfluidic model for single-cell capillary obstruction by Plasmodium falciparum-infected erythrocytes." Proc Natl Acad Sci U S A **100** (25): 14618-14622.

Sieuwerts, A. M., J. Kraan, et al. (2009). "Anti-epithelial cell adhesion molecule antibodies and the detection of circulating normal-like breast tumor cells." J Natl Cancer Inst **101** (1): 61-66.

Silly, H., H. Samonigg, et al. (1992). "Micrometastatic tumour cells in bone marrow in colorectal cancer." Lancet **340** (8830): 1288.

Slade, M. J. and R. C. Coombes (2007). "The clinical significance of disseminated tumor cells in breast cancer." Nat Clin Pract Oncol **4** (1): 30-41.

Sledge, G. W., Jr. (2006). "Circulating tumor cells in breast cancer: blood will tell." Clin Cancer Res **12** (21): 6321-6322.

Smirnov, D. A., D. R. Zweitzig, et al. (2005). "Global gene expression profiling of circulating tumor cells." Cancer Res **65** (12): 4993-4997.

Smith, J. C. and D. Figeys (2006). "Proteomics technology in systems biology." Mol Biosyst **2** (8): 364-370.

Sorger, P. K. (2008). "Microfluidics closes in on point-of-care assays." Nat Biotechnol **26** (12): 1345-1346.

Spinney, L. (2006). "Cancer: caught in time." Nature **442** (7104): 736-738.

Stebbing, J. and L. R. Jiao (2009). "Circulating tumour cells as more than prognostic markers." The Lancet Oncology **In Press, Corrected Proof**.

Steeg, P. S. (2006). "Tumor metastasis: mechanistic insights and clinical challenges." Nat Med **12** (8): 895-904.

Steen, S., J. Nemunaitis, et al. (2008). "Circulating tumor cells in melanoma: a review of the literature and description of a novel technique." Proc (Bayl Univ Med Cent) **21** (2): 127-132.

Tan, S. J., L. Yobas, et al. (2009). "Microdevice for the isolation and enumeration of cancer cells from blood." Biomed Microdevices **11** (4): 883-892.

Terpe, H. J., S. Storkel, et al. (1996). "Expression of CD44 isoforms in renal cell tumors. Positive correlation to tumor differentiation." Am J Pathol **148** (2): 453-463.

Thorsen, T., S. J. Maerkl, et al. (2002). "Microfluidic large-scale integration." Science **298** (5593): 580-584.

Toner, M. and D. Irimia (2005). "Blood-on-a-chip." Annu Rev Biomed Eng **7**: 77-103.

Van Vliet, K. J., G. Bao, et al. (2003). "The biomechanics toolbox: experimental approaches for living cells and biomolecules." Acta Materialia **51** (19): 5881-5905.

Vankrunkelsven, S., D. Clicq, et al. (2004). "A novel microstep device for the size separation of cells." Electrophoresis **25** (10-11): 1714-1722.

Weiss, L. (1990). "Metastatic inefficiency." Adv Cancer Res **54**: 159-211.

Weiss, L. (1992). "Biomechanical interactions of cancer cells with the microvasculature during hematogenous metastasis." Cancer Metastasis Rev **11** (3-4): 227-235.

Weiss, L. and D. S. Dimitrov (1984). "A fluid mechanical analysis of the velocity, adhesion, and destruction of cancer cells in capillaries during metastasis." Cell Biophys **6** (1): 9-22.

Weiss, L. and D. S. Dimitrov (1986). "Mechanical aspects of the lungs as cancer cell-killing organs during hematogenous metastasis." J Theor Biol **121** (3): 307-321.

Weiss, L., J. P. Harlos, et al. (1988). "Metastatic patterns of renal carcinoma: an analysis of 687 necropsies." J Cancer Res Clin Oncol **114** (6): 605-612.

Weiss, L. and G. W. Schmid-Schonbein (1989). "Biomechanical interactions of cancer cells with the microvasculature during metastasis." Cell Biophys **14** (2): 187-215.

Weiss, L. and P. M. Ward (1983). "Cell detachment and metastasis." Cancer Metastasis Rev **2** (2): 111-127.

Wenqi, D., W. Li, et al. (2009). "EpCAM is overexpressed in gastric cancer and its downregulation suppresses proliferation of gastric cancer." J Cancer Res Clin Oncol **135** (9): 1277-1285.

Wheeler, A. R., W. R. Throndset, et al. (2003). "Microfluidic device for single-cell analysis." Anal Chem **75** (14): 3581-3586.

Whitesides, G. M. (2003). "The 'right' size in nanobiotechnology." Nat Biotechnol **21** (10): 1161-1165.

Whitesides, G. M. (2006). "The origins and the future of microfluidics." Nature **442** (7101): 368-373.

Whitesides, G. M., E. Ostuni, et al. (2001). "Soft lithography in biology and biochemistry." Annual Review of Biomedical Engineering **3**: 335-373.

Wicha, M. S. (2006). "Cancer stem cells and metastasis: lethal seeds." Clin Cancer Res **12** (19): 5606-5607.

Wilding, P., L. J. Kricka, et al. (1998). "Integrated cell isolation and polymerase chain reaction analysis using silicon microfilter chambers." Anal Biochem **257** (2): 95-100.

Yamashita, T., A. Budhu, et al. (2007). "Activation of Hepatic Stem Cell Marker EpCAM by Wnt {beta}-Catenin Signaling in Hepatocellular Carcinoma." Cancer Res **67** (22): 10831-10839.

Yap, B. and R. D. Kamm (2005). "Mechanical deformation of neutrophils into narrow channels induces pseudopod projection and changes in biomechanical properties." J Appl Physiol **98** (5): 1930-1939.

Yasumoto, K., T. Osaki, et al. (2003). "Prognostic value of cytokeratin-positive cells in the bone marrow and lymph nodes of patients with resected nonsmall cell lung cancer: a multicenter prospective study." Ann Thorac Surg **76** (1): 194-201; discussion 202.

Zhang, Y., C. W. Lo, et al. (2006). "Replica molding of high-aspect-ratio polymeric nanopillar arrays with high fidelity." Langmuir **22** (20): 8595-8601.

Zieglschmid, V., C. Hollmann, et al. (2005). "Detection of disseminated tumor cells in peripheral blood." Crit Rev Clin Lab Sci **42** (2): 155-196.

Zolota, V., A. C. Tsamandas, et al. (2002). "Expression of CD44 protein in renal cell carcinomas: association with p53 expression." Urol Oncol **7** (1): 13-17.

Zovato, S., G. Opocher, et al. (2009). "7144 Predictive value and biologic significance of circulating tumor cells (CTC) in sporadic and von hippel lindau (VHL) renal cancer." European Journal of Cancer Supplements **7** (2): 436-437.